Quantifying and Mitigating Antifungal Tolerance in the Pathogenic Yeast *Candida auris*

by

Samira Rasouli Koohi

A thesis submitted in partial fulfillment of the requirements for the degree of

Master of Science

Department of Physics
University of Alberta

Abstract

Candida auris is an emerging pathogen that has been detected on five continents and is linked to resistance against the main three classes of antifungal drugs used to treat invasive infections, leading to healthcare-associated outbreaks. Tolerance refers to the ability of a drug-susceptible fungal strain to grow slowly in the presence of an antifungal drug at concentrations above the minimum inhibitory concentration (MIC). This phenomenon can be reversed when the drug pressure is eliminated [1–3].

In this thesis, we examined the presence of tolerant subpopulations against several antifungal drugs, including fluconazole, itraconazole, caspofungin, voriconazole, posaconazole, amphotericin B, and anidulafungin. We obtained five *Candida auris* isolates from clinical samples collected at the Public Health Lab-Alberta Precision Laboratories.

I employed the microdilution assay to determine the MIC and conducted the disk diffusion assay (DDA) to determine the radius of the zone of inhibition (RAD). Images of the DDA were analyzed using *diskImageR* and *imageJ* software to quantify the fraction of growth (FOG) within the zone of inhibition (ZOI). Slow growing colonies within the ZOI were considered as tolerant subpopulations. The FOG within the ZOI served as a variable to quantify the degree of tolerance. Additionally, I measured supra-MIC growth (SMG) as another variable to quantify tolerance, which determined the growth in drug concentrations above MIC.

After 48 hours of drug treatment, an increase in SMG was observed for certain antifungal drug- *C. auris* isolate combinations. To explore whether tolerance was a non-genetic or genetic trait, I sub-cultured the colonies growing inside and outside the ZOI. I then repeated the DDA, MIC, and

SMG experiments. The isolates from inside and outside the ZOI did not exhibit any changes in the RAD, MIC, or SMG. These findings suggests that a non-genetic mechanism may underlie tolerance in *C. auris*. The potential synergy between various antifungals and an adjuvant, chloroquine, was then assessed against *C. auris*, *C. parapsilosis*, and *I. orientalis*. I found that the antifungal drug fluconazole when combined with the adjuvant chloroquine, reduced or eliminated tolerance in *C. auris*. Finally, I performed a numerical simulation to investigate the diffusion concentration profile of antifungal drugs within agar media. My findings revealed a concentration gradient, with higher drug concentrations observed near the center of the ZOI and lower concentrations at the periphery of the ZOI, which explains why the tolerant colonies were often observed at the edge of the ZOI; that is that tolerance is a drug-dependent phenomenon.

Preface

I confirm that the research described in this thesis is original. I carried out the research under the supervision of Dr. Daniel Charlebois. The majority of my thesis research (Chapter 2) was published in the peer-reviewed journal *Biomedicines* under the title "Identification and Elimination of Antifungal Tolerance in *Candida auris*"; the other co-authors of this article were Dr. Shamanth A. Shankarnarayan, who guided me on PCR protocols, assisted with the Chloroquine experiment, and co-wrote this article, and Clare Maristela Galon who replicated the Chloroquine experiment. I also presented these results orally at the "UA Bacterial AMR & Pathogenesis Research Talks" at University of Alberta (2022) and as a poster at the AMR – One Health Consortium in Banff (2022). The second part of my thesis research on the effect of drug diffusion on antifungal tolerance (Chapter 3) was presented as a poster at the AMR – One Health Consortium in Banff (2023). Finally, I co-authored a perspective article on the topic of "Does Transcriptional Heterogeneity Promote Genetic Drug Resistance?" (K.S. Farquhar, S. Rasouli Koohi, D.A. Charlebois, *BioEssays*, 2021).

ACKNOWLEDGEMENT

Table of Contents

Table of Figures

Chapter1

1 Introduction

1.1 Antifungal Resistance

An important medical advance that revolutionised healthcare procedures was the discovery of antimicrobial agents. They are compounds that are either natural, seminatural (semisynthetic), or synthetic and may either eradicate or inhibit the growth of germs. Antimicrobials are effective against many different types of microorganisms, including bacteria, fungi, viruses, and protozoa [4,5]. Antimicrobials which have an impact on bacteria and fungi are called antibiotics and antifungal respectively. Antimicrobials have an impact on animal and food production in addition to being crucial for human health directly [4]. Microorganisms have developed resistance to antimicrobials as their use expanded, and therefore some infections can no longer be treated with current drugs [6]. When microorganisms stop being susceptible to one or more antimicrobial agents, they are said to be antimicrobial-resistant. Microorganisms are referred as multidrug-resistant when they are resistant to at least one antibiotic in three or more drug classes [7] and they are pan drug-resistant microbes if they are resistant to all available antimicrobials [8,9].Antimicrobial resistance (AMR) is a complex worldwide problem. The development of AMR is mostly attributed to both human and veterinary medicine [10,11]. The Canadian Council of Academies (CCA) estimated that the escalating issue of AMR remains a pressing concern in recent years [12,13], particularly in 2022 [14–16], with infections increasingly posing treatment challenges worldwide. In 2019, nearly five million deaths were attributed to drug-resistant bacterial infections, of which 1.27 million were directly linked to AMR [12–14]. Alarming forecasts predict that AMR could lead to annual reductions in global GDP ranging from 1.1% to 3.8% by 2050. In specific regions such as Australia, Canada, Europe, and the United States, projections indicate a staggering 2.4 million cumulative deaths attributable

to AMR by 2050 [12,17], along with cumulative healthcare costs totaling $134 billion. In Canada, as of 2018, 26% of infections were resistant to first-line treatments, resulting in over 14,000 deaths, with 5,400 directly attributed to AMR and incurring an economic cost of roughly $2 billion in 2018 [18]. This challenge has persisted and intensified in recent years, with AMR rates continuing to climb for many priority pathogens. Access to effective antimicrobial drugs, especially when first-line treatments prove ineffective, remains a significant concern. Additionally, the lack of alternative treatment options for patients with specific conditions or intolerances, coupled with prohibitive costs, further underscores the gravity of this issue. Even last-resort antimicrobial drugs currently in use can have adverse effects, and as resistance rates surge, the financial burden of addressing these challenges is on the rise [12]. A worldwide issue, invasive fungal diseases cause 1.7 million fatalities annually [19–21]. Despite the major adverse impacts that pathogenic fungi have on human health worldwide, there are currently just three main classes of antifungal medications available to treat invasive infections, all of which have drawbacks such as host toxicity, poor pharmacokinetics, or a narrow spectrum of efficacy [22]. However, the number of antibiotics reported extends up to 39 classes [23]. As a result of fungi being eukaryotic and more similar to human cells, with respect to other microorganisms like bacteria, finding effective antifungal medicines has become more challenging for scientists. Therefore, the study of antifungal agent resistance has lagged behind that of antibacterial agent resistance [24]. Antifungal resistance (AFR) is a widespread issue that has a detrimental effect on patient care, particularly when it comes to invasive or systemic fungal infections.

1.2   Candida auris

One of the most important resistance pathogens is *Candida auris*. *Candida auris* (*C. auris*) is a species of yeast that belongs to the *Candida* genus, which is a large group of fungi [25,26]. There are a number of species that are commonly implicated in human infections, including opportunistic pathogenic fungi species, *C. albicans*, *C. glabrata*, *C. tropicalis*, *C. parapsilosis* and *Candida auris*, that are clinically significant. The most prevalent and extensively researched species, *C. albicans*, causes the majority of human *Candida* infections [27]. Other species are *C. glabrata* and *C. auris*, and they are linked to particular clinical symptoms and patterns of medication resistance [28]. It has been suggested that

global warming may have influenced *C. auris* selection [29]. Climate change could have facilitated the fungus in adjusting to the elevated body temperatures of birds and mammals, including humans [30]. According to some studies, birds and other animals with high body temperatures may have helped the fungus spread into cities and eventually infect people. Furthermore, it is still unknown how *C. auris* penetrates the epithelial layer without developing hyphae [31–34]. For a considerable time, *C. auris* was believed to be a haploid fungus; however, Shuru et al. recently made a groundbreaking discovery of the diploid form and spontaneous ploidy shifts in clinical isolates of *C. auris* [35]. With few effective treatments, a high mortality rate, and the potential of the microorganism to spread quickly in healthcare settings, the rise of pan-resistant *C. auris* strains in some regions is concerning [36].

It is well-known that the discovery dates back to 2009 in Japan where it was initially isolated from a patient's external ear, and it has since spread to various continents, exhibiting genetic diversity across different clades [37,38]. But there are some reports show that *C. auris* was introduced before this time in other countries like France [39]. In Japan, *C. auris* tends to remain localized in the ear and does not cause invasive illness by entering the bloodstream. However, in Korea, the same strain of *C. auris* has been linked to systemic infections [40]. First, it was categorized into four geographically limited clades: clade I (South Asia), clade II (East Asia), clade III (South Africa), and clade IV (South America). Additionally, there is evidence of a fifth clade reported from Iran [38,41–43] and recently, it was claimed that the sixth clade was discovered in Singapore [44]. It has infested more than 44 countries and all the continents except Antarctica [45]. As a member of the CTG clade[1], *C. auris* is more closely related to haploid and frequently drug-resistant species like *Candida lusitaniae* and *haemulonii*. This organism is difficult to identify using common identification methods and are commonly misidentified as *C. haemulonii* [37]. *C. auris* possesses remarkable ability to colonize and endure on surfaces within healthcare settings [46]. It demonstrates extended persistence on moist surfaces, surpassing *C. albicans*. Additionally, its metabolic activity

---

[1] The CTG clade includes fungi with a unique genetic trait where the CTG codon, typically encoding leucine, now codes for serine.

on surfaces remains sustained, resembling that of *C. parapsilosis*, which is recognized for colonizing skin and plastics [47].

Candidemia, a type of bloodstream infection, caused by *C. auris* can cause organ damage [48]. The death rate for this infection ranges from 30% to 70% [49]. Numerous virulence factors, including as secreted lipases and proteases, mannosyl transferases, oligopeptides, siderophore-based iron transporters, and biofilm formation, contribute to the pathogenicity of *Candida* species. These elements are crucial for the pathogen's invasion, colonisation, and acquisition of nutrition [33,34,50–52].

Antifungal resistance of *C. auris* causes a major challenge in treatment with high rates of resistance observed against azoles, echinocandins, and amphotericin B among clinical isolates [45,53–59]. Mechanisms of antifungal resistance in *C. auris* encompass gene mutations affecting drug targets (e.g., ERG11), efflux pumps (e.g., MDR1), and alterations in cell wall composition [57,59,60]. Genomic studies have provided insights into the genetic diversity and evolution of *C. auris* isolates [61,62]. Before going into detail into the mechanism of action of antifungals and resistance mechanisms, the different forms of AMR will be defined.

1.3 AMR Terminology

Tolerant Cells: In yeasts, "tolerant cells" refer to cells that can endure the presence of drugs or other stimuli that would ordinarily inhibit their proliferation. They can grow slowly in concentration of drug above MIC level. The majority of the time, tolerant cells are not dormant, but they can exhibit a range of adaptive processes that enable them to withstand the toxicity of the drugs. This may include adjustments to cellular metabolism, the activation of stress response pathways, or adjustments to gene expression. Antifungal Tolerance is quantified as the fraction of growth above the MIC [1,63].

Heteroresistance: A phenomenon known as heteroresistance occurs when a subset of the cells in a population of yeast, exhibit varying degrees of resistance to a particular stressor, such as an antifungal drug [64]. This means that while the majority of cells in the population may be sensitive to the drug and unable to survive, a small proportion of cells either

naturally possess resistance to the medication or have evolved resistance mechanisms that allow them to survive and continue to grow in its presence [63,65].

Susceptible: A pathogen is considered susceptible to a specific antimicrobial agent when its growth is inhibited, or it is killed during in vitro susceptibility test by a concentration of the drug that is known to be associated with a high probability of successful treatment [66].

Resistant: When a pathogen is suppressed during an in vitro susceptibility test by a drug concentration that is linked to a high likelihood of therapeutic failure, the pathogen is said to be resistant to that particular antimicrobial agent [66].

Persister Cells: There are a small portion of the bacterial population known as persister cells that goes into a growth-arrested or slow-growth stage. These cells are not genetically altered or dysfunctional. They help bacteria survive in rapidly changing settings by acting as a reservoir within bacterial populations. While the number of normal bacterial cells decreases after antibiotic therapy, persister cells are able to tolerate and be alive in presence of antibiotics. The phenotypic drug tolerance shown in persister cells is thought to be mostly influenced by epigenetic[1] inheritance. Drug-resistant mutants may evolve as a result of the persister cells' slow rate of development in combination with the stress-related mutations [67–69]. They are frequently referred to as "dormant" and "viable but non-culturable" cells. The phenomenon of bacterial persistence is seen as a sort of adaptive resistance since it permits germs to tolerate difficult conditions and may aid in the generation of drug-resistant variants [70,71].

The terms "persister cells" and " heteroresistance" are sometimes used interchangeably in the context of microbial populations, while there may be some differences depending on the specific research field or organism being studied. Yeast tolerance and bacterial persistence are frequently reversible. If the stress or selection pressure is removed, the tolerant or persistent cells can revert to a more susceptible or actively growing state. When the stressor,

---

[1] Epigenetic alterations refer to genetic modifications that influence gene function without altering the DNA sequence itself.

like an antimicrobial agent, is removed from the environment in the case of tolerant yeast cells, the yeast cells can recover and resume normal growth and division [1].

The focus of this thesis is on the identification, quantification, and elimination of tolerance in *C. auris*.

1.4 Different Antifungals

1.4.1 Triazoles

The class of antifungals known as azoles contains two or three nitrogen-containing heterocyclic five-membered chemical rings, namely imidazole and triazole. These drugs possess a wide range of applications and exhibit fungistatic[1] properties. Triazole antifungals include fluconazole, itraconazole, posaconazole, and voriconazole [72]. Azoles also target cell membrane and cytochrome P450-dependent enzymes, in particular C14-demethylase (Figure 1), are inhibited by them [22]. These enzymes contribute to ergosterol's (the main fungal sterol) production which is a major sterol produced by fungi. By inhibiting the synthesis of ergosterol the fungal cell growth will be arrested [24]. Azole resistance mechanisms in certain fungi, such as *Candida* species, often involve the activation of membrane-associated efflux pumps. These pumps recognize various chemicals and contribute to multidrug resistance. Additionally, azole resistance can be caused by alterations in the sterol biosynthesis pathway due to point mutations and promoter insertions [24,73]. Drug target overexpression is another mechanism [22].

1.4.2 Polyenes

The polyene class of antifungal drugs include nystatin, amphotericin B, and pimaricin. They are a type of broad-spectrum antifungal drugs with a cyclic amphiphilic macrolide substructure which are produced by a species of Streptomyces bacteria [74]. They are known as fungicidal[2] drug. The alternating conjugated double bonds which make the macrolide ring structure of the polyene molecules give them their name. The mechanism of

---

[1] Fungistatic refer to antifungal agents that hinder the growth of fungi without causing the death of the fungi.
[2] Fungicidal agents are the drugs that kill fungal pathogens.

action of this drug is binding to the ergosterol (Figure 1) which is a sterol presents in fungi cell membrane. As a result, ergosterol will be extracted from lipid bilayers and pores will be made in cell membrane and there will be intracellular ion leakage and the changes of membrane potential. Then, active transport mechanism within the cell membrane will be disrupted. In resistant fungi, mutations develop and enhance synthetic pathway for other sterols and replace with ergosterol which the drug is no longer effective on it [22,75,76]. In my thesis amphotericin B was used.

1.4.3 Echinocandins

Echinocandins are fungicidal drugs that represent a novel category of antifungal medications that function through the inhibition of β (1, 3)-D-glucan synthase (Figure 1), a crucial enzyme required for maintaining the structural integrity of the fungal cell wall. Caspofungin became the inaugural drug within this category to receive approval. micafungin and anidulafungin are two other echinocandins [77].
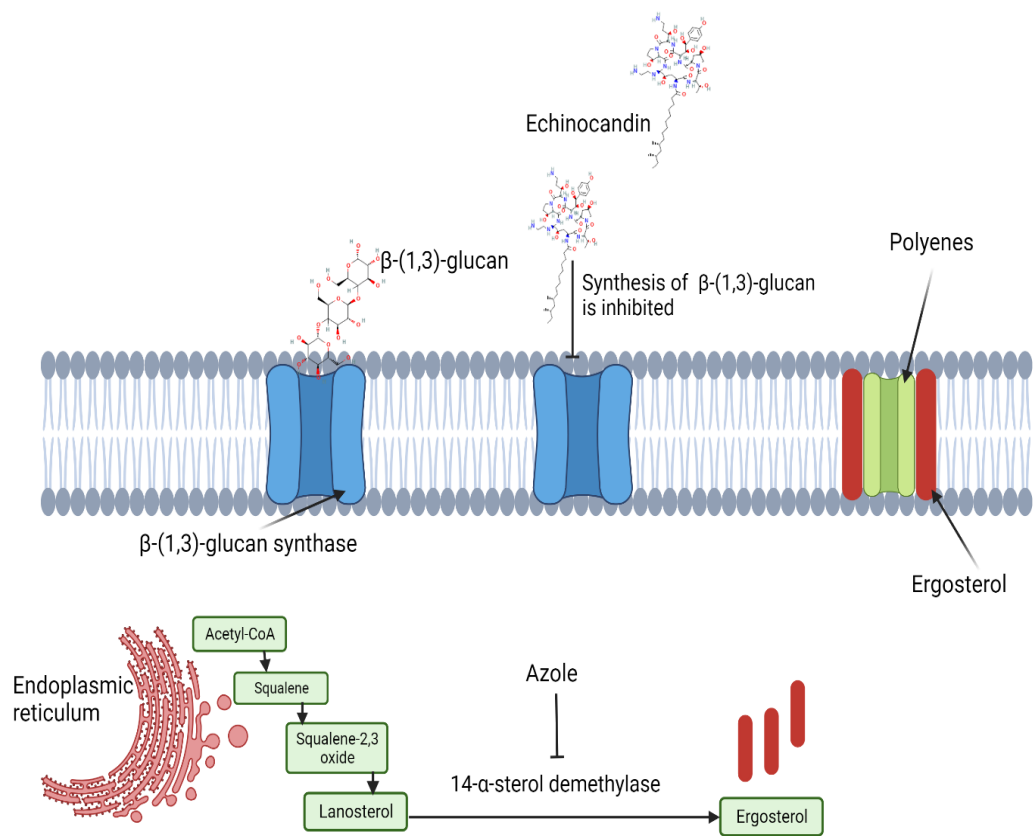
Figure 1. Mechanism of action of antifungals. Echinocandins non-competitively binding to a subunit of the enzyme and blocking the β-(1,3)-d-glucan synthesis. Polyene agents by binding to ergosterol form pores in the fungal cell membrane through which K+ and Mg++ can leak out of the cell. Azoles inhibit the enzyme cytochrome P450-dependent 14-α-sterol demethylase, required for the conversion of lanosterol to ergosterol. This figure was generated using BioRender (2023).

1.5   Genomic Plasticity

The ability of an organism's entire genome to change or adapt is known as genomic plasticity. This phenomenon in microorganism genomes allowing cells to quickly alter their genomes in response to changes in their environment [78]. Phenotypic plasticity is when organisms with the same genetic makeup can develop different traits in response to varying environmental conditions [79–81]. This plasticity can arise either from genetics or as a result of the physical and chemical processes during development and also result from interaction between the organism and its environment [82]. For example, temperature can directly impact development without genetic modification [81]. Additionally, heritable epigenetic

changes like DNA methylation can also lead to persistent developmental variations. Some suggest that plasticity can be genetically based and evolved, focusing on changes in gene expression patterns in response to the environment [83]. This includes the concept of reaction norms [83] and the adaptability of gene expression [84]. Fungal pathogens can develop drug resistance due to changes in their genomes as well as particular point mutations that boost the synthesis of drug targets or efflux pumps [85]. When cells divide, sometimes they are with an abnormal number of chromosomes which is called aneuploidy [86,87]. However, some recent studies suggest that aneuploid yeast cells might actually help cells adapt to new environments. Researchers found that when yeast cells had the abnormal number of chromosomes, they became better at handling stress and resisting drugs. This might happen because having different numbers of chromosomes changes the number of certain genes in the cell, making the cell more diverse and adaptable. So, even though aneuploidy is usually a mistake, it can sometimes be a way for cells to quickly become better at surviving in different conditions [86–88]. Some azole drug-resistant strains of *C. albicans* duplicate a portion of chromosome 5 to form an isochromosome[1]. The azole target Erg11 and the drug efflux regulator Tac1 are produced by additional genes as a result of this alteration [22,89]. Guanghua Huang and their colleagues used a *C. auris* that was susceptible to fluconazole in their experiment [88]. They exposed it to more and more fluconazole concentrations, and over time, the fungus became resistant to the drug. To understand why this happened, they looked at the fungus's genes. They found that the resistant fungus had an extra piece of chromosome 5 in its genes. Without the fluconazole, the fungus went back to being sensitive and lost that extra piece of chromosome 5. They also saw that this extra chromosome had genes related to resistance to the drugs. Additionally, they found some changes in certain genes (*TAC1B, RRP6*, and *SFT2*) in all the resistant fungus they tested. This extra chromosome 5 seems to help the fungus become resistant to fluconazole quickly, and it might be an important way for *C. auris* to become drug-resistant as it evolves.

---

[1]An isochromosome is an abnormal chromosome that appears as a mirror image of itself, consisting of two copies of either the short arm or the long arm.

Another way resistance develops is through loss of heterozygosity (LOH) events, in which some antifungal resistance-related gene regions mutate. LOH can arise from a variety of factors, including degradation, deletion, imbalanced rearrangement, gene conversion, mitotic recombination, or the loss of an entire chromosome. When one of the two alleles at a particular genetic locus is removed from the genome of an organism, called loss of heterozygosity, causes homozygosity, where both alleles are the same [90,91]. This can influence the expression of certain genes. Because of the allelic imbalance caused by LOH, which is the loss of one allele, heterozygous somatic cells become homozygous. LOH is described as the loss of one parent's genetic contribution to a cell [91]. Segmental aneuploidies, in which particular chromosomal segments have an abnormally high number of copies, are also thought to have a role in the development of resistance [22,92]. In the context of *C. albicans*, lineages that evolve with drug concentrations close to their MIC50 (the minimum inhibitory concentration of drug that reduces growth by 50%) tend to develop higher MIC50 levels, along with acquiring distinct segmental aneuploidies and copy number variations (CNVs). This is in contrast to lineages evolving with drug concentrations above MIC50, which undergo diverse mutational changes and experience an increase in drug tolerance (here the ability of a subpopulation of cells to grow above their MIC50) [92]. The activation of stress responses in cellular physiology leads to a reduction in antibiotic susceptibility for various antibiotics. This activation can stimulate resistance mechanisms, encourage the adoption of resistant lifestyles such as biofilm, and induce resistance mutations. These stress response pathways are essential for pathogen survival in the face of various environmental challenges and are crucial for mitigating the stress induced by antifungal agents [22,93]. Heat shock proteins (HSPs) are molecular chaperones that respond to stress and facilitate correct protein folding. Specifically, Hsp90, a well-preserved molecular chaperone, plays a central role in coordinating stress response signaling that governs fungal drug resistance. Hsp90 aids in the proper folding and functioning of client proteins, and its activity is intricately regulated by interactions with co-chaperones and modifications after translation. In the fungal pathogen *Candida albicans*, Hsp90 contributes to drug resistance and virulence by supporting various signal transducers' stability [94,95]. Azole resistance in *C. auris* involves mutations in the ERG3 gene, leading to the inhibition of toxic sterol accumulation caused by azole-mediated Erg11 inhibition. This mechanism

has been observed in related pathogens like C. albicans and C. parapsilosis, and ERG3 mutations have also emerged in *C. auris* following echinocandin exposure [22,96,97].

1.6   Definition of Tolerance to Antimicrobial Agents

Tolerance to antifungal drug concentrations exceeding the MIC is a phenomenon [1], overlooked according to prevailing clinical recommendations. Distinguishing between tolerance and resistance could offer valuable insights into the reasons behind treatment failures in specific contexts. Antifungal tolerance is characterized by a subset of tolerant cells that exhibit slow growth in drug concentrations exceeding the MIC, usually becoming visually apparent after time intervals longer than the standard clinical 24-hour MIC measurement period [3]. *C. auris* populations exhibit genetic and phenotypic heterogeneity, which is another factor to consider. Genetic variations within *C. auris* can result in diverse responses to antifungal drugs, which may lead to the development of tolerance. Under different stress conditions, changes in the total number of chromosomes might occur, resulting in improved tolerance to antifungal medications and enabling tolerance to antifungals even in the absence of past exposure [22,98]. For example, research in *C. albicans* suggests that exposure to certain stress-causing agents, chemotherapeutic hydroxyurea can lead to an abnormal number of a specific chromosome, making the fungus more resistant to caspofungin [99,100]. CNV is the phenomenon in which parts of the genome are duplicated and the number of duplications can vary between individuals within the same species. For instance, by accelerating the acquisition of genomic variety, this genomic plasticity plays a critical role in the development of azole resistance in C. albicans. CNVs, which are identified by the duplication of particular genomic areas, frequently include distinctive lengthy inverted repeat sequences on either side. The majority of these variants, which are present across the genome, contain genes linked to drug resistance. What is important in this phenomenon is reversibility in the next generation after the removal of the stress condition which indicates that it is either non-genetic in nature or it is a genetically encoded stress response mechanism. This was observed in an experiment performed on *C. parapsilosis* [101]. This research explores how aneuploidy affects the way *C. parapsilosis* adapts to stressful conditions. The researchers exposed *C. parapsilosis* to two stress-inducing substances: tunicamycin (TUN), which stresses the endoplasmic reticulum, and aureobasidin A (AbA), which inhibits sphingolipid biosynthesis. They selected the cells that managed to grow in the presence of these stressors. What they found was that aneuploidy, specifically having an extra copy of chromosome 6, helped the fungus adapt to both TUN and AbA. This suggests that *C. parapsilosis* can adjust to different types of stress by changing its chromosome numbers, showing that its genetic makeup is quite flexible. Then they checked the number of chromosomes after reducing the drug concentration in next generation and found that the change will be reversed suggesting that this phenomenon can be a mechanism in tolerant subpopulation [101] .

Other mechanisms for tolerance including random fluctuations and non-genetic factors [102,103] are explained in the following sections.

1.7   Non-Genetic Heterogeneity

Non-genetic variability among genetically similar cells is well studied in cancer biology [103] For many years, researchers have been aware of the genetic diversity among tumor cells, posing challenges to the treatment of cancer. Research employing flow cytometry has demonstrated that the abundance of a specific protein can fluctuate among genetically identical cells. These are heritable when modulated by gene regulatory networks [104,105] and can potentially act as a temporary substrate for natural selection, even in the absence of mutations [106,107]. This phenomenon accounts for the observed population heterogeneity, resulting in subpopulations exhibiting distinct responses to environmental stresses. This finding underscores the complexity of cellular behavior and adds to our understanding of how cells within the same group can exhibit differences in gene expression and protein levels. In diverse biological systems, including human blood progenitor cells, cancer cells, and microorganisms, non-genetic heterogeneity plays a crucial role in shaping outcomes. This heterogeneity arises from variations in gene expression profiles, leading to distinct phenotypic traits in seemingly identical populations of cells [105,107,108].

Microorganisms, including bacteria and yeast, also exhibit non-genetic phenotypic variability that can confer resistance to environmental stressors. This adaptability highlights the importance of non-genetic factors in population fitness [108]. The central role of phenotypic diversification in evolution allows species to adapt and thrive in challenging environmental conditions [109].Researchers, using Saccharomyces cerevisiae, investigated the reasons and outcomes of cell-to-cell variation in gene expression, aiming to understand its advantages or disadvantages. They found that increased variability in gene expression, influenced by the TATA box sequence, could be beneficial in adapting to abrupt environmental changes. Their study involved introducing mutations in a synthetic promoter and showed that TATA-containing promoters enabled rapid cell responses, adaptability to sudden environmental stress [110]. In another research [111] scientists explored how gene expression noise, both intrinsic and extrinsic, affects the fitness of cell populations in response to environmental stress. They conducted experiments using two closely related

budding yeast strains; one with precise noise control and one with constant low noise. The study aimed to understand how increased noise might benefit cells under high stress and impact their ability to adapt to prolonged stress. While their findings confirmed that extrinsic noise could enhance fitness under acute stress and influence gene expression in prolonged stress, they observed that strains with high and low extrinsic noise showed similar responses to prolonged stress. This suggests that noise-induced phenotypic contributes to stress resilience in the short term but may not be essential for long-term adaptation [111].

1.8   Stochastic Nature of Gene Expression

Indeed, investigating stochastic gene expression is crucial for understanding why genetically identical cells can exhibit variations in drug resistance. This stochastic phenomenon in gene expression may lead to the emergence of subpopulations with different traits and levels of tolerance. Even when cells have the same genetic makeup, the random nature of gene expression can result in diversity within a population, which can be important for adaptation, survival, and response to environmental changes [112,113]. Gene expression involves the transfer of information from DNA to mRNA to protein, with regulatory regions like promoters controlling transcription. Stochastic gene expression refers to the inherent randomness in this process, resulting in variations in mRNA and protein levels among seemingly identical cells. This noise can be intrinsic or extrinsic, originating from various sources such as cell division, age, and environmental fluctuations [114]. Despite the assumption of uniformity in clonal cell populations, noise-induced variability can have both detrimental and beneficial consequences [115]. While fluctuations may disrupt cellular regulation, they can also provide phenotypic diversity for natural selection to act upon, influencing responses to perturbations like drug treatments and offering a fitness advantage in changing environments [112]. These reactions occur as a result of collisions between molecules undergoing Brownian motion, leading to unpredictable timing of individual reactions and fluctuations in molecular population levels [113].The extent of these fluctuations becomes less noticeable in systems with a large number of molecules, such as test tubes, where the relative amplitudes of these fluctuations are effectively averaged out. In such cases, deterministic equations are suitable for describing the system's behavior [113].

1.9 Susceptibility Assessments

Antimicrobial sensitivity testing is the measurement of the susceptibility of a microorganism to an antimicrobial drug. The two mainly used susceptibility tests are Disk Diffusion Assay (DDA) and Broth Microdilution Assay (MBDA) which are explained in below.

1.9.1 Disk Diffusion assay

A disk diffusion assay, also known as the Kirby-Bauer test, is a method used in microbiology to determine if a microorganism is susceptible to a specific antimicrobial agent. In this method an antimicrobial disk will be placed on agar media and after 24 hours, the diameter of the zone of inhibition will be measured and compared with CLSI standards to distinguish between susceptible and resistant strains [116].

1.9.2 Microdilution Assay

A microdilution assay is a laboratory technique used to determine the minimum inhibitory concentration (MIC) of an antimicrobial agent against a specific microorganism by using a 96-well plate (Figure 2). For this purpose, a gradient of different concentration of antimicrobial solution is added to the wells of the plate and a similar amount of microorganism inoculum will be added to the wells and after 24 hours incubation period the well with 50 % of growth inhibition will be considered as MIC_{50}.
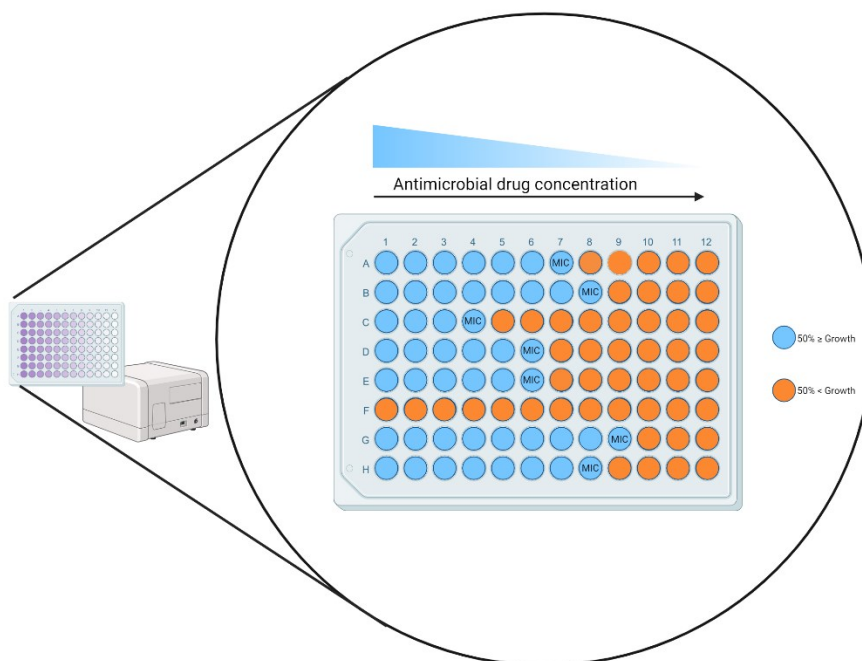
Figure 2. The illustration depicts the broth microdilution method. Featuring concentration gradients on the plates and consistent inoculum sizes of microorganisms. The concentration at which 50% of the growth is inhibited is defined as the MIC (minimum inhibitory concentration). The outcomes are measurable through absorbance readings obtained via a plate reader. This figure was generated using BioRender (2023).

1.10 Identification of Tolerance by Utilizing *diskImageR*

diskImageR [117,118] is a computational pipeline utilized for the analysis of photographs obtained from disk diffusion assays. Its purpose is to assess the level of drug susceptibility by measuring the radius of inhibition. In addition, it evaluates two key aspects of subpopulation growth, namely the fraction of growth occurring within the zone of inhibition, and the rate of change in growth from non-inhibitory to inhibitory drug concentrations. This methodology was initially introduced by Berman et al. The application of *diskImageR* was demonstrated in investigating the response of Candida albicans, a human fungal pathogen, to the antifungal drug fluconazole under various strain backgrounds and growth conditions. *diskImageR* employs two readily accessible software programs that are compatible with any computational platform: the statistical programming language R (R Core Team 2014) [119] and the image analysis program ImageJ [120] (figure 3). To measure tolerance, the growth of subpopulations exhibiting slow growth in drug concentrations

above the MIC can be quantified. Established methods for quantifying tolerance include SMG observed in BMDAs and the FoG within the ZOI observed in disk diffusion assays. These two parameters can be obtained using *diskImageR* [117,118,121–123].
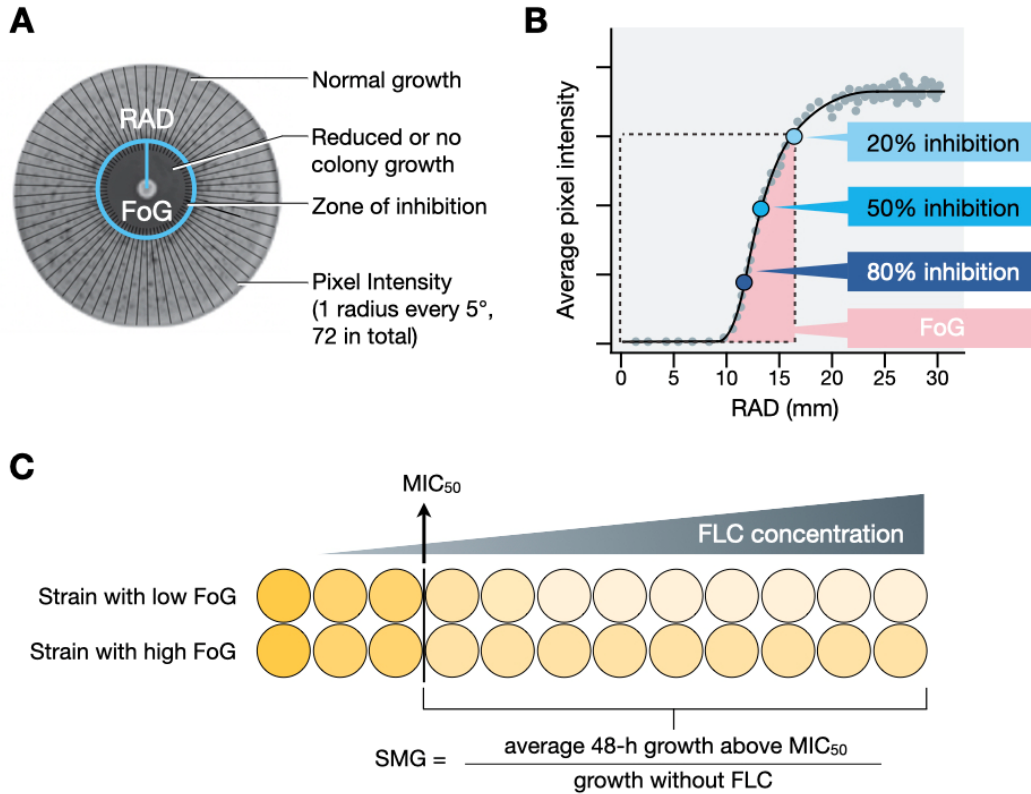
Figure 3. *The process of evaluating drug responses in both disk diffusion and liquid broth microdilution assays.* In the diskImageR analysis (A), pixel intensity is measured to gauge cell density by capturing data at 72 radii spaced every 5 degrees originating from the antifungal disc. The average radius (RAD) (B) serves as an indicator of susceptibility, with the minimum inhibitory concentration (MIC) inversely correlated with RAD. Different levels of growth reduction (20%, 50%, and 80%) relative to the maximum radius are denoted by light, medium, and dark blue dots. The fraction of growth within the inhibition zone (FoG) is calculated at the RAD threshold, considering the area under the curve in pink, divided by the maximum area. An illustration of MIC and supra-MIC growth (SMG) computations (C) is provided. MIC50, indicating the concentration at which 50% growth is inhibited, is calculated at 24 hours relative to growth without the drug, in this case, fluconazole (FLC). SMG is determined by assessing the average growth per well above the MIC and dividing it by the level of growth without FLC. This figure was adapted from Rosenberg 2020, CC BY 4.0 (https://creativecommons.org/licenses/by/4.0/).

1.11 Drug Diffusion in Disk Diffusion Assay

One method of susceptibility assessment is disk diffusion assay. Simulation assay will help to understand more about how drug diffuses within agar media. It will help us to explain the growth behavior of antifungal resistant subpopulations on agar.

1.11.1 Diffusion

Robert Brown's discovery of Brownian motion in the 19th century contributed to the development of diffusion theory and provided evidence for the existence of atoms [113,124]. The constant movement of particles due to thermal energy leads to their random motion and collisions, causing them to disperse from high to low concentration areas. This phenomenon, known as Brownian motion, is essential for diffusion. Diffusion plays a crucial role in biological processes like passive molecular transport and substance exchange across cell membranes [125]. The Einstein relation and Stokes' law provide insights into how temperature, particle size, and fluid viscosity affect diffusion. Higher temperatures and smaller particle sizes increase the diffusion coefficient and reduce drag forces, respectively, resulting in faster diffusion. Stokes' formula is given by:

$$\zeta = 6\pi\eta R \tag{1}$$

Where ζ is viscosity friction coefficient, η is viscosity, R is radius of the particle, and the coefficient 6π is obtained experimentally for the context of viscous drag experienced by a particle moving through a fluid. The force of viscosity on a small sphere moving through a viscous fluid is given by:

$$F_d = 6\pi\eta R v \tag{2}$$

Where F_d is the drag force – known as Stokes' drag, η is viscosity and v is the flow velocity relative to the particle. As the viscosity of the fluid increases, the drag force also increases,

resulting in a decrease in the speed of the particle through the fluid. Similarly, larger particles experience higher drag forces, which impede their motion. Finally, the velocity of the particle relative to the fluid affects the magnitude of the drag force, faster-moving particles experience a greater drag.

Then Einstein relation is as follow:

$$\zeta D = k_B T \qquad (3)$$

from which we obtain the Stokes-Einstein formula:

$$D = \frac{k_B T}{6\pi\eta R} \qquad (4)$$

This equation shows that as temperature (T) increases the diffusion coefficient (D) also increases, leading to faster diffusion. A smaller particle radius (R) will result in higher diffusion coefficient and faster diffusion.

1.11.2 Diffusion Equation

The diffusion equation provides a mathematical description of how a diffusing substance's concentration varies over time and space. It is formulated as a partial differential equation (equation 5), establishing a relationship between the rate of concentration change, the diffusion coefficient, and the Laplacian of the concentration field [125–129].

$$\frac{\partial C}{\partial t} = D\nabla^2 C \qquad (5)$$

Where $\frac{\partial C}{\partial t}$ is the rate of change of concentration with respect to time.

D is the diffusion coefficient, which depends on the properties of the diffusing substance and the medium it's moving through.

∇^2 is the Laplacian operator, which represents the spatial variation in concentration.

1.11.3 Steady-State Diffusion

The concentration profile doesn't change over time in steady-state diffusion. The steady-state diffusion equation describes the steady-state behaviour of diffusion [129–132].

$$\frac{d^2c}{dx^2} = 0 \tag{6}$$

1.11.4 Fick's First Law of Diffusion

Mathematical descriptions of diffusion can be found in Fick's laws of diffusion [129], which consist of two distinct principles that elucidate various aspects of the diffusion process [125–128,133]:

Fick's first law describes the rate of diffusion by considering the concentration gradient and the diffusivity of the medium. The concentration gradient is determined by the change in concentration over a specified distance. This law states that, the rate of diffusion is directly proportional to the concentration gradient:

$$J = -D\left(\frac{dc}{dx}\right) \tag{7}$$

Where J is the diffusion flux, or the amount of material that flows per unit time and area, D is the diffusion coefficient, depending on the properties of the material and the environment, and $\frac{dc}{dx}$ is the rate of change of the concentration gradient.

The equation indicates that the diffusion flux is directly proportional to the concentration gradient, where the diffusion coefficient serves as a constant related to the rate of diffusion. The negative sign in the equation signifies that diffusion consistently occurs from regions of high concentration to those of low concentration, down the gradient.

Fick's second law offers an explanation to how the concentration of a diffusing substance alters over time. It asserts that the rate at which the concentration changes is directly proportional to the second derivative of the concentration with respect to distance:

Where $\frac{dc}{dt}$ is the rate of change of concentration with respect to time, and $\frac{\partial^2 c}{\partial x^2}$ is the second derivative of the concentration with respect to distance:

$$\frac{\partial c}{\partial t} = D\left(\frac{\partial^2 c}{\partial x^2}\right) \qquad (8)$$

Both Fick's laws of diffusion find wide applications in calculating diffusion across diverse systems encompassing gases, liquids, and solids.

These laws can be used to effectively model a variety of scenarios involving diffusion, including the dispersion of gases in the atmosphere, the movement of water and nutrients within soil, the diffusion of impurities within semiconductor materials, and the diffusion of antifungal agents on the surface of solid media.

To solve these equations, the goal is to identify the concentration profile c(x,t) that satisfies the equation, along with any required initial and boundary conditions.

Various approaches exist for solving this equation, encompassing both analytical and numerical methods.

Analytical solutions are achievable for straightforward scenarios characterized by simple initial and boundary conditions, as well as a constant diffusion coefficient. In such cases, the solution often adopts a Gaussian function of the following form [125,126,128,133–135] (Figure 4):

$$c(x, t) = \frac{1}{\sqrt{4\pi Dt}} \cdot exp\left(-\frac{x^2}{4Dt}\right) \qquad (9)$$

This equation represents the concentration profile, where c(x,t) denotes the concentration at position x and time t, D represents the diffusion coefficient, and $\sqrt{4\pi Dt}$ is a normalization factor. The exponential term, $exp\left(-\frac{x^2}{4Dt}\right)$ accounts for the spatial and temporal characteristics of the diffusion process. The mathematical constant π represents the ratio of a circle's circumference to its diameter. The exponential function, represented by exp, calculates the value of e raised to a given power. According to the formula, the concentration of the diffusing substance diminishes exponentially both as time passes (t increases) and as one moves away from the origin (x = 0).
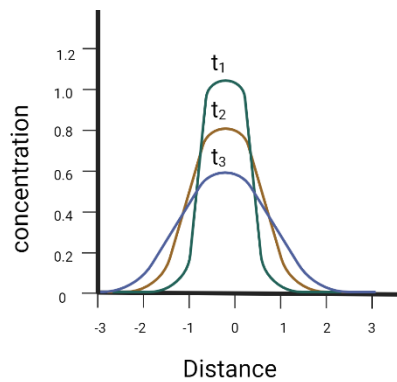
Figure 4. Illustration of the Gaussian concentration profile, a common analytical solution to Fick's laws of diffusion. This figure is generated using BioRender (2023).

This solution describes the spread of a concentration pulse with a Gaussian shape over time. The standard deviation of the Gaussian distribution increases with the square root of time, indicating that the diffusion process causes the concentration profile to spread out over time.

Numerical methods are commonly employed to solve the diffusion equation in more involved scenarios characterized by variable diffusion coefficients or complex initial and boundary conditions. These methods involve discretizing the spatial and temporal domains and utilizing numerical algorithms to estimate the solution at discrete points in space and time [136]. A popular numerical method for resolving Fick's second law is the finite difference approach. In this approach, a difference quotient is used to estimate the second derivative, and the resulting set of linear equations is then solved. Additional numerical techniques available for solving the diffusion equation include the finite element method

21

and the spectral method. These techniques present various approaches for approximating the concentration profile properly in systems with intricate initial boundary conditions, changing diffusion coefficients, or both [131,133,134,137].

Fick's second law can be extended to two dimensions to describe diffusion in two-dimensional systems. The equation becomes:

$$\frac{\partial c}{\partial t} = D \left(\frac{\partial^2 c}{\partial x^2} + \frac{\partial^2 c}{\partial y^2} \right) \tag{10}$$

Solving this equation involves finding the concentration profile c (x,y,t) that satisfies the equation and any given initial and boundary conditions. This can be done using numerical methods such as finite difference or finite element methods [134,136].

To model disk diffusion assay in chapter 3, I employ Include an explanation to support the validity of the 2D assumption comprising a drug circular diffusing source located at the center of a square domain, where the concentration remains zero at the boundaries. The initial distribution of the drug concentration can be described by the following profile:

$$c(x,y,0) = 0 \quad \text{for } x^2 + y^2 > r^2 \tag{11}$$

$$c(x,y,0) = c_0 \quad \text{for } x^2 + y^2 \leq r^2 \tag{12}$$

where r is the radius of the circular source and c_0 is the initial concentration within the source.

This equation specifies that at time t = 0, the concentration c at any point (x, y) in the two-dimensional system is determined based on the conditions: if the point lies outside the circular region with a radius of r (given by $x^2 + y^2 > r^2$), the concentration is 0; if the point lies inside or on the circular region (given by $x^2 + y^2 \leq r^2$), the concentration is c_0. Using finite difference methods, the concentration profile can be calculated at each time step by approximating the second derivatives with difference quotients. The resulting system of linear equations can be solved using iterative methods such as Gauss-Seidel or Jacobi. The concentration profile will evolve over time, spreading out from the circular source and diffusing through the domain. The exact form of the concentration profile will depend on the specific initial and boundary conditions of the problem, as well as the diffusion

coefficient [128,138,139].

1.11.5 Solving Fick's Second Law Using a Finite Difference Approximation

We can discretize the domain of interest into a grid of points with spacing x and y in the x and y directions, respectively, before applying the finite difference method to Fick's second law. We also discretize the time into discrete time steps with spacing Δt. Then, we can approximate the second partial derivatives of the concentration with respect to x and y (c(i,j)) using central differences:

$$\frac{\partial^2 c}{\partial x^2} \approx \frac{c(i+1,j) - 2c(i,j) + c(i-1,j)}{\Delta x^2} \tag{13}$$

$$\frac{\partial^2 c}{\partial y^2} \approx \frac{c(i,j+1) - 2c(i,j) + c(i,j-1)}{\Delta y^2} \tag{14}$$

where c(i,j) represents the concentration at the grid point (i,j).

We can substitute these approximations into Fick's second law [equation (10)] to obtain a finite difference equation:

$$\frac{c(i,j,t+\Delta t) + c(i,j,t)}{\Delta t} \tag{15}$$
$$= D$$
$$\cdot \left[\frac{c(i+1,j,t) - 2c(i,j,t) + c(i-1,j,t)}{\Delta x^2} \right.$$
$$\left. + \frac{c(i,j+1,t) - 2c(i,j,t) + c(i,j-1,t)}{\Delta y^2} \right]$$

This equation relates the concentration at each grid point (i,j) at time t+Δt to the concentration at the same point at time t, as well as the concentrations at neighboring points

23

at time t. D is assumed to be constant in this equation.

The equation 15 can be rearranged to solve for the concentration at time t+Δt at each grid point [129,132,139]:

$$c(i,j,t+\Delta t) = c(i,j,t) + D\frac{\Delta t}{\Delta x^2} \cdot \big(c(i+1,j,t) - 2c(i,j,t) + c(i-1,j,t)\big) + D\frac{\Delta t}{\Delta y^2} \cdot \big(c(i,j+1,t) - 2c(i,j,t) + c(i,j-1,t)\big) \tag{16}$$

The above equation enables the calculation of concentration values at each grid point and time step by iteratively considering the concentrations from the previous time step and neighboring grid points. This iterative process can be repeated until the concentration profile reaches a steady state or until a specific time criterion is met. By performing these computations, the evolving concentration distribution can be accurately determined over time.

In summary, Fick's second law can be solved using difference approximation, where the partial derivatives are approximated using central differences and the finite difference equation is solved iteratively to obtain the concentration profile at each time step.

1.11.6 Estimation of diffusion coefficient *D*

The diffusion coefficient characterizes the rate at which a substance diffuses through a medium. This intrinsic property of the material can be determined through experimental measurements specific to the substance and medium under consideration. Robbins et al. set up an experiment and measurement technique to develop visualize and quantify diffusion in model foods, specifically gels made of agar [140]. The researchers tracked the diffusion of aqueous solutions containing different concentrations of two dyes (rhodamine 6G and methylene blue) within agar gels at three different temperatures (30°C, 50°C, and 70°C) until equilibrium was reached. Using image analysis techniques, they examined the nature

of the diffusion process, specifically the amount of dye that diffused into the gel. The diffusion coefficient, D, was estimated using Fick's second law of diffusion [140]. Alternatively, theoretical models can be utilized to estimate the diffusion coefficient in situations where experimental data may be limited or unavailable [141–143].

One way to estimate the diffusion coefficient is by using the Stokes-Einstein equation (Equation (4))[125,133,143,144]:

$$D = \frac{kT}{6\pi\eta r}$$

However, we first need to determine the effective radius of the antifungal molecule we assume that it is spherical. To estimate the radius, we can use the molecular weight and assume the molecule has a density similar to water. The formula to calculate the radius (r) is:

$$r = \left(\frac{3m}{4\pi\rho}\right)^{1/3} \qquad (17)$$

Once the diffusion coefficient has been estimated, it can be used in the finite difference approximation of Fick's second law, as shown previously. It is important to note that the choice of the diffusion coefficient can have a significant impact on the behavior of the system being modeled. Therefore, it is important to choose an appropriate value based on the specific situation being studied.

Chapter 2

2 Identification and Elimination of Antifungal Tolerance in Candida auris

S Rasouli Koohi, SA Shankarnarayan, CM Galon, DA Charlebois

Article

Identification and Elimination of Antifungal Tolerance in *Candida auris*

Samira Rasouli Koohi [1,†] , Shamanth A. Shankarnarayan [1,†] , Clare Maristela Galon [1] and Daniel A. Charlebois [1,2,*]

1 Department of Physics, University of Alberta, Edmonton, AB T6G 2R3, Canada
2 Department of Biological Sciences, University of Alberta, Edmonton, AB T6G 2E9, Canada
* Correspondence: dcharleb@ualberta.ca
† These authors contributed equally to this work.

Abstract: Antimicrobial resistance is a global health crisis to which pathogenic fungi make a substantial contribution. The human fungal pathogen *C. auris* is of particular concern due to its rapid spread across the world and its evolution of multidrug resistance. Fluconazole failure in *C. auris* has been recently attributed to antifungal "tolerance". Tolerance is a phenomenon whereby a slow-growing subpopulation of tolerant cells, which are genetically identical to susceptible cells, emerges during drug treatment. We use microbroth dilution and disk diffusion assays, together with image analysis, to investigate antifungal tolerance in *C. auris* to all three classes of antifungal drugs used to treat invasive candidiasis. We find that (1) *C. auris* is tolerant to several common fungistatic and fungicidal drugs, which in some cases can be detected after 24 h, as well as after 48 h, of antifungal drug exposure; (2) the tolerant phenotype reverts to the susceptible phenotype in *C. auris*; and (3) combining azole, polyene, and echinocandin antifungal drugs with the adjuvant chloroquine in some cases reduces or eliminates tolerance and resistance in patient-derived *C. auris* isolates. These results suggest that tolerance contributes to treatment failure in *C. auris* infections for a broad range of antifungal drugs, and that antifungal adjuvants may improve treatment outcomes for patients infected with antifungal-tolerant or antifungal-resistant fungal pathogens.

Keywords: adjuvant; antifungal tolerance/resistance; broth microdilution assay; *Candida auris*; disk diffusion assay; diskImageR; human fungal pathogen

1. Introduction

Antimicrobial resistance (AMR) threatens the advances of modern medicine. Antifungal resistance contributes significantly to the AMR problem [1,2], especially among immunocompromised patients [3,4]. A multitude of biological, sociological, and economic factors result in hundreds of millions of serious fungal infections and between 1 and 1.5 million fungal infection-related deaths per year globally [5,6]. AMR, among fungi, is of particular concern due to the limited number of classes of drugs available to treat invasive fungal infections (i.e., fungistatic azoles as well as fungicidal polyenes and echinocandins) [7]. This threat is exacerbated by the fact that no new class of antifungal drugs has reached the market in over a decade [8,9]. Climate change is also predicted to increase the prevalence of fungal infections, as fungi adapt to warmer temperatures to increase their geographic range and overcome the thermal protection barrier of their warm-blooded hosts [10].

Candida species of yeast are the most common causes of fungal infections [11]. One *Candida* species that is increasingly of concern is *Candida auris* [12], due to its resistance to antifungal drugs and healthcare-associated outbreaks [13]. *C. auris* has now been reported on all inhabited continents and in over 47 countries [14,15]. Particularly concerning, is that *C. auris* is multidrug resistant (i.e., non-susceptible to at least one agent in three or more

classes of antimicrobials) [16–18], and, in some cases, it has been found to be pandrug-resistant (i.e., non-susceptible to all agents in all antimicrobial classes) [18,19]. *C. auris* has mortality rates of up to 45% among patients with bloodstream infections [20].

"Tolerance" is a phenomenon whereby a slow-growing subpopulation of cells, which are thought to be genetically identical to susceptible cells, emerges during antifungal drug treatment [21]. Antifungal tolerance is distinct from antifungal resistance, in that resistance is the result of heritable genetic changes and resistant cells grow above the minimum inhibitory concentration (MIC) in a concentration-dependent manner (i.e., MIC increases in resistance, but it does not increase in tolerance). In contrast, tolerance is a reversible phenomenon whereby cells grow slowly above MIC (i.e., they exhibit growth at "supra-MIC"). Tolerance manifests from the phenotypic heterogeneity intrinsic to a given fungal isolate, such that any cell within an isogenic population can reproduce the fractions of susceptible and tolerant cells present prior to the initiation of antifungal treatment. Cross tolerance has been observed in *C. albicans*, whereby strains tolerant to posaconazole also exhibit tolerance to other azole drugs [22]. Though the molecular mechanisms underlying tolerance in *Candida* species are still largely unknown, preliminary studies have shown that tolerance is associated with multiple genetic components that differ between isolates, including Hsp90-faciliated azole tolerance in *C. auris* [23]. Aneuploidy has also been shown to alter antifungal tolerance in *C. albicans* [24,25]. It is unknown if *C. auris* is tolerant to non-azole classes of antifungal drugs.

Clinical assays have not been designed to detect antifungal tolerance [26,27]. Quantitatively measuring tolerances of infecting isolates may provide prognostic insights concerning the success of mono- and combination-antifungal therapies [28]. Broth microdilution assays and disk diffusion assays, coupled with the image analysis software diskimageR, have been successfully used to quantify antifungal tolerance in research laboratories [29]. Most clinical diagnostic tests are performed on cultures grown for 24 h and therefore cannot detect drug-tolerant cells, which are typically visually evident after 48 h of growth [21]. Tolerance, along with host factors, immune status, and pharmacological issues [30], may explain why some patients do not respond to drug therapy despite being infected with fungi that have been determined, by traditional antimicrobial susceptibility testing methods, to be susceptible to a particular drug (i.e., cells that do not grow above MIC at 24 h, the standard endpoint MIC measurement for *Candida* species) [21,28]. "Trailing growth" (the clinical term for tolerance) leads to poor response to fluconazole in *C. tropicalis* in wax moth larvae [31] and mouse models [32], and high levels of tolerance are associated with *C. albicans* infections in patients treated with fluconazole [33].

Adjuvant drugs have the potential to sustain the vital functions of antimicrobial drugs [21]. Non-antifungal agents have been shown to enhance the effectiveness of azole drugs against resistant *Candida* species and other pathogenic fungi, including *Aspergillus fumigatus*, *Cryptococcus neoformans*, and the dimorphic fungus *Histoplasma capsulatum* [34–36]. Specifically, the antimalarial drug chloroquine, in combination with fluconazole, exhibited enhanced antifungal activity against *C. albicans*, *C. tropicalis*, *C. glabrata*, *C. parapsilosis*, and *C. krusei* (teleomorph is known as *Issatchenkia orientalis* and *Pichia kudriavzevii* [11]) isolates in vitro [37]. Whether or not tolerance and resistance to azoles or to other classes of antifungal drugs can be eliminated in *C. auris* using adjuvant antifungal therapies, remains to be investigated. Another study explored the activity of doxycycline, pyrvinium pamoate, along with chloroquine, as adjuvants in combination with fluconazole in clinical *C. albicans* isolates, and found increased antifungal activity [29]. Chloroquine is a member of the quinoline family and is used to treat diseases including malaria, amebiasis, rheumatoid arthritis, discoid, and systemic lupus erythematosus [38–40]. Chloroquine causes iron depletion, leading to a decrease in membrane sterol availability and downregulates the *ERG11* gene [41]. We hypothesize that the combining chloroquine with common antifungal drugs will eliminate antifungal tolerance in *C. auris*.

The main aims of our study are to use broth microdilution and disk diffusion assays, together with diskImageR, to investigate if tolerance to all three classes of antifungal

28

drugs occurs in *C. auris*, and if this tolerance can be eliminated by adjuvant antifungal therapy. We find that *C. auris* is tolerant to several fungistatic and fungicidal drugs: fluconazole, itraconazole, posaconazole, voriconazole, amphotericin B, and caspofungin. We demonstrate that antifungal tolerance is detectable at 24 h, as well as at 48 h, and that tolerance is a reversible phenomenon. Finally, we are reporting for the first time that in some isolates combining antifungal drugs with the adjuvant chloroquine eliminates tolerance and resistance in *C. auris*.

2. Materials and Methods

2.1. Strains, Media, and Growth Conditions

C. auris isolates were obtained from clinical samples from the Alberta Precision Laboratories (APL)—Public Health Laboratory (ProvLab).

All strains and isolates (Table S1) were preserved in 25% glycerol at −80 °C until further use. The strains and isolates were revived by culturing from frozen stock on YPD agar plates (yeast extract: Sigma Aldrich, #8013-01-2; bacto peptone: Difco, #9295043) and incubated at 35 °C for 48 h. Fresh subcultures were made on YPD agar plates and incubated at 35 °C for 24 h prior to conducting microbroth dilution and disk diffusion assays (Section 2.3).

2.2. DNA Extractions, PCR, and Sequencing

The initial identification of all *C. auris* isolates was performed using matrix-assisted laser desorption ionization—time of flight (MALDI-TOF) mass spectrometry [42,43] by the APL—ProvLab. The molecular identity of these isolates was confirmed by amplifying and sequencing the Internal Transcribed Spacer (ITS) region of ribosomal DNA. The primers ITS-5 (5′-GGAAGTAAAAGTCGTAACAAGG-3′) and ITS-4 (5′-TCCTCCGCTTATTGATATGC-3′) were used to amplify the ITS region (Integrated DNA Technologies). Genomic DNA was extracted using manual phenol–chloroform–isoamyl alcohol method [44]. The concentration of the extracted DNA was measured using a microvolume μDrop Plate (Thermo Fisher Scientific, Mississauga, ON, Canada, #N12391). The template and the primers were mixed in concentrations of 7.5 ng/μL and 0.25 μM, respectively, to a final volume of 10 μL. Sanger sequencing was then performed using a 3730 Genetic Analyzer (Thermo Fisher Scientific, Mississauga, ON, Canada, #A41046) at the Molecular Biology Services Unit at the University of Alberta. The resulting sequences were subjected to nucleotide BLAST analysis [45], which revealed 100% similarly to the standard strains. The *C. auris* isolates' ITS sequences were submitted to NCBI with the accession number OP984814-OP984818.

2.3. Broth Microdilution and Disk Diffusion Assays

The MIC for each isolate was first determined via broth microdilution assays following CLSI M27 guidelines [46]. All the isolates were tested in 96-well U-bottom microwell plates (Thermo Fisher Scientific, Mississauga, ON Canada, #163320) against fluconazole (Sigma-Aldrich, Oakville, ON, Canada, #F8929) (0.12–64 μg/mL), amphotericin B (Sigma-Aldrich, Canada, #A9528) (0.03–16 μg/mL), itraconazole (Sigma-Aldrich, Oakville, ON, Canada, #16657) (0.03–16 μg/mL), posaconazole (Sigma-Aldrich, Oakville, ON, Canada, #SML2287) (0.03–16 μg/mL), voriconazole (Sigma-Aldrich, Oakville, ON Canada, #P20005) (0.03–16 μg/mL), micafungin (Sigma-Aldrich, Oakville, ON, Canada, #208538) (0.015–8 μg/mL), caspofungin (Sigma-Aldrich, Oakville, ON, Canada, #179463-17-3) (0.015–8 μg/mL), and anidulafungin (Sigma-Aldrich, Oakville, ON, Canada, #166663-25-8) (0.03–16 μg/mL). These antifungals were dissolved in DMSO (fluconazole, itraconazole, voriconazole, posaconazole, anidulafungin, and amphotericin B) or water (caspofungin and micafungin); the concentration of the antifungal microwell plates were twice the final concentration tested with the inoculum added. Freshly cultured *Candida* species (*C. auris*, *C. parapsilosis* (ATCC 22019), and *I. orientalis* (ATCC 6258)) at 24 h of incubation at 35 °C were used as inoculum. Inoculum of 100 μL consisting of $2\text{–}5 \times 10^3$ cells were used to inoculate the

antifungal microwell plates. After inoculation, the microwell plates were incubated at 35 °C and evaluated after 24 h and 48 h to determine the MICs.

Disk diffusion assays (DDAs) were carried out as per CLSI M44-A2 guidelines [47] against fluconazole (25 μg), itraconazole (50 μg), posaconazole (5 μg), voriconazole (1 μg), amphotericin B (20 μg), and caspofungin (5 μg). MHA medium with 2% dextrose (Sigma Aldrich, Oakville, ON, Canada, #50-99-7) and 0.5 μg/mL methylene blue dye (Sigma Aldrich, Oakville, ON, Canada, #03978) was used to perform the disk diffusion assays. After 24 h of growth, 5–10 colonies were picked and liquid suspensions of *C. auris* were made by reconstituting colonies in 2 mL of normal saline (Sigma Aldrich, Oakville, ON, Canada, #S8776). The optical density (OD) was measured using a Varioskan LUX microplate reader (Thermo Fisher Scientific, Mississauga, ON, Canada, #N16044) at 530 nm, and adjusted to an OD of 0.09–0.13, which corresponded to $1–5 \times 10^6$ cells/mL. The adjusted solution was utilized to swab on the Muller–Hinton agar (MHA) using sterile cotton swabs (Fisher Scientific, Saint-Laurent, Quebec, Canada, #22-029-683). An antifungal disk was placed on each plate after inoculating and drying the agar plates. The plates were then incubated for 24 to 48 h at 35 °C. All experiments were performed in triplicate.

2.4. Photography and Image Preprocessing

Photographs of each disk diffusion plate were taken after 24 h and 48 h at the maximum possible resolution (6000 by 4000 pixels with an aspect ratio of 3:2) using a Canon EOS Rebel SL3 camera with a Canon EF-S 35 mm f/2.8 Macro IS STM macro lens. The camera settings were as follows: ISO 800, white balance, picture type "neutral", time 1/100 s, center focused against a plain black background from a fixed distance. The photos were taken and then the size of each photograph was standardized by cropping the edges and bringing all images to the same resolution.

2.5. Quantifying Tolerance via Supra-MIC Growth and Fraction of Growth

Tolerant subpopulations grow slowly in drug concentrations above MIC [21]. We used established methods to quantify tolerance, namely, supra-MIC growth from microbroth dilution assays and the fraction of growth (FoG) in the zone of inhibition (ZOI) from disk diffusion assays (Section 2.3).

The MIC for each isolate was determined using CLSI supplement M60 guidelines [48]. The MIC readings were recorded at 24 h and 48 h post inoculation. Tentative breakpoints provided by the Centers for Disease Control and Prevention for *C. auris* were considered to differentiate them as susceptible or resistant [49]. *I. orientalis* and *C. parapsilosis* were used as reference strains to ensure that the antifungal MIC range in each experiment was within CLSI guidelines.

Supra-MIC growth (*SMG*) was determined by subjecting the antifungal microwell plates used for measuring MICs to spectrophotometric reading at 630 nm after 24 h and 48 h of incubation at 35 °C. *SMG* was calculated as an average growth per well above MIC-normalized to total growth without antifungals [28]:

$$SMG = \frac{average\ growth\ per\ well\ above\ MIC}{growth\ without\ antifungal} \tag{1}$$

The software program diskImageR [29] analyses photographs of disk diffusions assays. diskImageR utilizes the image processing program ImageJ [50] and the programming language *R* [51]. We used diskImageR to measure the tolerance and resistance of *C. auris* isolates to fungistatic and fungicidal drugs from photographs of the disk diffusion assay plates (Section 2.4; Figures S1 and S2). All disk diffusion experiments were repeated in triplicate using antifungal disks placed in the center of MHA plates incubated at 35 °C for 24 and 48 h (Figure S3). After the photographs were imported by diskImageR into ImageJ, the size of each photograph was standardized and the "find particles" macro was used to find the center of the antimicrobial diffusion disk. The radius of the ZOI (RAD) and the FoG in the ZOI were measured where 20%, 50%, and 80% of growth was inhibited (RAD_{20},

RAD$_{50}$, and RAD$_{80}$, and FoG$_{20}$, FoG$_{50}$, and FoG$_{80}$, respectively). The RAD measures the degree of susceptibility/resistance, and FoG measures the degree of tolerance. The RAD for all disk diffusions assay plates were also measured manually (using a ruler), and the FoGs were also analyzed using ImageJ [52]. ImageJ analysis for estimating pixel intensity to obtain FoG was carried out by importing photographs to ImageJ software and setting "on" the measurements such as "mean grey value", minimum and maximum grey "area", and fixing the "area" for ZOI. The "measure" macro was then used to measure the pixel intensity. For photographs of 48 h DDA plates, the same parameters were restored to their 24 h counterparts, and the pixel intensity was measured within ZOI. When there are colonies at border of the ZOI (e.g., Figure S3B), diskImageR considers it as the area outside of the ZOI, and the measured RAD is smaller than the manually measured RAD; consequently, the FoG$_{20}$ measured by diskImageR is also inaccurate. Therefore, in these cases, the RAD was obtained by manually measuring the RAD and by measuring the FoG using ImageJ (Figure S4) [50]. When isolates were highly tolerant, resulting in many colonies in the ZOI (Figure S5B) or complete confluence in the ZOI (Figure S5D) after 48 h, diskImageR reported RAD and FoG as "NA" (Not Applicable).

2.6. Experiments to Determine Effectiveness Adjuvant-Antifungal Treatment

The synergies among antifungals (fluconazole, itraconazole, posaconazole, voriconazole, amphotericin B, and caspofungin) and adjuvant (chloroquine) against *C. auris*, *C. parapsilosis*, and *I. orientalis* were evaluated using DDAs (Section 2.3) and broth microdilution methods with minor modifications. For DDAs, a syringe-filtered chloroquine diphosphate salt (Sigma-Aldrich, #C6628) solution was added to MHA media after autoclaving to a final concentration of 1031.8 µg/mL. After inoculation of *C. auris* and the control strains, the MHA plates containing chloroquine were incubated in the dark as chloroquine light sensitive. These plates were read and photographed at 24 h and 48 h. *C. auris* isolates and control strains were lawn cultured (i.e., the entire surface of the agar plate was covered by swabs dipped in the liquid culture) on the MHA plates containing chloroquine with and without antifungal disks, to respectively determine the effect of antifungal chloroquine and chloroquine alone on *C. auris*. Whereas for the broth microdilution method, the concentration for different antifungal drugs were as mentioned in Section 2.3 and the chloroquine concentration ranged from 8 to 512 µg/mL. Synergistic activity of chloroquine with different antifungals was tested using the checkerboard method as previously described [37]. Both antifungal drugs (50 µL) and chloroquine (50 µL) were dispensed to sterile 96 well U bottom microtiter plates and prepared inoculum (100 µL) as per Section 2.3 was inoculated. Plates were then incubated at 35 °C. MIC and SMG results were read at 24 h and 48 h.

3. Results

3.1. Identification of Resistance in C. auris from Broth Microdilution Assays

To determine if the *C. auris* isolates were resistant to the antifungal drugs used in our study, we performed antifungal susceptibility testing at 24 and 48 h using the broth microdilution method (Section 2.3). The MICs for the *C. auris* isolates indicated that three isolates were susceptible to the fungicidal and fungistatic drug tested, whereas *C. auris* isolate 2 was not susceptible to fluconazole, and *C. auris* isolate 5 was not susceptible to fluconazole, voriconazole, caspofungin, and amphotericin B (Figure 1 and Table S2). The quality control strains *C. parapsilosis* and *I. orientalis* were within the recommended ranges. No change in MIC was observed at 24 and 48 h except for *C. auris* isolates 1 and 2 against amphotericin B.
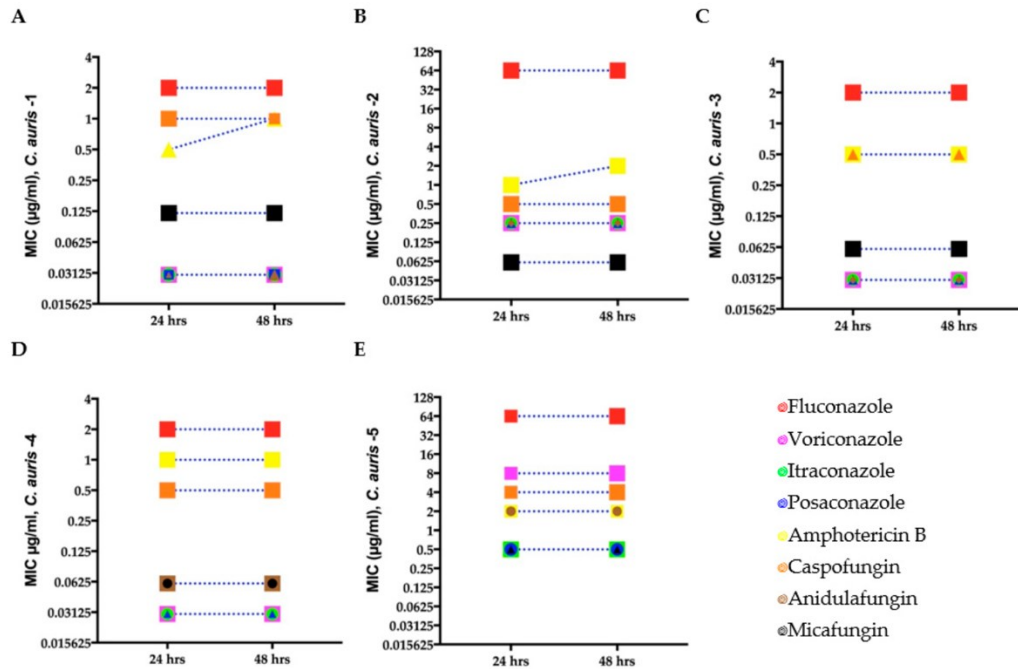
Figure 1. Minimum inhibitory concentration (MIC) for clinical *C. auris* isolates (**A**–**E**) growing in antifungal microwell plates to determine susceptibility/resistance to antifungal drugs. Mean MICs of five clinical *C. auris* isolates measured after 24 and 48 h for four fungistatic drugs (fluconazole, itraconazole, posaconazole, and voriconazole) and two fungicidal drugs (amphotericin B and caspofungin). Different symbols denote *C. auris* isolates with the same MIC.

3.2. Identification of Resistance in C. auris from Disk Diffusion Assays

To confirm the resistance of the *C. auris* isolates determined by the broth microdilution assays (Section 3.1), we performed the corresponding disk diffusion assays. In agreement with the microbroth dilution method, resistance was noted in *C. auris* isolate 2 for fluconazole and *C. auris* isolate 5 for fluconazole and voriconazole (RAD = 0 mm in all three instances; Figure 2B,E). However, *C. auris* isolate 5 exhibited a ZOI to amphotericin B (RAD = 7 mm) and caspofungin (RAD = 6 mm) at 24 h (Figure 2E). As expected, and in agreement with previous work [28], there was an inverse correlation between RAD and MIC (Pearson test, $r = -0.58$, $p = 0.007$).
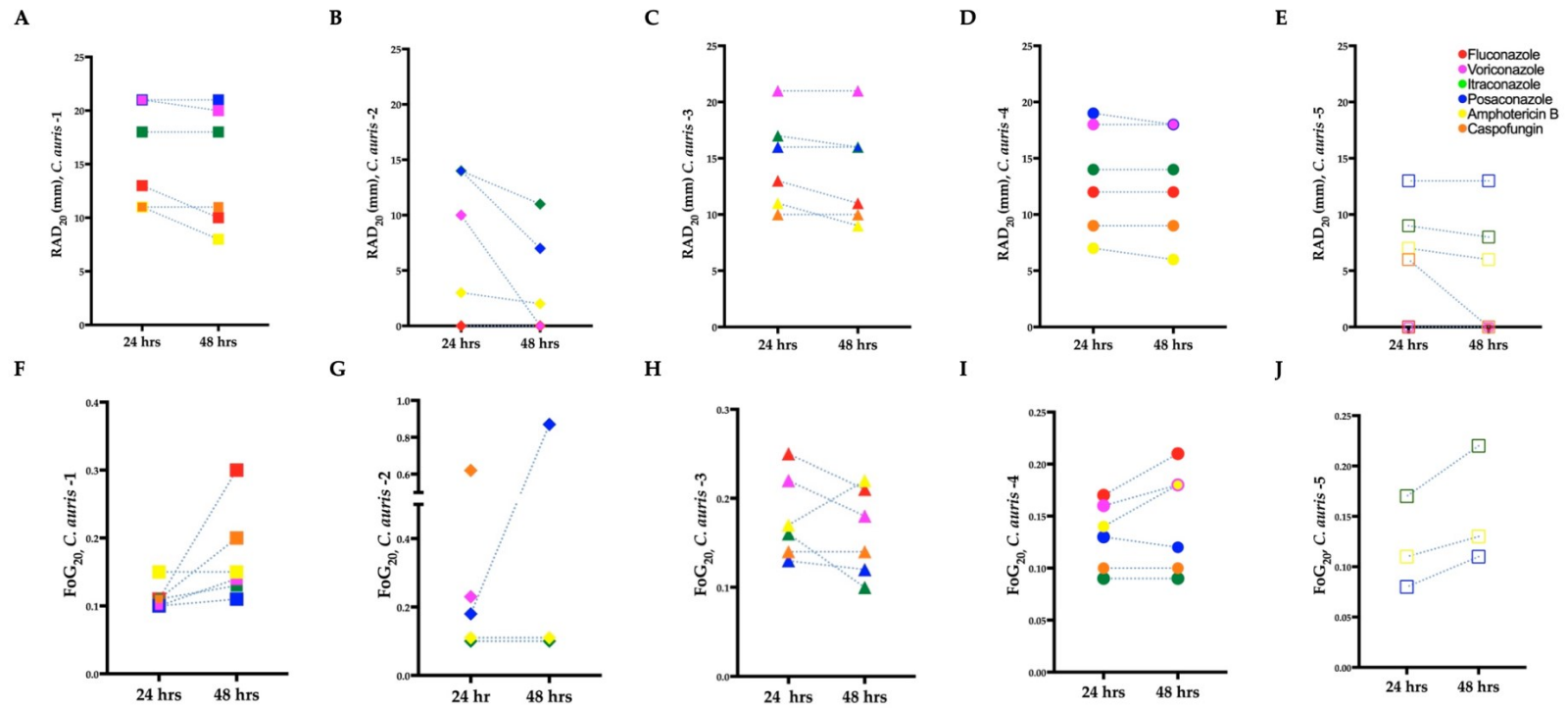
Figure 2. Radius of the zone of inhibition (RAD) (**A–E**) and fraction of growth in the zone of inhibition (FoG$_{20}$) (**F–J**) for *C. auris* isolates treated with antifungal drugs. Mean RAD where 20% of growth is inhibited (RAD$_{20}$) at 24 and 48 h. (**B**) Mean FoG where 20% of growth is inhibited (FoG$_{20}$) 24 and 48 h. *C. auris* isolate 2 treated with caspofungin at 48 h is not plotted in (**B**), as it exhibited FoG in the entire ZOI (i.e., a "NA" data point was generated by diskImageR [29]); the reduction in RAD and FoG$_{20}$ for *C. auris* isolate 3 in (**C**) and (**H**), respectively, is due to the exclusion of FoG$_{20}$ within the ZOI by diskImageR (see Section 2.5 for details). *C. auris* isolate 5 exhibited resistances to fluconazole and caspofungin.

3.3. Identification of Tolerance in C. auris from Broth Microdilution Assays

To determine if tolerant subpopulations existed within the non-resistant *C. auris* isolates, we carried out an SMG analysis (Section 2.5). A statistically significant increase in SMG was observed after 48 h for *C. auris* isolate 1 to fluconazole and itraconazole (Independent *t*-test, $p = 0.009$ and $p = 0.001$, respectively), *C. auris* isolates 2 and 4 to voriconazole (Independent *t*-test, $p = 0.0009$ and $p = 0.0014$, respectively), and *C. auris* isolate 2 to caspofungin (Independent *t*-test, $p = 0.006$), indicating the presence of tolerance (Figure 3B,D). There was also a non-significant increase in SMG at 48 h for *C. auris* isolates 3 and 4 to fluconazole, *C. auris* isolates 2, 3, and 5 to itraconazole, *C. auris* isolates 1, 2, 3, 4, and 5 to posaconazole, *C. auris* isolates 1, 3, and 5 to voriconazole, and *C. auris* isolate 1 and 5 to amphotericin B. No tolerance was observed for *C. auris* isolate 4 to itraconazole and caspofungin, and *C. auris* isolates 2, 3, and 4 to amphotericin B (Figure 3F–I). There was a decrease in SMG for *C. auris* isolate 1 against amphotericin B. This occurred because the growth of isolates in wells without antifungals increased over 48 h, which in turn reduced the SMG (as described in Equation (1)).

Figure 3. Tolerance from supra-MIC growth (SMG) for clinical *C. auris* isolates grown in antifungal microwell plates. (**A–E**) Mean SMG of tolerant isolates after 24 and 48 h. (**F–I**) Mean SMG of non-tolerant isolates after 24 and 48 h. *C. auris* 5 was resistant to fluconazole and caspofungin hence tolerance/non-tolerance could not be determined for these isolate–antifungal combinations.

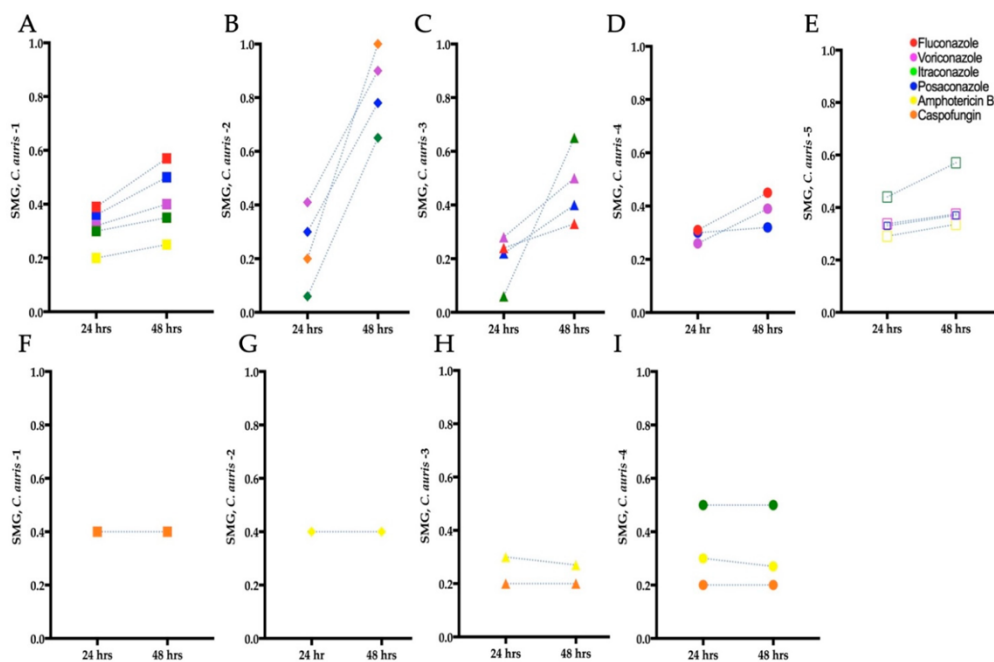### 3.4. Identification of Tolerance in C. auris from Disk Diffusion Assays

To confirm the tolerance of the *C. auris* isolates determined by the broth microdilution assays (Section 3.3), we performed the corresponding DDAs. All the *C. auris* isolates with higher SMG exhibited higher FoG_{20} at 48 h (Figure 2F–J). The FoG_{20} within the ZOI ranged between 0.08 and 0.62 and 0.09 and 0.87 at 24 and 48 h, respectively (Figure 2). *C. auris* isolate 2 exhibited the highest FoG_{20} against caspofungin at 24 h (0.62) and against posaconazole at 48 h (0.87). Similarly, at 24 h the highest pixel intensity occurred for *C. auris*

isolate 3 against posaconazole (195, Figure 4A) and the highest SMG occurred for *C. auris* isolate 2 against caspofungin (1.0, Figure 4A). At 48 h, the highest pixel intensity and SMG were measured for *C. auris* isolate 2 against voriconazole (197 and 0.90, respectively; Figure 4B).
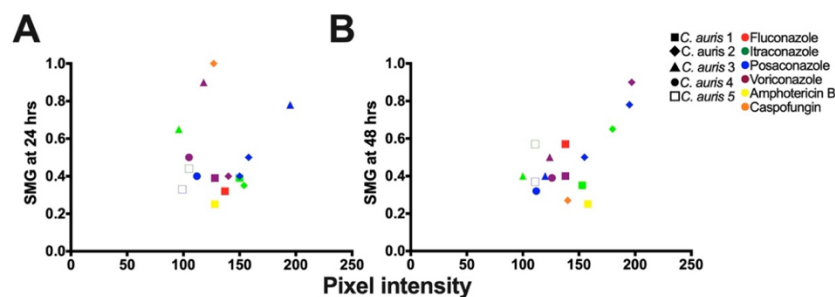
Figure 4. Correlation analysis for mean supra-MIC growth (SMG) and mean pixel intensity measured by ImageJ [51] to determine tolerance. (**A**) Analysis performed after 24 h of growth ($R^2 = 0.3128$; Pearson correlation test, $p = 0.0469$). (**B**) Analysis performed after 48 h of growth ($R^2 = 0.2862$; Pearson correlation test, $p = 0.0085$).

There was no correlation between FoG_{20} and RAD levels (Pearson test, $r = -0.25$, $p = 0.28$), as expected based on previous work which established that the FoG_{20} and RAD measure different drug responses [28,29]. The was significant correlation between SMG measured by diskImageR and pixel intensity measured by *ImageJ* (Figure 4), which occurred as both SMG and pixel intensity increase when tolerant subpopulations are present.

Overall, there was no significant difference between diskImageR and manual readings of the RAD (Independent *t*-test, $p = 0.5634$ and $p = 0.8453$ for readings at 24 h and 48 h, respectively; Figure S4). There was also no significant difference for FoG_{20} readings using diskImageR and ImageJ at 24 h (Unpaired *t*-test, $p = 0.35$). However, there was a statistically significant difference for FoG_{20} reading using diskImageR and ImageJ at 48 h (Unpaired *t*-test, $p = 0.022$). The difference in these FoG_{20} readings resulted from the fact that diskImageR was unable to distinguish the border of the ZOI among tolerant isolates, which was obscured by tolerant colonies at 48 h.

Among reference strains, only *C. parapsilosis* exhibited tolerance to fluconazole and voriconazole (Figure S6). The FoG_{20} and SMG for fluconazole and voriconazole is presented in Table S3. No tolerance was observed for the other antifungal drugs considered in this study against *C. parapsilosis*. *I. orientalis* did not exhibit tolerance to any of the antifungal agents tested.

3.5. Tolerance in C. auris Is a Reversable Phenomenon

Next, we investigated if the antifungal tolerance that we discovered in *C. auris* was a reversible phenomenon. To investigate this, we sub-cultured colonies growing inside and outside of the ZOI and repeated the microbroth dilution and disk diffusion experiments (Figure S7). There was no difference between the MICs of original colonies and colonies from inside and outside ZOI at both 24 and 48 h (Table S4). RAD, FoG_{20}, and SMG, obtained from *C. auris* colonies isolated from inside and outside the ZOI, also did not show any statistically significant differences. These results indicate that the antifungal-tolerant colonies in our experiments could reversibly generate antifungal-susceptible colonies.

3.6. Elimination of Tolerance and Resistance in C. auris via Adjuvant-Antifungal Treatment

To eliminate the tolerance observed in our clinical *C. auris* isolates (Sections 3.3 and 3.4), a previously known adjuvant chloroquine [37] was combined with the antifungal drugs

fluconazole, itraconazole, posaconazole, voriconazole, amphotericin B, and caspofungin. Chloroquine-antifungal disk diffusion assays and broth microdilution assays were performed on all five clinical *C. auris* isolates, as well as on the *C. parapsilosis* and *I. orientalis* reference strains (Table S1). Chloroquine alone did not have any antifungal effect on either *C. auris* isolates or the reference strains (Figure S9).

Tolerance and resistance were reduced or eliminated in some of our clinical *C. auris* isolates by combing chloroquine with antifungal drugs. *C. auris* isolate 1 showed an increase in RAD for fluconazole, posaconazole, amphotericin B, and caspofungin in presence of chloroquine compared to the RAD measured with these antifungal drugs alone at 48 h (Figure 5A–J). Similar results were found for: *C. auris* isolate 2 for posaconazole, voriconazole, amphotericin B, and caspofungin; *C. auris* 3 for fluconazole, posaconazole, voriconazole, amphotericin B, and caspofungin; *C. auris* isolate 4 for itraconazaole and amphotericin B; and *C. auris* isolate 5 for itraconazole and caspofungin (elimination of resistance for caspofungin), which all displayed an increase in RAD when these antifungal drugs were combined with chloroquine. Correspondingly, the FoG_{20} was reduced in presence of chloroquine for *C. auris* isolate 1 when combined with posaconazole, amphotericin B, and caspofungin (Figure 5K–T). However, no effect was observed when chloroquine was combined with fluconazole, itraconazole, or voriconazole. Similar adjuvant antifungal FoG_{20} results were obtained for *C. auris* isolate 2 against posaconazole, voriconazole, amphotericin B, and caspofungin; *C. auris* isolate 3 against fluconazole, itraconazole, posaconazole, voriconazole, amphotericin B, and caspofungin; *C. auris* isolate 4 against amphotericin B; and *C. auris* isolate 5 against itraconazole and caspofungin. No effect of chloroquine was observed for *C. auris* isolate 4 against fluconazole and posaconazole, nor for *C. auris* isolate 5 against amphotericin B. The FoG_{20} for *C. auris* isolate 2 for voriconazole and caspofungin and *C. auris* isolate 5 for caspofungin could not be measured at 48 h without chloroquine as there was no ZOI. However, we were able to measure the ZOI in some of these isolates in the presence of chloroquine, indicating an adjuvant effect of chloroquine on tolerance as well as on resistance. The reference strain *I. orientalis* (resistant to fluconazole) exhibited a ZOI against fluconazole when supplemented with chloroquine (Table S5; Figure S8). However, *C. parapsilosis* was not significantly affected by the presence of chloroquine (Table S5; Figure S8).

Similar effects on antifungal tolerance were obtained in adjuvant antifungal broth microdilution assays (Figure 6). Tolerance decreased for all chloroquine–antifungal drug combinations in the following isolates: *C. auris* isolate 1 (except for itraconazole), *C. auris* isolate 2 (except for voriconazole and itraconazole), *C. auris* isolate 3, *C. auris* isolate 4 (except for fluconazole), and *C. auris* isolate 5 (except for posaconazole and amphotericin B) all exhibited reduced SMG with chloroquine–antifungal drug at 48 h compared to SMG at 24 h with chloroquine–antifungal drug. As *C. auris* isolate 2 was resistant to fluconazole, SMG was not calculated. However, chloroquine did not show any effect on *C. auris* isolate-2 against itraconazole and voriconazole at 48 h compared to 24 h which is in concordance with disk diffusion assay. Whereas the SMG for *C. auris* isolate 5 was reduced against itraconazole. However, SMG could not be calculated to fluconazole and caspofungin, due to the growth at highest concentration. Similar to the disk diffusion assays, chloroquine did not show any effect on *C. auris* isolate 1 against itraconazole, *C. auris* isolate 2 against voriconazole and itraconazole, *C. auris* isolate 4 against fluconazole, and *C. auris* isolate-5 against posaconazole and amphotericin B. The MICs of all the *C. auris* isolates and control strains remained unchanged in presence of chloroquine.
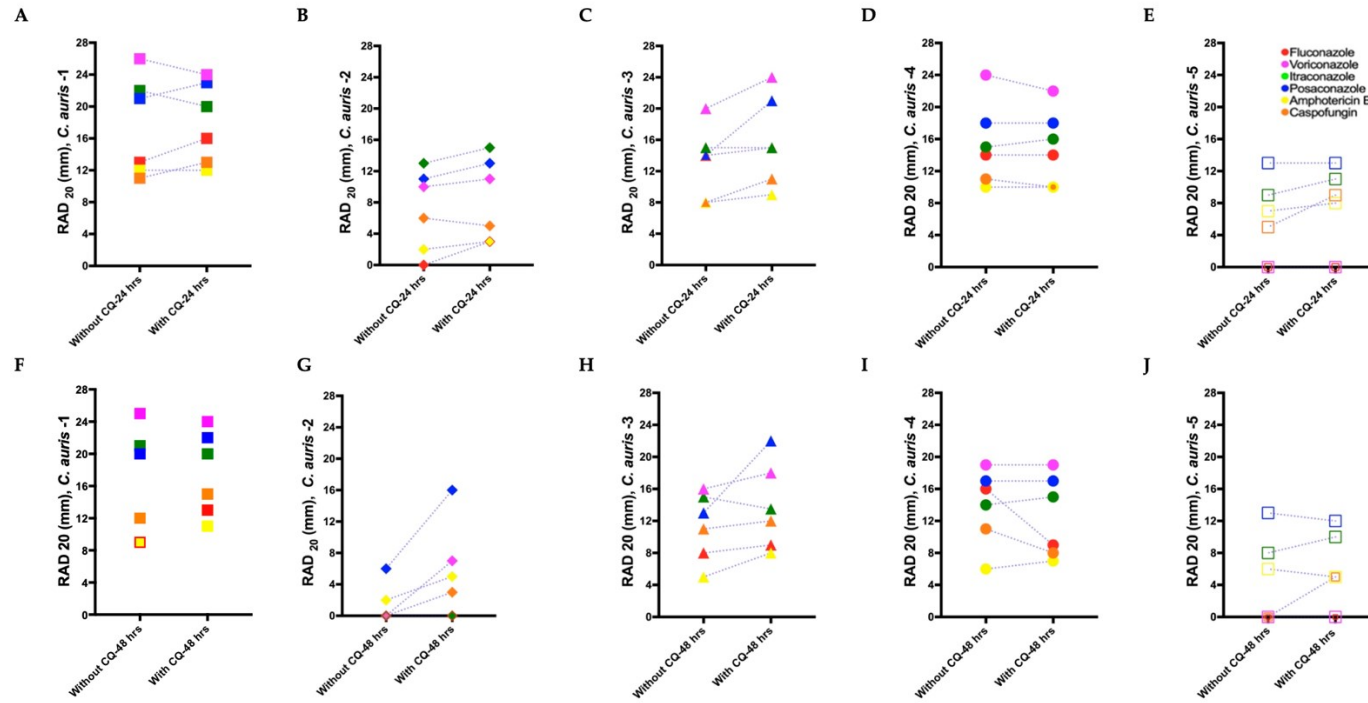
Figure 5. *Cont.*
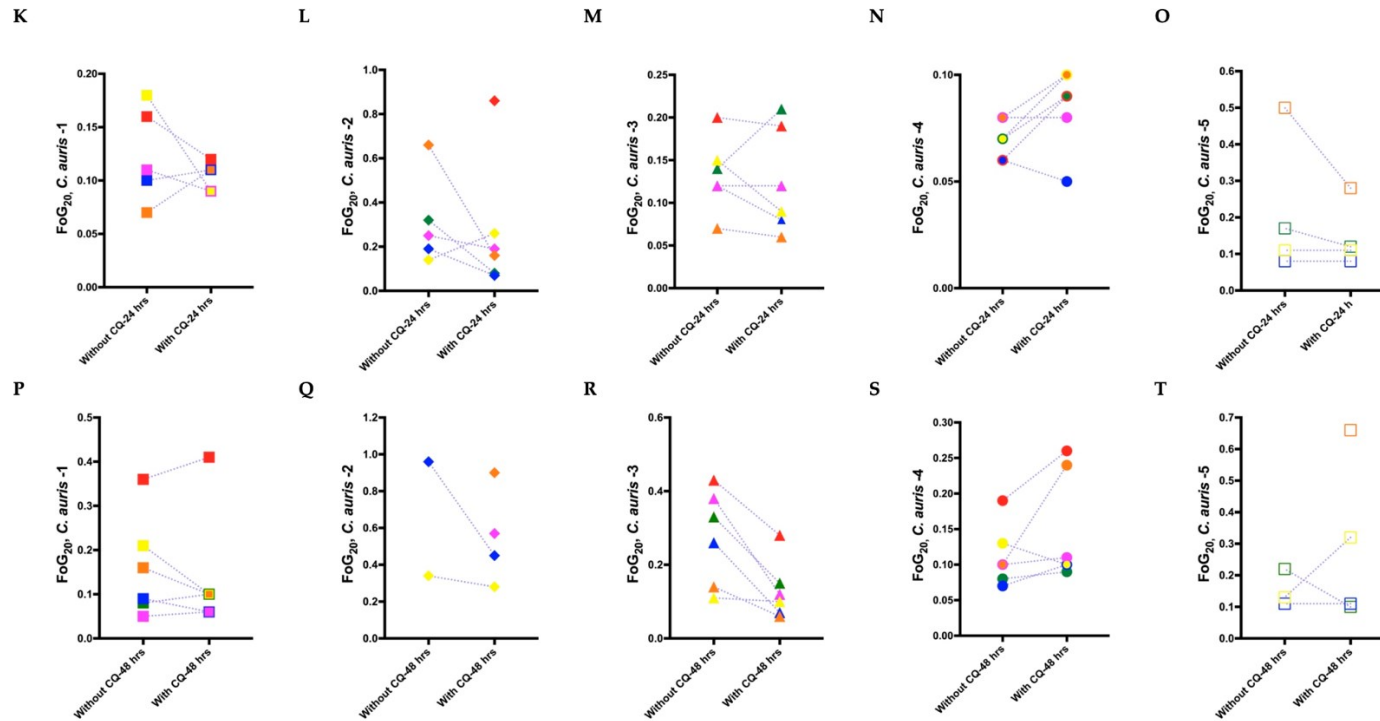
Figure 5. Radius of the zone of inhibition (RAD) and fraction of growth in the zone of inhibition (FoG$_{20}$) measurements for *C. auris* isolates for adjuvant antifungal disk diffusion assays. (**A–E**) Mean RAD measured for the *C. auris* isolates at 24 h against antifungal drugs with and without the adjuvant chloroquine. (**F–J**) Mean RAD measured for the *C. auris* isolate at 48 h against antifungal drugs with and without chloroquine. (**K–O**) Mean FoG$_{20}$ measured using diskImageR [29] for all *C. auris* isolates at 24 h against antifungal drugs with and without chloroquine. (**P–T**) Mean FoG$_{20}$ measured using diskImageR for the *C. auris* isolates at 48 h against antifungal drugs with and without chloroquine. Note that the single data points in (**L**), (**Q**), and (**T**) at 48 h are due to the mitigation of resistance in presence of chloroquine, as FoG$_{20}$ could not be measured for these isolates at 24 h because of their resistance to the corresponding antifungal drugs.
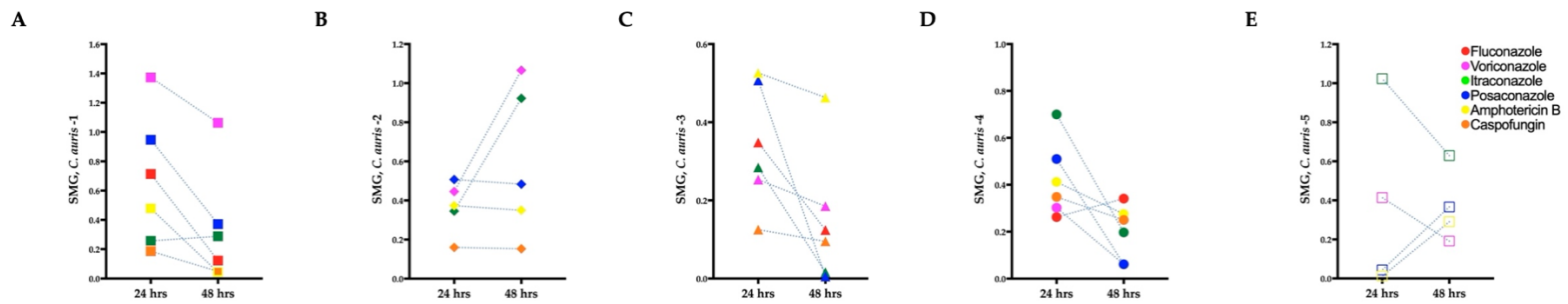
Figure 6. Supra-MIC growth (SMG) of *C. auris* isolates 1 to 5 (**A–E**) for adjuvant antifungal broth microdilution assays. Chloroquine did not show any adjuvant effect on C. auris isolate 1 when combined with itraconazole, nor for *C. auris* isolate 2 when combined with itraconazole or voriconazole at 48 h compared to 24 h. Similarly, no adjuvant effect was noted for *C. auris* isolate 4 against fluconazole nor for *C. auris* isolate 5 against posaconazole and amphotericin B. Since *C. auris* isolate 2 is resistant to fluconazole and *C. auris* isolate 5 is resistant to fluconazole and caspofungin, the SMGs were not calculated for these isolate–adjuvant–antifungal combinations.

4. Discussion

We report for the first time that some clinical *C. auris* isolates are tolerant to fungistatic drugs (fluconazole, voriconazole, itraconazole, and posaconazole) and to fungicidal drugs (amphotericin B and caspofungin). We also found azole tolerance in *C. parapsilosis* (fluconazole and voriconazole), but not in *I. orientalis* which was intrinsically resistant to fluconazole. We were able to detect tolerance after 24 h, as well as after 48 h by FoG_{20}, of antifungal treatment using diskImageR [29] and ImageJ [52]. These findings suggest that a distinct subpopulation among *C. auris* was able to survive and grow slowly in the presence of different antifungal drugs. Since *C. auris* is a multidrug-resistant pathogen, the presence of tolerance further narrows treatment options. Previous reports suggest that tolerant subpopulations among infecting *Candida* species are strongly associated with mortality among candidemia patients [53]. Therefore, clinical diagnostic laboratories should also test for antifungal tolerance along with standard antifungal susceptibility/resistance tests to increase the efficacy of antifungal treatment. Furthermore, existing tolerance quantification methods could be adapted to detect tolerance after 24 h and 48 h to broaden the scope of standard antimicrobial susceptibility testing in medical diagnostic laboratories. The fluconazole tolerance that we observed in *C. auris* was in agreement with previous studies on *C. albicans* [28] and *C. auris* [23], as well as with related clinical studies on "trailing growth" (reduced but persistent visible growth of *Candida* species in fluconazole concentrations above MIC [32,54,55]).

The tolerance to fungistatic and fungicidal drugs observed in some of the clinical *C. auris* isolates in our study appears to be a reversible phenomenon, as previously described for clinical *C. albicans* isolates [56]. The tolerant cells growing inside the ZOI upon subculture are indistinguishable from the parental population, suggesting the presence of phenotypic heterogeneity instead of genetic variation. *C. auris* isolates cultured from inside and outside the ZOI did not show any significant changes in the average RAD, MIC, or SMG levels. This reversible tolerance that we observed in *C. auris* may result from stochastic phenotype switching or an induced response activated by the presence of antifungal drugs inside of the cell. The general mechanism underlying tolerance in *C. auris* remains to be elucidated in future work, to be aided, for instance, by mathematical modeling and synthetic biology [57], tracking single cell growth and gene expression trajectories in microfluidic devices [58,59], as well as genetic sequence and aneuploidy analyses [60].

The tolerance in some of our *C. auris* isolates was reduced or eliminated in vitro by combining azole, polyene, and echinocandin antifungal drugs with the antimalarial drug chloroquine. Chloroquine reduced tolerance for some *C. auris* isolate–antifungal combinations, while chloroquine did not have an adjuvant effect for other combinations. The mechanism underlying this strain-dependent phenomenon remains to be elucidated. Combining chloroquine with antifungal drugs had a partial effect on resistance in some of the *C. auris* isolates investigated in this study. Specifically, *C. auris* isolate 5, which was resistant to caspofungin and voriconazole (RAD = 0 mm), had a small increase in the ZOI (RAD < 12 mm) in presence of chloroquine. Correspondingly, *C. auris* isolate 2 had no ZOI for caspofungin, but had a small ZOI (RAD = 6 mm) in presence of chloroquine. The RADs for these cases were smaller than those for the sensitive *C. auris* isolates in our experiments. Chloroquine did not affect the MICs of the *C. auris* isolates in our study. Chloroquine also affected fluconazole resistance in *I. orientalis* (Table S5), though tolerant subpopulations in *C. parapsilosis* were unaffected by chloroquine. Altogether, these results suggest that combining chloroquine with antifungal drugs may have a partial mitigation effect on resistance in *C. auris*. Though the mechanism of action is unknown, it is likely related to iron depletion caused by chloroquine and its downregulation of the *ERG11* gene [35,41]. Iron depletion is known to decrease membrane sterols and increase membrane fluidity, leading to increased uptake of antifungal drugs into the cell [61]. The downregulation of *ERG11* gene, which synthesizes lanosterol alpha demethylase enzyme, is also known to be an important rate-limiting enzyme for the synthesis of ergosterol [62].

Due to the limited number of *C. auris* isolates that we were able to acquire, the results presented in this study serve as a proof of concept that *C. auris* is tolerant to fungistatic and fungicidal drugs, and that this antifungal tolerance can be mitigated by using chloroquine as an adjuvant. Further in vitro validation of these results in additional *C. auris* isolates, as well as subsequent investigations using in vivo model systems, will be pursued in future research. Another limitation of our study is that we did not have access to patient details and antifungal treatment history due to privacy regulations.

Overall, this study advances our understanding of antifungal treatment failure in *C. auris* and identifies opportunities for the clinical detection of antifungal tolerance as well as the development of targeted adjuvant antifungal therapies against tolerant and resistant invasive candidiasis.

Supplementary Materials: The following supporting information can be downloaded at: https://www.mdpi.com/article/10.3390/biomedicines11030898/s1, Table S1: *Candida* isolates and strains; Table S2: minimum inhibitory concentrations (MICs) of *C. auris* isolates; Table S3: mean MIC, SMG, FoG$_{20}$, and RAD for reference strains *Issatchenkia orientalis* and *C. parapsilosis* measured at 24 and 48 h for different antifungal drugs. Table S4: reversibility of tolerance phenotype in *Candida auris*. Table S5: effect of chloroquine (CLQ) on reference strains *Issatchenkia orientalis* and *Candida parapsilosis*. Figure S1: quantification of antifungal tolerance in a disk diffusion assay using the image analysis program diskImageR [29]. Figure S2: detecting tolerance in *Candida auris* from disk diffusion assays (DDAs) using diskImageR. Figure S3: representative disk diffusion assays (DDA) images of fluconazole (FLU) tolerance in *Candida auris* and *Candida parapsilosis*. Figure S4: comparison between diskImageR and manual radius of the zone of inhibition (RAD) measurements. Figure S5: azole tolerance in *Candida auris*. Figure S6: azole tolerance in *Candida parapsilosis* reference strain. Figure S7: reversibility of tolerance in a representative *Candida auris* isolate 2 against voriconazole. Figure S8: disk diffusion assays (DDAs) of antifungal adjuvant treatment in *Candida auris* isolates and *Issatchenkia orientalis* and *Candida parapsilosis* reference strains. Figure S9: *Candida auris* isolates and *Candida parapsilosis* and *Issatchenkia orientalis* reference strains growing on Mueller–Hinton agar (MHA) media with chloroquine.

References

1. Perlin, D.S.; Rautemaa-Richardson, R.; Alastruey-Izquierdo, A. The Global Problem of Antifungal Resistance: Prevalence, Mechanisms, and Management. *Lancet Infect. Dis.* **2017**, *17*, e383–e392. [CrossRef] [PubMed]
2. Gow, N.A.R.; Johnson, C.; Berman, J.; Coste, A.T.; Cuomo, C.A.; Perlin, D.S.; Bicanic, T.; Harrison, T.S.; Wiederhold, N.; Bromley, M.; et al. The Importance of Antimicrobial Resistance in Medical Mycology. *Nat. Commun.* **2022**, *13*, 5352. [CrossRef] [PubMed]
3. Alangaden, G.J. Nosocomial Fungal Infections: Epidemiology, Infection Control, and Prevention. *Infect. Dis. Clin. North Am.* **2011**, *25*, 201–225. [CrossRef] [PubMed]
4. Andes, D.R.; Safdar, N.; Baddley, J.W.; Alexander, B.; Brumble, L.; Freifeld, A.; Hadley, S.; Herwaldt, L.; Kauffman, C.; Lyon, G.M.; et al. The Epidemiology and Outcomes of Invasive Candida Infections among Organ Transplant Recipients in the United States: Results of the Transplant-Associated Infection Surveillance Network (TRANSNET). *Transpl. Infect. Dis.* **2016**, *18*, 921–931. [CrossRef] [PubMed]
5. O'Neill, J. Tackling Drug-Resistant Infections Globally: Final Report and Recommendations: The Review on Antimicrobial Resistanc. 2016. Available online: https://Amr-Review.Org (accessed on 10 November 2022).
6. Woolhouse, M.; Farrar, J. Policy: An Intergovernmental Panel on Antimicrobial Resistance. *Nature* **2014**, *509*, 555–557. [CrossRef]
7. Krysan, D.J. The Unmet Clinical Need of Novel Antifungal Drugs. *Virulence* **2017**, *8*, 135–137. [CrossRef]
8. Wall, G.; Lopez-Ribot, J.L. Current Antimycotics, New Prospects, and Future Approaches to Antifungal Therapy. *Antibiotics* **2020**, *9*, 445. [CrossRef]
9. McCarty, T.P.; Pappas, P.G. Antifungal Pipeline. *Front. Cell. Infect. Microbiol.* **2021**, *11*, 1–11. [CrossRef]
10. Nnadi, N.E.; Carter, D.A. Climate Change and the Emergence of Fungal Pathogens. *PLoS Pathog.* **2021**, *17*, e1009503. [CrossRef]
11. Turner, S.A.; Butler, G. The Candida Pathogenic Species Complex. *Cold Spring Harb. Perspect. Med.* **2014**, *4*, a019778. [CrossRef]
12. Cendejas-Bueno, E.; Kolecka, A.; Alastruey-Izquierdo, A.; Theelen, B.; Groenewald, M.; Kostrzewa, M.; Cuenca-Estrella, M.; Gómez-López, A.; Boekhout, T. Reclassification of the Candida Haemulonii Complex as Candida Haemulonii (C. Haemulonii Group I), C. Duobushaemulonii Sp. Nov. (C. Haemulonii Group II), and C. Haemulonii Var. Vulnera Var. Nov.: Three Multiresistant Human Pathogenic Yeasts. *J. Clin. Microbiol.* **2012**, *50*, 3641–3651. [CrossRef] [PubMed]
13. Forsberg, K.; Woodworth, K.; Walters, M.; Berkow, E.L.; Jackson, B.; Chiller, T.; Vallabhaneni, S. Candida Auris: The Recent Emergence of a Multidrug-Resistant Fungal Pathogen. *Med. Mycol.* **2019**, *57*, 1–12. [CrossRef] [PubMed]
14. Chow, N.A.; Gade, L.; Tsay, S.V.; Forsberg, K.; Greenko, J.A.; Southwick, K.L.; Barrett, P.M.; Kerins, J.L.; Lockhart, S.R.; Chiller, T.M.; et al. Multiple Introductions and Subsequent Transmission of Multidrug-Resistant Candida Auris in the {USA}: A Molecular Epidemiological Survey. *Lancet Infect. Dis.* **2018**, *18*, 1377–1384. [CrossRef]
15. Centers for Disease Control and Prevention Tracking Candida Auris: Candida Auris Fungal Diseases CDC. Available online: https://www.cdc.gov/fungal/candida-auris/tracking-c-auris.html (accessed on 1 April 2021).
16. Arendrup, M.C.; Patterson, T.F. Multidrug-Resistant Candida: Epidemiology, Molecular Mechanisms, and Treatment. *J. Infect. Dis.* **2017**, *216*, S445–S451. [CrossRef] [PubMed]
17. Rhodes, J.; Fisher, M.C. Global Epidemiology of Emerging Candida Auris. *Curr. Opin. Microbiol.* **2019**, *52*, 84–89. [CrossRef] [PubMed]
18. Magiorakos, A.-P.; Srinivasan, A.; Carey, R.B.; Carmeli, Y.; Falagas, M.E.; Giske, C.G.; Harbarth, S.; Hindler, J.F.; Kahlmeter, G.; Olsson-Liljequist, B.; et al. Multidrug-Resistant, Extensively Drug-Resistant and Pandrug-Resistant Bacteria: An International Expert Proposal for Interim Standard Definitions for Acquired Resistance. *Clin. Microbiol. Infect.* **2012**, *18*, 268–281. [CrossRef]
19. Lyman, M.; Forsberg, K.; Reuben, J.; Dang, T.; Free, R.; Seagle, E.E.; Sexton, D.J.; Soda, E.; Jones, H.; Hawkins, D.; et al. Notes from the Field: Transmission of Pan-Resistant and Echinocandin-Resistant Candida Auris in Health Care Facilities — Texas and the District of Columbia, January–April 2021. *MMWR. Morb. Mortal. Wkly. Rep.* **2021**, *70*, 1022–1023. [CrossRef] [PubMed]
20. Chen, J.; Tian, S.; Han, X.; Chu, Y.; Wang, Q.; Zhou, B.; Shang, H. Is the Superbug Fungus Really so Scary? A Systematic Review and Meta-Analysis of Global Epidemiology and Mortality of Candida Auris. *BMC Infect. Dis.* **2020**, *20*, 827. [CrossRef]
21. Berman, J.; Krysan, D.J. Drug Resistance and Tolerance in Fungi. *Nat. Rev. Microbiol.* **2020**, *18*, 319–331. [CrossRef]
22. Kukurudz, R.J.; Chapel, M.; Wonitowy, Q.; Adamu Bukari, A.-R.; Sidney, B.; Sierhuis, R.; Gerstein, A.C. Acquisition of Cross-Azole Tolerance and Aneuploidy in Candida Albicans Strains Evolved to Posaconazole. *G3 Genes|Genomes|Genetics* **2022**, *12*, jkac156. [CrossRef]
23. Kim, S.H.; Iyer, K.R.; Pardeshi, L.; Muñoz, J.F.; Robbins, N.; Cuomo, C.A.; Wong, K.H.; Cowen, L.E. Genetic Analysis of Candida Auris Implicates Hsp90 in Morphogenesis and Azole Tolerance and Cdr1 in Azole Resistance. *MBio* **2019**, *10*, e02529-18. [CrossRef]
24. Healey, K.R.; Kordalewska, M.; Ortigosa, C.J.; Singh, A.; Berrío, I.; Chowdhary, A.; Perlin, D.S. Limited ERG11 Mutations Identified in Isolates of Candida Auris Directly Contribute to Reduced Azole Susceptibility. *Antimicrob. Agents Chemother.* **2018**, *62*, e01427-18. [CrossRef]
25. Mount, H.O.; Revie, N.M.; Todd, R.T.; Anstett, K.; Collins, C.; Costanzo, M.; Boone, C.; Robbins, N.; Selmecki, A.; Cowen, L.E. Global Analysis of Genetic Circuitry and Adaptive Mechanisms Enabling Resistance to the Azole Antifungal Drugs. *PLoS Genet.* **2018**, *14*, e1007319. [CrossRef]
26. Coenye, T.; De Vos, M.; Vandenbosch, D.; Nelis, H. Factors Influencing the Trailing Endpoint Observed in Candida Albicans Susceptibility Testing Using the CLSI Procedure. *Clin. Microbiol. Infect.* **2008**, *14*, 495–497. [CrossRef] [PubMed]

27. Arendrup, M.C.; Cuenca-Estrella, M.; Lass-Flörl, C.; Hope, W.; Arendrup, M.C.; Hope, W.W.; Flörl, C.; Cuenca-Estrella, M.; Arikan, S.; Barchiesi, F.; et al. EUCAST Technical Note on the EUCAST Definitive Document EDef 7.2: Method for the Determination of Broth Dilution Minimum Inhibitory Concentrations of Antifungal Agents for Yeasts EDef 7.2 (EUCAST-AFST). *Clin. Microbiol. Infect.* **2012**, *18*, E246–E247. [CrossRef]

28. Rosenberg, A.; Ene, I.V.; Bibi, M.; Zakin, S.; Segal, E.S.; Ziv, N.; Dahan, A.M.; Colombo, A.L.; Bennett, R.J.; Berman, J. Antifungal Tolerance Is a Subpopulation Effect Distinct from Resistance and Is Associated with Persistent Candidemia. *Nat. Commun.* **2018**, *9*, 2470. [CrossRef]

29. Gerstein, A.C.; Rosenberg, A.; Hecht, I.; Berman, J. DiskimageR: Quantification of Resistance and Tolerance to Antimicrobial Drugs Using Disk Diffusion Assays. *Microbiology* **2016**, *162*, 1059–1068. [CrossRef] [PubMed]

30. Lepak, A.J.; Andes, D.R. Antifungal Pharmacokinetics and Pharmacodynamics. *Cold Spring Harb. Perspect. Med.* **2014**, *5*, a019653. [CrossRef] [PubMed]

31. Bhattacharya, S.; Holowka, T.; Orner, E.P.; Fries, B.C. Gene Duplication Associated with Increased Fluconazole Tolerance in Candida Auris Cells of Advanced Generational Age. *Sci. Rep.* **2019**, *9*, 5052. [CrossRef]

32. Astvad, K.M.T.; Sanglard, D.; Delarze, E.; Hare, R.K.; Arendrup, M.C. Implications of the EUCAST Trailing Phenomenon in Candida Tropicalis for the In Vivo Susceptibility in Invertebrate and Murine Models. *Antimicrob. Agents Chemother.* **2018**, *62*, e01624-18. [CrossRef]

33. Colombo, A.L.; Guimarães, T.; Sukienik, T.; Pasqualotto, A.C.; Andreotti, R.; Queiroz-Telles, F.; Nouér, S.A.; Nucci, M. Prognostic Factors and Historical Trends in the Epidemiology of Candidemia in Critically Ill Patients: An Analysis of Five Multicenter Studies Sequentially Conducted over a 9-Year Period. *Intensive Care Med.* **2014**, *40*, 1489–1498. [CrossRef] [PubMed]

34. Islahudin, F.; Khozoie, C.; Bates, S.; Ting, K.-N.; Pleass, R.J.; Avery, S. V Cell Wall Perturbation Sensitizes Fungi to the Antimalarial Drug Chloroquine. *Antimicrob. Agents Chemother.* **2013**, *57*, 3889–3896. [CrossRef]

35. Levitz, S.M.; Harrison, T.S.; Tabuni, A.; Liu, X. Chloroquine Induces Human Mononuclear Phagocytes to Inhibit and Kill Cryptococcus Neoformans by a Mechanism Independent of Iron Deprivation. *J. Clin. Investig.* **1997**, *100*, 1640–1646. [CrossRef] [PubMed]

36. Newman, S.L.; Gootee, L.; Brunner, G.; Deepe, G.S. Chloroquine Induces Human Macrophage Killing of Histoplasma Capsulatum by Limiting the Availability of Intracellular Iron and Is Therapeutic in a Murine Model of Histoplasmosis. *J. Clin. Investig.* **1994**, *93*, 1422–1429. [CrossRef] [PubMed]

37. Li, Y.; Wan, Z.; Liu, W.; Li, R. Synergistic Activity of Chloroquine with Fluconazole against Fluconazole-Resistant Isolates of Candida Species. *Antimicrob. Agents Chemother.* **2015**, *59*, 1365–1369. [CrossRef]

38. Bjelle, A.; Björnham, A.; Larsen, A.; Mjörndal, T. Chloroquine in Long-Term Treatment of Rheumatoid Arthritis. *Clin. Rheumatol.* **1983**, *2*, 393–399. [CrossRef]

39. Powell, S.J. Therapy of Amebiasis. *Bull. N. Y. Acad. Med.* **1971**, *47*, 469–477.

40. Dima, A.; Jurcut, C.; Chasset, F.; Felten, R.; Arnaud, L. Hydroxychloroquine in Systemic Lupus Erythematosus: Overview of Current Knowledge. *Ther. Adv. Musculoskelet. Dis.* **2022**, *14*, 1759720X211073001. [CrossRef]

41. Lan, C.-Y.; Rodarte, G.; Murillo, L.A.; Jones, T.; Davis, R.W.; Dungan, J.; Newport, G.; Agabian, N. Regulatory Networks Affected by Iron Availability in Candida Albicans. *Mol. Microbiol.* **2004**, *53*, 1451–1469. [CrossRef]

42. Singhal, N.; Kumar, M.; Kanaujia, P.K.; Virdi, J.S. MALDI-TOF Mass Spectrometry: An Emerging Technology for Microbial Identification and Diagnosis. *Front. Microbiol.* **2015**, *6*, 791. [CrossRef]

43. Dingle, T.C.; Butler-Wu, S.M. Maldi-Tof Mass Spectrometry for Microorganism Identification. *Clin. Lab. Med.* **2013**, *33*, 589–609. [CrossRef]

44. Turenne, C.Y.; Sanche, S.E.; Hoban, D.J.; Karlowsky, J.A.; Kabani, A.M. Rapid Identification of Fungi by Using the ITS2 Genetic Region and an Automated Fluorescent Capillary Electrophoresis System. *J. Clin. Microbiol.* **1999**, *37*, 1846–1851. [CrossRef] [PubMed]

45. National Library of Medicine. Available online: https://blast.ncbi.nlm.nih.gov/Blast.cgi?PROGRAM=blastn&BLAST_SPEC=GeoBlast&PAGE_TYPE=BlastSearch (accessed on 12 October 2022).

46. CLSI. *Reference Method for Broth Dilution Antifungal Susceptibility Testing of Yeasts*; Clinical and Laboratory Standards Institute: Wayne, PA, USA, 2017.

47. CLSI. *Method for Antifungal Disk Diffusion Susceptibility Testing of Yeasts: Approved Guideline—Second Edition*, 2nd ed.; Clinical and Laboratory Standards Institute: Wayne, PA, USA, 2008; ISBN 1562385321.

48. CLSI. *Performance Standards for Antifungal Susceptibility Testing of Yeasts*, 1st ed.; CLS.; Clinical and Laboratory Standards Institute: Wayne, PA, USA, 2017.

49. CDC 2019 Antifungal Susceptibility Testing and Interpretation | Candida Auris | Fungal Diseases | CDC. Available online: https://www.cdc.gov/fungal/candida-auris/c-auris-antifungal.html (accessed on 24 December 2019).

50. ImageJ. Available online: https://imagej.nih.gov/ij/ (accessed on 28 July 2022).

51. R Core Team. *R: A Language and Environment for Statistical Computing*; R Foundation for Statistical Computing: Vienna, Austria, 2018.

52. Abràmoff, M.D.; Magalhães, P.J.; Ram, S.J. Image Processing with ImageJ. *Biophotonics Int.* **2004**, *11*, 36–41. [CrossRef]

53. Levinson, T.; Dahan, A.; Novikov, A.; Paran, Y.; Berman, J.; Ben-Ami, R. Impact of Tolerance to Fluconazole on Treatment Response in Candida Albicans Bloodstream Infection. *Mycoses* **2021**, *64*, 78–85. [CrossRef] [PubMed]

54. Marcos-Zambrano, L.J.; Escribano, P.; Bouza, E.; Guinea, J. Susceptibility of Candida Albicans Biofilms to Caspofungin and Anidulafungin Is Not Affected by Metabolic Activity or Biomass Production. *Med. Mycol.* **2016**, *54*, 155–161. [CrossRef]
55. Delarze, E.; Sanglard, D. Defining the Frontiers between Antifungal Resistance, Tolerance and the Concept of Persistence. *Drug Resist. Updat.* **2015**, *23*, 12–19. [CrossRef]
56. Farquhar, K.S.; Rasouli Koohi, S.; Charlebois, D.A. Does Transcriptional Heterogeneity Facilitate the Development of Genetic Drug Resistance? *BioEssays* **2021**, *43*, 2100043. [CrossRef]
57. Farquhar, K.S.; Flohr, H.; Charlebois, D.A. Advancing Antimicrobial Resistance Research Through Quantitative Modeling and Synthetic Biology. *Front. Bioeng. Biotechnol.* **2020**, *8*, 583415. [CrossRef]
58. Jo, M.C.; Liu, W.; Gu, L.; Dang, W.; Qin, L. High-Throughput Analysis of Yeast Replicative Aging Using a Microfluidic System. *Proc. Natl. Acad. Sci. USA* **2015**, *112*, 9364–9369. [CrossRef]
59. Charlebois, D.A.; Hauser, K.; Marshall, S.; Balázsi, G. Multiscale Effects of Heating and Cooling on Genes and Gene Networks. *Proc. Natl. Acad. Sci. USA* **2018**, *115*, E10797–E10806. [CrossRef]
60. Yang, F.; Lu, H.; Wu, H.; Fang, T.; Berman, J.; Jiang, Y. Aneuploidy Underlies Tolerance and Cross-Tolerance to Drugs in Candida Parapsilosis. *Microbiol. Spectr.* **2021**, *9*, e00508-21. [CrossRef] [PubMed]
61. Prasad, T.; Chandra, A.; Mukhopadhyay, C.K.; Prasad, R. Unexpected Link between Iron and Drug Resistance of Candida Spp.: Iron Depletion Enhances Membrane Fluidity and Drug Diffusion, Leading to Drug-Susceptible Cells. *Antimicrob. Agents Chemother.* **2006**, *50*, 3597–3606. [CrossRef] [PubMed]
62. Ostrowsky, B.; Greenko, J.; Adams, E.; Quinn, M.; O'Brien, B.; Chaturvedi, V.; Berkow, E.; Vallabhaneni, S.; Forsberg, K.; Chaturvedi, S.; et al. Candida Auris Isolates Resistant to Three Classes of Antifungal Medications—New York, 2019. *MMWR Morb. Mortal. Wkly. Rep.* **2020**, *69*, 6–9. [CrossRef] [PubMed]

Chapter 3

3 Diffusion

3.1 Objectives

The objective of this chapter is to investigate the diffusion of antifungal agents within agar media, specifically focusing on the observations made during the antifungal tolerance experiments on C. auris in Chapter 2. Specifically, when conducting the disk diffusion assays, it was observed that within the inhibition zone, colonies exhibiting tolerance to the antifungal agent have a higher intensity in the region near the outer boundary of the inhibition zone. This prompted further inquiry into the underlying factors contributing to this spatial distribution of tolerant colonies. We hypothesized that within the 48 hours, the drug concentration is lower compared to the central region around disc, and that tolerance may be a drug concentration dependent phenomenon governed by diffusion in the agar medium (Figure 5).
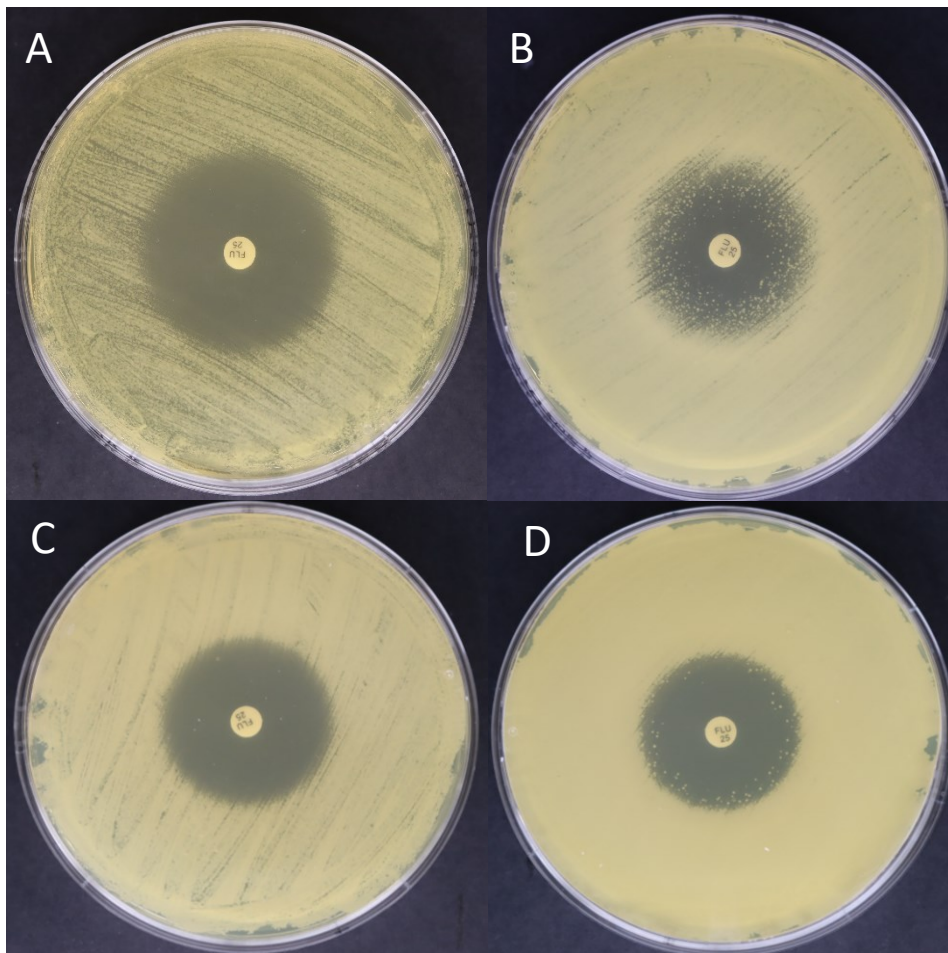
Figure 5. The DDA results. In some cases, it showed a higher intensity of tolerant colonies in the region near the outer boundary of the inhibition zone. (A) C.auris isolate 1 after 24 hours, (B) C.auris isolate 1 after 48 hours, (C) C.parapsilosis after 24 hours, (A) C.parapsilosis after 48 hours.

While there is no direct precedent for the specific research I am undertaking, I found two studies that explored related aspects. The first employed a diffusion approximation method to calculate MIC based on the Assay DDA [118]. The second utilized a finite element computational model based on Fick's second law of diffusion in a two-temperature agar diffusion bioassay to quantify nisin concentration [143].

3.2   Method

3.2.1   Diffusion Coefficient Estimation

The diffusion coefficient was calculated using the Stokes-Einstein equation [equation (4), chapter 1] which takes into account the physicochemical properties of the antifungals such as temperature and viscosity and radius which were calculated using molecular weight, density and viscosity. Information regarding these properties can be obtained from the PubChem database [145]. If the antifungal drug shape is a sphere, the radius will be calculated by [equation (17) chapter 1]. Furthermore, viscosity measurements were conducted using an Anton Paar viscometer. For measuring viscosity of the agar media, a shear rate of 1000 s^{-1} was applied, and it measures 10 times every minute at 35°C. The Python code is available in Code S1.

3.2.2   Modeling Antifungals Diffusion in the Disk Diffusion Method: Finite Difference Approximation Method

To model the diffusion of antifungal in the agar using the finite difference method, we can discretize the agar plate into a grid of points and approximate the diffusion equation [equation (10) chapter 1] using finite differences [132–134,136,138].

To solve this equation (15) in chapter 1, we can initialize a two-dimensional array to represent the concentration of antibiotic at each grid point and set the initial concentration at the center of the grid to the concentration of the antibiotic in the disk. We then iterate over

each time step, and for each time step, we can iterate over each grid point, using the values of the neighboring grid points at the previous time step to update the concentration at the current grid point [131,132,134,136,137].

The Python code to solve the finite difference equation for a circular disk of antifungal in the center of a square grid is available in Code S2 and S3.

3.2.3   Geometry and Initial conditions

In this study, a controlled experimental setup was assumed to examine the diffusion behavior of caspofungin, an antifungal agent. A well with a diameter of 35 mm was centrally positioned on an 85 mm diameter agar plate, and it was filled with a predetermined concentration of 1 microgram per ml of caspofungin. To investigate the diffusion process, a grid-based analysis was employed, with grid sizes of 0.1 mm in both the x and y directions. The initial condition was established such that at time t = 0, the concentration inside the well was equivalent to the initial concentration, while the concentration at all other locations on the plate was set to zero. Notably, a no-flux boundary condition was imposed on all plate boundaries, ensuring that there is no net flux of caspofungin across the plate boundaries. This boundary condition can be mathematically expressed [143] as shown in equation (5): enabling a quantitative representation of the diffusion process within the experimental system.

$$-n(-D\nabla c) = 0 \tag{7}$$

The diffusion of the antifungal can be affected by many factors, such as the size of the disk, the concentration of the antifungal in the disk and the diffusion coefficient of the antifungal in the medium. These factors were optimized to ensure that the assay is sensitive and specific, and that the results are reproducible.

The diffusion coefficient of the drug in the agar medium is dependent on the physical properties of the drug and the medium, such as the size and shape of the drug molecule, the viscosity of the medium, and the temperature [125,126,128,143]. The diffusion coefficient

can be measured experimentally or calculated theoretically. The diffusion of a drug within the agar medium during the disk diffusion assay gives rise to a concentration gradient surrounding the disk. This gradient is influenced by the drug's concentration within the disk, its diffusion coefficient, and the distance from the disc. Numerical methods, such as finite difference or finite element methods [131,137], can be employed to calculate the drug concentration at any spatial location and time within the medium (see Chapter 1, 1.11.5). Understanding the physics of diffusion in this assay is crucial for elucidating drug diffusion mechanisms and determining factors that impact the size of the inhibition zone surrounding the disk. By optimizing assay conditions based on diffusion, it becomes possible to enhance the sensitivity, specificity, and reproducibility of the assay results [130]. In our experiment, we established the presence of a central well on the agar plate (we assumed a square with 85 mm length), which the well was identical in size to the antifungal disc used in our previous experiment detailed in Chapter 2. The antifungal drug we employed for this study was caspofungin, and we maintained the same concentration as in the previous experiment, which was 5 μg/ml. The plate has square mesh size of 0.1 mm.

3.3   Drug Diffusion Simulation Results

The simulation aimed to explore the diffusion behavior of the drug over a 48-hour period and investigate the relationship between drug concentration and the radius of inhibition.

Figure 5 illustrates the diffusion pattern of the drug within the agar plate over time. The diffusion constant was calculated as 9.942×10^{-12} m^2/s (Appendix S16). The viscosity which was measured for this experiment was 0.03 ± 0.003 Pa.s and the density of water was consider of the drug solvent. The simulation results confirmed our initial assumption that within the first 48 hours, the concentration at the center of the plate was consistently higher compared to the concentration at the border of inhibition (Figure 6). This finding supports the hypothesis that the higher concentration at the center contributes to the inhibition of microbial growth in that region. The simulation was repeated by different diffusion constants (Figure S10-15) to show that the difference in diffusion constant has no effect on this conclusion.

To quantitatively analyze the diffusion process, we plotted the radius of inhibition against the drug concentration over time, as shown in Figure 7. The plot demonstrates that as the drug concentration increases, the radius of inhibition expands, indicating a greater area of microbial growth inhibition. This correlation confirms the effectiveness of the disk diffusion method in evaluating the susceptibility of microorganisms to antifungal drugs.

While our simulation provides valuable insights into the diffusion behavior of the drug within the 2D environment and supports the hypothesis regarding the distribution of colonies in the border area, several factors must be considered. First, the 2D nature of our simulation does not account for the full 3D diffusion characteristics of the drug diffusion in experimental method. Furthermore, the drug release mechanism of the antifungal disc in a time-dependent manner, a key variable in reality, remains undefined in our model. These complexities, in combination with the lack of depth considerations in the agar medium, introduce uncertainty when directly comparing our simulation results to experimental data.

Overall, my drug diffusion simulations model the diffusion dynamics of antifungal in the disc diffusion method. It also highlights the importance of considering experimental conditions and limitations when interpreting simulation results and emphasizes the need for further experimental validation to enhance the predictive capabilities of such simulations.
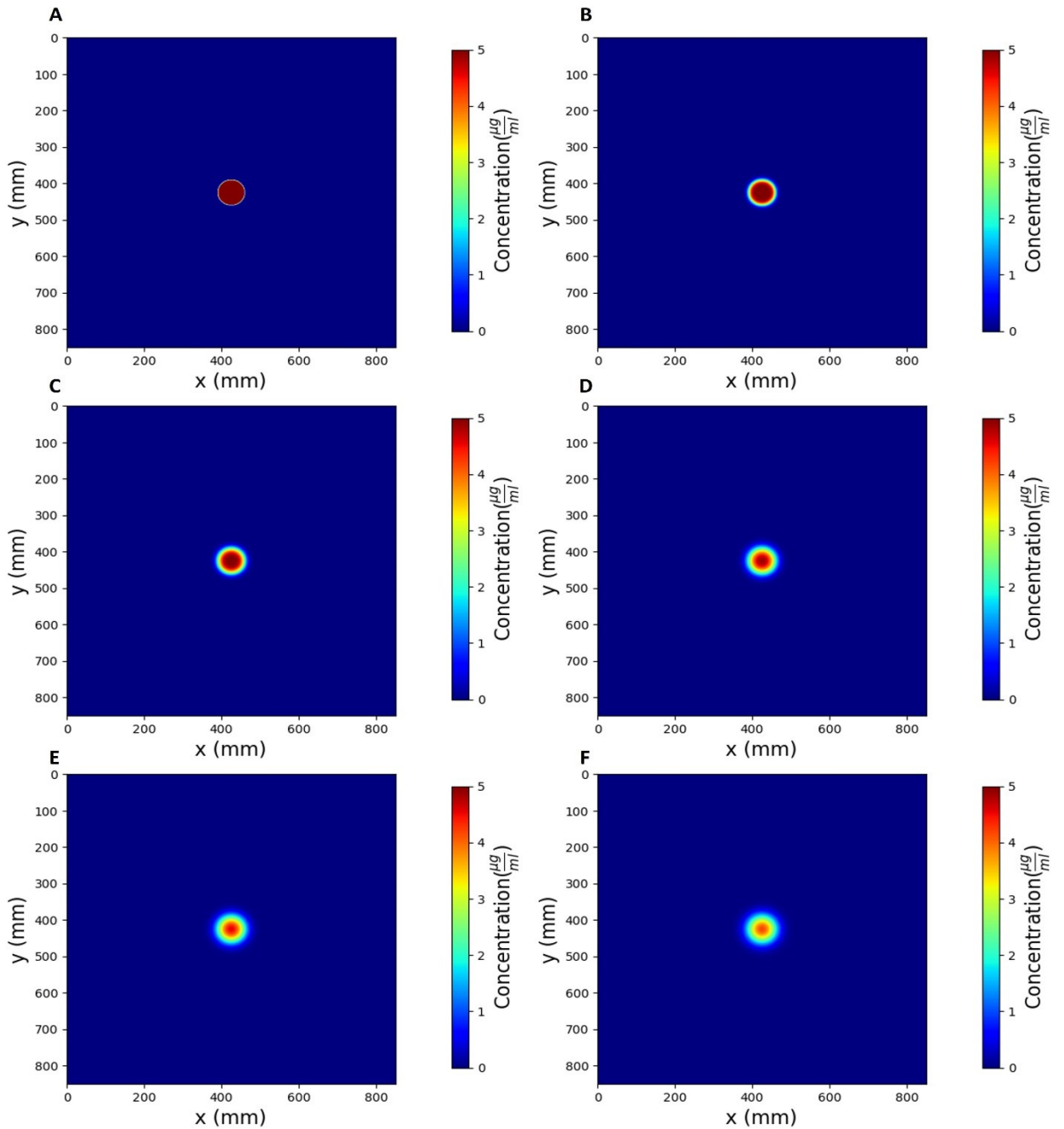
Figure 6. Temporal and spatial evolution of caspofungin diffusion in disk diffusion assay (D =9.94 × 10⁻¹² m²/s). Diffusion of 5 µg/ml caspofungin (same concentration used in experimental test) in disk diffusion assay in x and y direction (mm) at (A)1 h, (B) 6 h, (C)12 h, (D) 24 h, (E) 36 h and (F) 48h with diffusion constant equal to 9.94 × 10⁻¹² m²/s. Red color shows the highest concentration and dark blue shows the lowest concentration. During diffusion always the concentration of caspofungin in high at the center and lower at the outer edge of the inhibition zone.

50
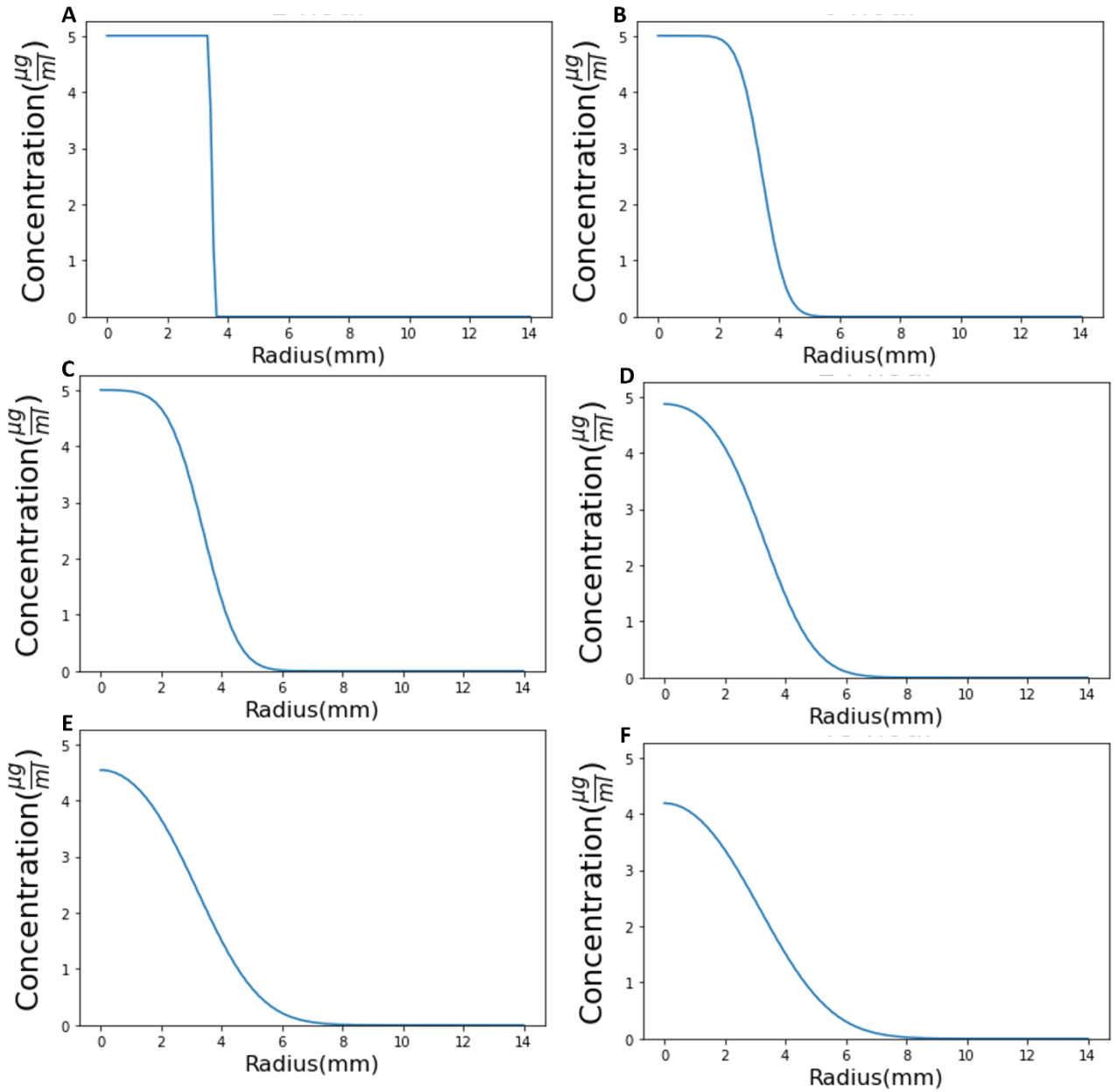
Figure 7. Temporal Variation of Caspofungin Concentration in the Zone of Inhibition (D = 9.94 × 10⁻¹² m²/s). The concentration gradient (µg/ml) of caspofungin in zone of inhibition (mm) at (A) 1h, (B) 6 h, (C) 12 h, (D) 24 h, (E) 36 h and (F) 48 h with diffusion constant equal to 9.947 × 10⁻¹² m²/s. The initial concentration of caspofungin was assumed to be 5 µg/ml (same concentration used in experimental test).

Chapter 4

4   Conclusion

This thesis addresses the significant challenges posed by *Candida auris*. This pathogen causes invasive infections, is resistant to crucial antifungal drugs, and contributes to healthcare-related outbreaks [36,37,45,51]. The broader issue of antimicrobial resistance affects human and veterinary medicine and has substantial socioeconomic implications. Antifungal tolerance further complicates the treatment landscape. Investigating the causes of recurrent infections and treatment failures becomes paramount.

Chapter 2 of my thesis focuses on identifying and eliminating antifungal tolerance in clinical *Candida auris* isolates. The innovative *diskImageR* tool [117,118] played a pivotal role, facilitating the measurement of the fraction of growth (FoG) inside the zone of inhibition (ZoI) and the calculation of Supra-MIC Growth (SMG) at both 24 and 48 hours. However, a significant challenge appeared during our analysis. In certain cases, before the 48-hour, when the ZoI was fully covered with colonies, *diskImageR* faced limitations in measuring FoG accurately. To overcome this limitation, I have reverted to use *ImageJ* software [120] to manually measure FoG, ensuring precise data collection. Our findings revealed that these colonies inside the ZoI exhibited slow growth patterns, often becoming evident within the 24 to 48-hour window. Traditional diagnostic laboratory practices entail examining agar plates within 24 hours [146], potentially overlooking the presence of tolerant subpopulations during this critical timeframe. This oversight could contribute to recurrent infections and treatment failures, highlighting the pressing need for their timely detection. Investigating the nature of tolerance as either a genetic or non-genetic trait, I conducted sub-culturing experiments on colonies within and outside the Zone of Inhibition (ZOI). Subsequently, I repeated DDA, MIC, and SMG tests. Surprisingly, the isolates from both areas showed no alterations in terms of RAD, MIC, or SMG. These results suggest that tolerance in *C. auris* may be attributed to a non-genetic mechanism. However, further verification through genetic sequencing in future research is required to confirm this hypothesis. It is essential to acknowledge several limitations that warrant consideration in

the interpretation of our findings. Firstly, it is important to note that our study serves as a preliminary proof-of-concept investigation, carried out with a relatively small sample size of just five isolates. This sample size restriction may impact the generalizability of our results and underscores the need for broader studies in the future. Secondly, a lack of comprehensive patient treatment history data is another limitation. Understanding the prior treatments administered to these patients could have provided valuable context for the observed outcomes. Lastly, it's vital to emphasize that our research was conducted in vitro, within a controlled laboratory environment. As such, we cannot directly extrapolate our findings to in vivo conditions, where additional variables and complexities may come into play, including the potential presence or absence of tolerance. Therefore, while our study offers valuable insights, further research, encompassing larger sample sizes, comprehensive patient histories, and in vivo studies, is imperative to gain a more complete understanding of the implications of our findings in real-world clinical scenarios.

Chapter 3 of my research thesis explore the intricate world of drug diffusion through simulation. This chapter aims to explore the dynamics of antifungal agents within agar media, with a particular focus on the intriguing observations made during the disk diffusion assay. Specifically, I observed that colonies demonstrating tolerance to antifungal agents exhibited heightened intensity in the region near the outer boundary of the inhibition zone. This observation spurred our hypothesis that, within the 48-hour window, drug concentration might be relatively lower in the border area compared to the central region, suggesting that tolerance could be a drug concentration-dependent phenomenon influenced by diffusion within the agar medium that this finding is in agreement with Rosenberg et al. research finding [147].

I, calculated the diffusion coefficient, a critical parameter for our simulations, using the Stokes-Einstein equation, which considers the diffusive properties of the antifungal drugs. Viscosity measurements, conducted using an Anton Paar viscometer, played a pivotal role in my calculations. My modeling approach utilized the finite difference approximation method in Python to simulate antifungal drug diffusion over a 48-hour period and investigate the correlation between drug concentration and the radius of inhibition. My simulation results confirmed that within the first 48 hours, the concentration near the plate's

center consistently exceeds that at the border of inhibition, supporting our proposition that heightened drug concentration at the center contributes to microbial growth inhibition in that region. Nonetheless, it is vital to acknowledge certain limitations within our simulation approach. Notably, our model is two-dimensional and does not account for the three-dimensional diffusion of the drug within the agar medium. These considerations may introduce variances between simulated outcomes and experimental observations. However, I expect these errors to be minimal as our *C. auris* isolates grew on the surface of the agar medium, which was the same surface on to which I constrained my drug diffusion simulations.

In conclusion, my thesis research provides valuable insights into the intricate issues of antifungal tolerance and drug diffusion dynamics. It highlights the need to consider experimental conditions and limitations when interpreting simulation results and highlights the importance of adapting and optimizing tools like *diskImageR* for more accurate measurements. my research not only contributes to a deeper understanding of these crucial aspects but also lays the groundwork for future investigations and potential breakthroughs in the study of fungal infections and antimicrobial resistance. Collaborative efforts and sustained exploration are essential as we strive to effectively combat these formidable global health challenges.

As we conclude this phase of our research, we eagerly anticipate the promising opportunities of future work that lie ahead. Building upon the valuable insights gained from our current study, we recognize several crucial areas for further exploration and investigation.

1. Mechanisms of Tolerance: One of the key directions for our future research perspective will be to delve deep into unraveling the mechanisms underlying antifungal tolerance in *Candida auris*. Our preliminary findings from chapter 2, which showcased the repeatability and reversibility of the tolerance trait across generations, have laid a strong foundation for this pursuit. Understanding the intricacies of how tolerance is conferred, we can uncover new targets for therapeutic interventions and develop innovative strategies to combat *C. auris* infections more effectively.

2. Gene Expression Analysis: Investigating gene expression profiles will be a pivotal component of our future work. A comprehensive exploration of gene expression patterns in both tolerant and susceptible subpopulations can provide invaluable insights into the regulatory pathways that govern tolerance. This analysis will shed light on the specific genes and molecular pathways that are upregulated or downregulated in the presence of antifungal drugs. Such knowledge can pave the way for the development of targeted therapies that disrupt these pathways, ultimately rendering *C. auris* more susceptible to conventional antifungal agents.

3. Exploring Pharmacokinetics for a Comprehensive Understanding: While the current study successfully identifies tolerant subpopulations in Candida auris under various antifungal treatments, an exciting avenue for future research involves exploring the pharmacokinetics of these drugs. Investigating drug absorption, distribution, metabolism, and excretion could refine interpretations of observed concentration gradients, enhancing our understanding of drug-fungus interactions. This future work is crucial for translating laboratory findings into clinically relevant interventions, optimizing treatment strategies, and bridging the gap between research and real-world healthcare scenarios. The study sets the stage for subsequent research that aims to provide a comprehensive understanding of the complex dynamics between antifungal drugs and *Candida auris*.

4. Development of New Diagnostic Techniques: The identification of tolerant subpopulations is a critical factor in preventing recurrent infections and treatment failures highlighting the need for improved diagnostic techniques. In our future research, we aim to develop innovative diagnostic methods that can detect the presence of tolerant subpopulations more accurately and rapidly. These enhanced diagnostic tools will bridge the gap between research findings and clinical practice, enabling healthcare providers to make more informed treatment decisions and tailor therapies to individual patient needs. The studies using machine learning and image processing are currently underway in our group [148] and may lead to future developments in this direction.

4. Exploration of New Antifungal Strategies: Equipped with a better comprehension understanding of tolerance mechanisms and gene expression profiles, we aim to investigate

and create new antifungal techniques. These strategies may include the development of novel antifungal compounds that directly target pathways related to tolerance, potentially making use of combination therapies that work when combined with antifungal medications already on the market, or the repurposing of current pharmaceuticals with recognized effects on tolerance. Our objective will be to increase the antifungal therapy options available and their effectiveness against *Candida auris*. We have employed chloroquine as an adjuvant component alongside antifungal treatments, and our findings demonstrate its potential impact on reducing tolerance in certain instances. This combination approach has revealed promising results in addressing and mitigating tolerance issues.

As we embark on the path of future work, our focus will remain steadfast on unraveling the mechanisms that govern tolerance, understanding gene expression patterns, and innovating in the realm of diagnostics and antifungal therapies. By forging ahead in these directions, we aim to make meaningful contributions to the field of medical mycology, ultimately improving patient outcomes and addressing the global challenge posed by *Candida auris* infections.

5 Appendices

5.1 Supplementary Tables

Table S1. *Candida* isolates and strains. *Candida auris* and *Candida* reference strains *Issatchenkia orientalis* and *Candida parapsilosis* used in our study to investigate antifungal tolerance and resistance. *Issatchenkia orientalis* is also known by the binomial names *Candida krusei* and *Pichia kudriavzevii*.

Strain/Isolate Number	Genus	Species
1	*Candida*	*auris*
2	*Candida*	*auris*
3	*Candida*	*auris*
4	*Candida*	*auris*
5	*Candida*	*auris*
6	*Issatchenkia*	*orientalis*
7	*Candida*	*parapsilosis*

Table S2. Minimum inhibitory concentrations (MICs) of C. auris isolates. Mean MICs were measured in µg/mL after 24 and 48 h for a range of fungistatic and fungicidal drugs.

Antifungal drug	Hours of incubation	*C. auris* 1	*C. auris* 2	*C. auris* 3	*C. auris* 4	*C. auris* 5
Fluconazole	24	2	64	2	2	64
	48	2	64	2	2	64
Voriconazole	24	0.03	0.25	0.03	0.03	8
	48	0.03	0.25	0.03	0.03	8
Itraconazole	24	0.03	0.25	0.03	0.03	0.5
	48	0.03	0.25	0.03	0.03	0.5
Posaconazole	24	0.03	0.25	0.03	0.03	0.5
	48	0.03	0.25	0.03	0.03	0.5

Amphotericin B	24	0.5	1	0.5	1	2
	48	1	2	0.5	1	2
Caspofungin	24	1	0.5	0.5	0.5	4
	48	1	0.5	0.5	0.5	4
Anidulafungin	24	0.03	0.25	0.03	0.06	2
	48	0.03	0.25	0.03	0.06	2
Micafungin	24	0.12	0.06	0.06	0.12	0.5
	48	0.12	0.06	0.06	0.06	0.5

Table S3. Mean MIC, SMG, FoG20, and RAD for reference strains *Issatchenkia orientalis* and *C. parapsilosis* measured at 24 and 48 h for different antifungal drugs. MIC: minimum inhibitory concentration; SMG: supra-MIC growth; FoG: fraction of growth; RAD: radius of the zone of inhibition; NA: not available.

		MIC (μg/mL)	SMG at 24 h	SMG at 48 h	FoG_{20} at 24 h	FoG_{20} at 48 h	RAD at 24 h (mm)	RAD at 48 h (mm)
I. orientalis ATCC 6258	Fluconazole	32	NA	NA	0	0	0	0
	Itraconazole	0.12	0.62	0.62	0.09	0.09	14	14
	Voriconazole	0.25	0.65	0.25	0.09	0.1	12	12
	Posaconazole	0.06	0.16	0.5	0.09	0.11	12	12
	Amphotericin B	1	0.31	0.25	0.2	0.06	6	3
	Caspofungin	0.5	0.62	0.5	0.13	0.22	11	11
C. parapsilosis ATCC 22019	Fluconazole	2	0.41	0.47	0.13	0.13	15	13
	Itraconazole	0.03	0.53	0.45	0.1	0.1	14	14
	Voriconazole	0.03	0.34	0.66	0.13	0.16	18	18
	Posaconazole	0.03	0.5	0.5	0.08	0.07	16	16
	Amphotericin B	0.5	0.24	0.24	0.17	0.17	9	8
	Caspofungin	1	0.76	0.1	0.19	0.18	7	6

Table S4. Reversibility of tolerance phenotype among tolerant *Candida auris* isolates against different antifungal agents. Mean radius of the zone of inhibition (RAD), mean fraction of growth (FoG) in the zone of inhibition (ZOI), mean minimum inhibitory concentration (MIC), and mean supra-MIC growth (SMG) values obtained for C. auris isolates sub-cultured from inside and outside

the ZOI, and treated with the azole, polyene, and echinocandin antifungal drugs. MIC, RAD, FoG20, and SMG, obtained from C. auris colonies isolated from inside and outside the ZOI, also did not show any statistically significant differences (Independent t-test, $p > 0.05$ for all values).

Drug–isolate combination	Origin of the colonies tested	MIC in µg/ml	RAD_{20} at 24 h (mm)	RAD_{20} at 48 h (mm)	FoG_{20} at 24 h	FoG_{20} at 48 h	SMG at 24 h	SMG at 48 h
Fluconazole-C. auris 1	Original	2	13	10	0.14	0.21	0.38	0.57
	Inside ZOI	2	15	7	0.13	0.22	0.54	0.66
	Outside ZOI	2	14	8	0.15	0.43	0.62	0.64
Fluconazole- C. auris 3	Original	2	14	8	0.11	0.29	0.26	0.33
	Inside ZOI	2	10	10	0.20	0.83	0.20	0.77
	Outside ZOI	2	12	9	0.21	0.71	0.50	0.78
Fluconazole-C. auris 4	Original	2	14	10	0.12	0.24	0.30	0.45
	Inside ZOI	2	16	13	0.19	0.34	0.33	0.40
	Outside ZOI	2	13	11	0.08	0.20	0.46	0.55
Itraconazole-C. auris 1	Original	0.03	17	17	0.09	0.12	0.30	0.50
	Inside ZOI	0.03	17	17	0.06	0.09	0.26	0.48
	Outside ZOI	0.03	17	17	0.09	0.09	0.29	0.50
Itraconazole-C. auris 2	Original	0.25	10	0	0.09	NA	0.06	0.65
	Inside ZOI	0.25	15	0	0.13	NA	0.05	0.60
	Outside ZOI	0.25	15	0	0.09	NA	0.06	0.80
Itraconazole-C. auris 3	Original	0.03	11	0	0.11	NA	0.22	0.40
	Inside ZOI	0.03	12	0	0.08	NA	0.32	0.45
	Outside ZOI	0.03	15	0	0.14	NA	0.40	0.59
Itraconazole-C. auris 5	Original	0.5	16	0	0.13	0.11	0.44	0.57
	Inside ZOI	0.5	8	6	0.12	0.22	0.40	0.44
	Outside ZOI	0.5	9	8	0.11	0.25	0.58	0.61
Voriconazole-C. auris 1	Original	0.03	20	20	0.07	0.10	0.32	0.40
	Inside ZOI	0.03	23	18	0.11	0.18	0.37	0.40
	Outside ZOI	0.03	20	10	0.12	0.10	0.43	0.44
Voriconazole-C. auris 2	Original	0.25	9	0	0.15	NA	0.41	0.9
	Inside ZOI	0.25	11	0	0.20	NA	0.27	1.0
	Outside ZOI	0.25	10	0	0.31	NA	0.26	1.3
Voriconazole-C. auris 3	Original	0.03	23	17	0.06	0.25	0.28	0.50
	Inside ZOI	0.03	19	14	0.10	0.36	0.28	0.51
	Outside ZOI	0.03	19	17	0.11	0.38	0.30	0.60
Voriconazole-C. auris 4	Original	0.03	21	18	0.07	0.12	0.26	0.39
	Inside ZOI	0.03	21	19	0.09	0.12	0.21	0.28
	Outside ZOI	0.03	23	23	0.08	0.09	0.32	0.35
Posaconazole-C. auris 1	Original	0.03	19	19	0.09	0.08	0.36	0.50
	Inside ZOI	0.03	19	21	0.05	0.08	0.34	0.64
	Outside ZOI	0.03	20	20	0.10	0.07	0.32	0.67
Posaconazole-C. auris 2	Original	0.25	13	7	0.07	0.80	0.30	0.78
	Inside ZOI	0.25	14	8	0.09	0.64	0.28	0.67
	Outside ZOI	0.25	14	7	0.10	0.70	0.28	0.85
Posaconazole-C. auris 3	Original	0.03	16	15	0.07	0.16	0.22	0.40
	Inside ZOI	0.03	18	15	0.07	0.26	0.24	0.70
	Outside ZOI	0.03	17	18	0.07	0.19	0.25	0.87
Posaconazole-C. auris 4	Original	0.03	13	14	0.07	0.12	0.30	0.32
	Inside ZOI	0.03	20	20	0.07	0.09	0.30	0.42
	Outside ZOI	0.03	20	21	0.1	0.08	0.25	0.36
Posaconazole-C. auris 5	Original	0.5	12	12	0.07	0.09	0.33	0.37
	Inside ZOI	0.5	12	11	0.14	0.12	0.23	0.32
	Outside ZOI	0.5	11	10	0.12	0.12	0.30	0.35
	Original	0.5	11	12	0.13	0.15	0.2	0.25

|								
Amphotericin B- *C. auris* 1	Inside ZOI	0.5	7	6	0.12	0.15	0.2	0.6
	Outside ZOI	0.5	10	7	0.11	0.2	0.2	0.53
Caspofungin- *C. auris* 2	Original	0.5	8	0	0.22	NA	0.2	1
	Inside ZOI	0.5	8	0	0.26	NA	0.30	1
	Outside ZOI	0.5	8	0	0.25	NA	0.29	1

Table S5. Effect of chloroquine (CLQ) on *Issatchenkia orientalis* and *Candida parapsilosis* reference strains. Mean FoG_{20}: fraction of growth; Mean RAD: radius of the zone of inhibition. The *p*-value was obtained by comparing RAD at 48 h with and without chloroquine.

|		Without CLQ	With CLQ	Without CLQ	With CLQ	Paired t-test
		FoG_{20} at 48 h	FoG_{20} at 48 h	RAD (mm) at 48 h	RAD (mm) at 48 h	
C. parapsilosis ATCC 22019	Fluconazole	0.14	0.08	14	9	$p = 0.195$
	Posaconazole	0.07	0.06	17	16	$p = 0.272$
I. orientalis ATCC 6258	Fluconazole	NA	0.11	0	7	$p = 0.032$

5.2   Supplementary Figures
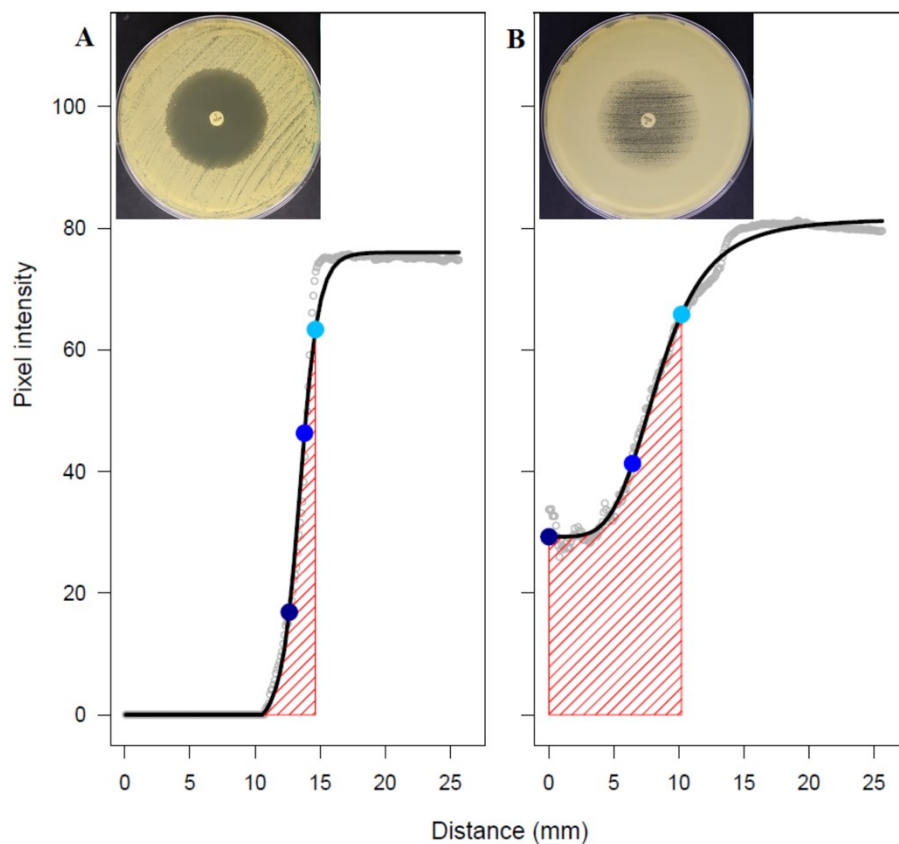
Figure S1. Quantification of antifungal tolerance in a disk diffusion assay using the image analysis program *diskImageR*. Pixel intensity corresponds to the cell density, and its average is measured for 72 radii every 5° from the center of the disk (grey dots). The radius of the zone of inhibition and fraction of growth are measured in three areas where 20%, 50%, and 80% of the growth is inhibited (light blue, blue, and dark blue circles, respectively) after (A) 24 h of incubation and (B) 48 h of incubation. The representative data in this figure was obtained from images of a disk diffusion assays for C. auris (isolate 2) exposed to posaconazole (insets of (A) and (B)).
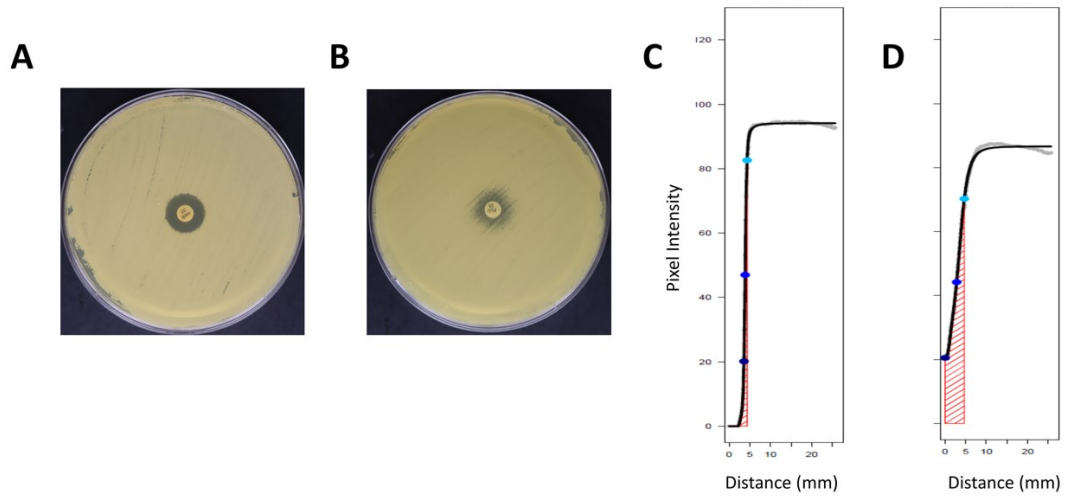
61

Figure S2. Detecting tolerance in Candida auris from disk diffusion assays (DDAs) using *diskImageR*. (A) Representative DDA image of *C. auris* (isolate 1) after 24 h of exposure to amphotericin B (AMB). (B) Representative DDA image of *C. auris* (isolate 1) after 24 h of exposure to fluconazole (FLU). (C) Quantification tolerance (shown in the pink zone) from the DDA shown to FLU in (A) using *diskImageR*. (D) Quantification tolerance from the DDA shown to AMB in (B) using *diskimageR*.
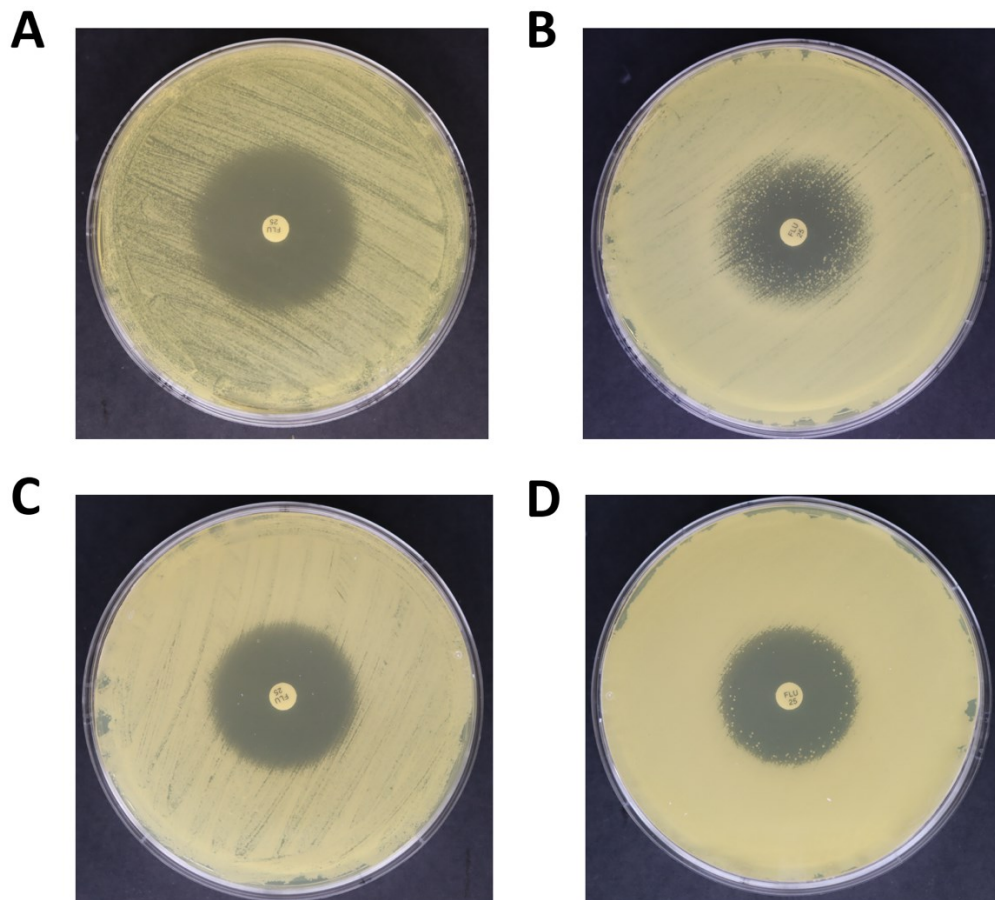
Figure S3. Representative disk diffusion assays (DDA) images of fluconazole (FLU) tolerance in *Candida auris* and *Candida parapsilosis*. (A) DDA of *C. auris* (isolate 1) after 24 h of exposure to FLU. (B) DDA of *C. auris* (isolate 1) after 48 h of exposure to FLU. (C) DDA of *C. parapsilosis* after 24 h of exposure to FLU. (D) DDA of *C. parapsilosis* after 48 h of exposure to FLU.
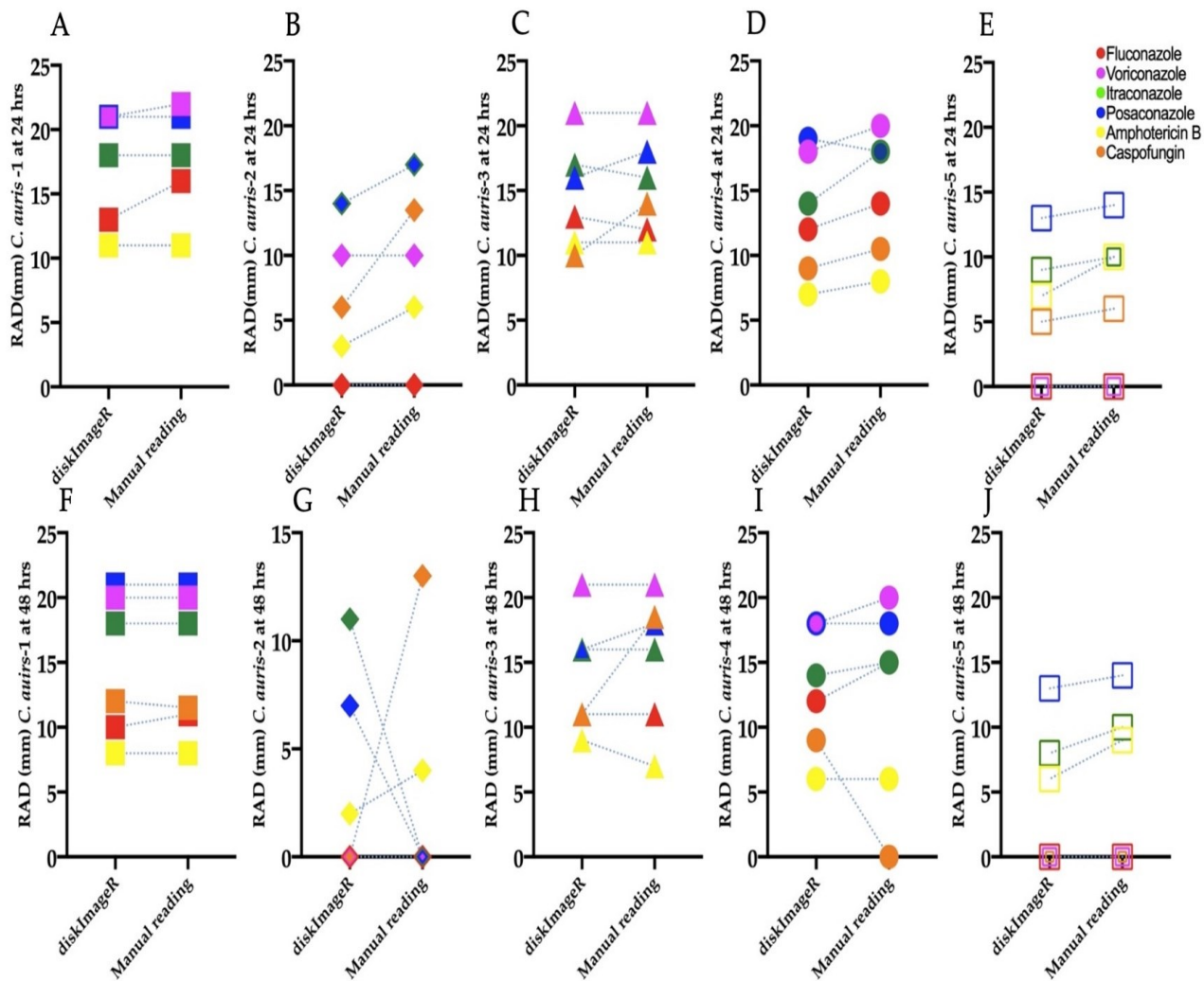
Figure S4. Comparison between *diskImageR* and manual radius of the zone of inhibition (RAD) measurements**. (A-E)** Mean RAD: radius of the zone of inhibition measured by *diskImageR* [29], and manually (see Section 2.5) at 24 h and (F-J) at 48 h.
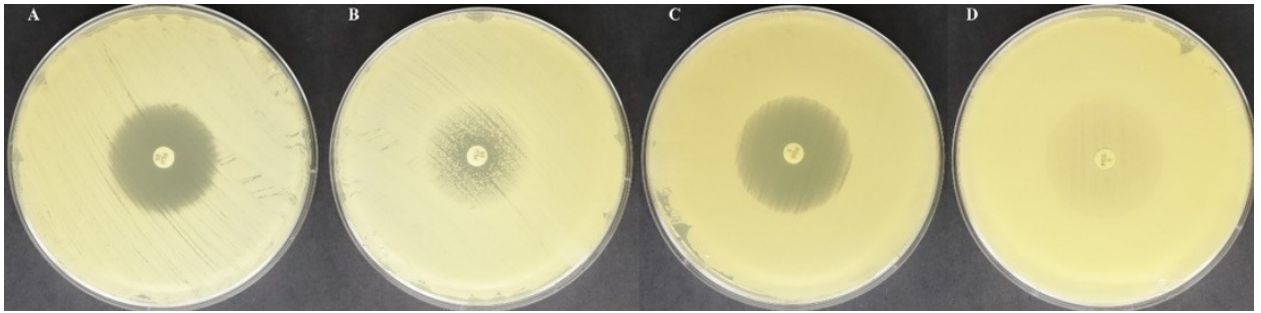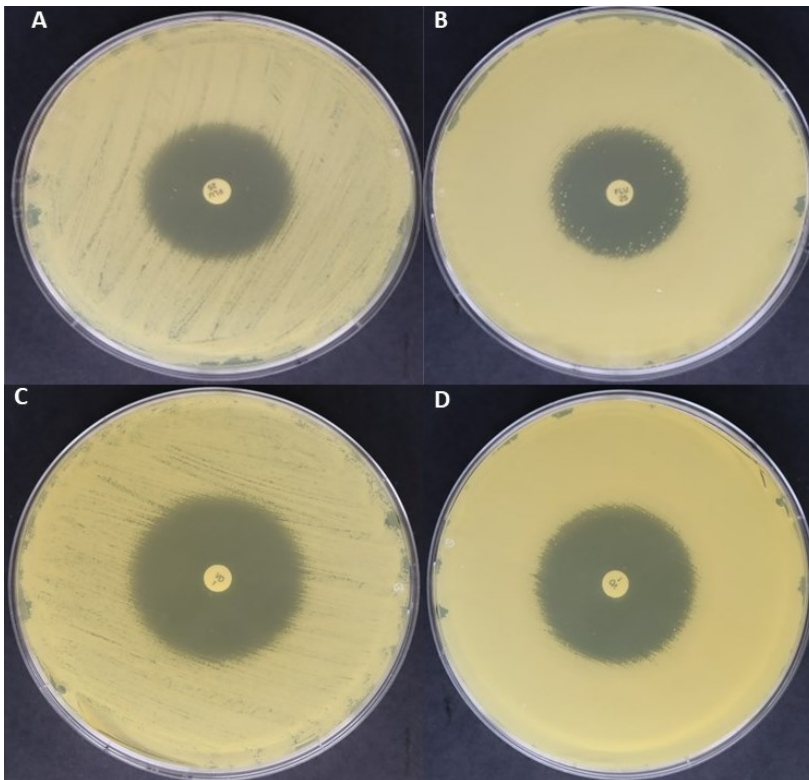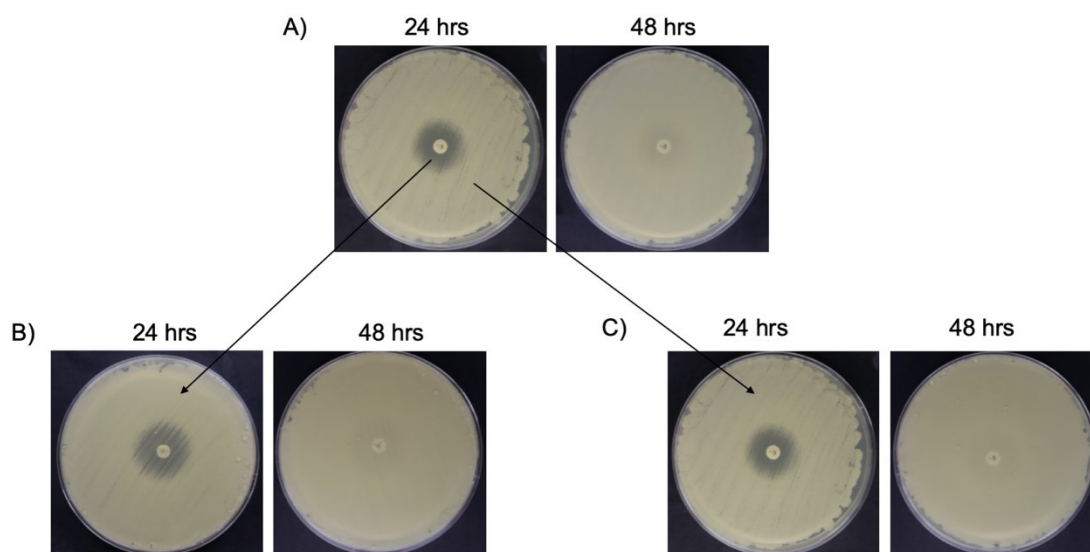
Figure S5. Azole tolerance in *Candida auris*. Disk diffusion assay (DDA) of fluconazole for *C. auris* (isolate 1) after (A) 24 h of growth and (B) 48 h of growth. DDA of posaconazole for *C. auris* isolate 2 after (C) 24 h of growth and (D) 48 h of growth.


Figure S6. Azole tolerance in the *Candida parapsilosis* reference strain. Tolerant *C. parapsilosis* colonies in the zone of inhibition (ZOI) after (A) 24 h and (B) 48 h of fluconazole treatment. Tolerant *C. parapsilosis* colonies in the ZOI after (C) 24 h and (D) 48 h of voriconazole treatment.

Figure S7. Reversibility of tolerance in a representative *Candida auris* isolate 2 against voriconazole. Disk diffusion assays after 24 and 48 h for (A) *C. auris* original isolate 2, (B) colonies isolated and sub-cultured from inside the zone of inhibition (ZOI) of the original plate, and (C) colonies isolated and sub-cultured from outside the ZOI of the original plate.
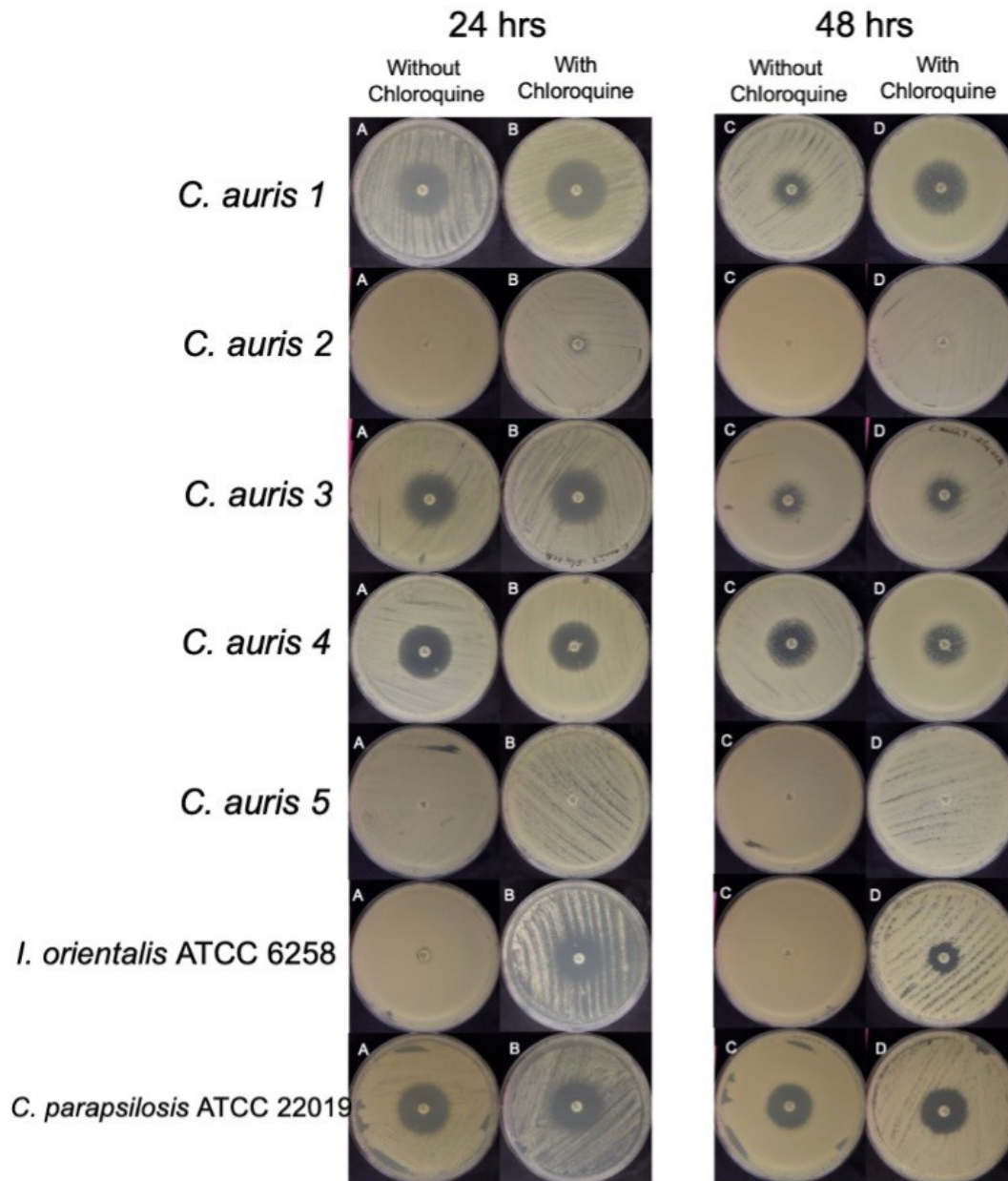
Figure S8. Disk diffusion assays (DDAs) of antifungal adjuvant treatment in *Candida auris* isolates and *Issatchenkia orientalis* and *Candida parapsilosis* reference strains. DDAs with fluconazole (FLU; 1st column) and with FLU combined with chloroquine (2nd column) against five *C. auris* isolates and two reference strains after 24 h (left) and 48 h (right).
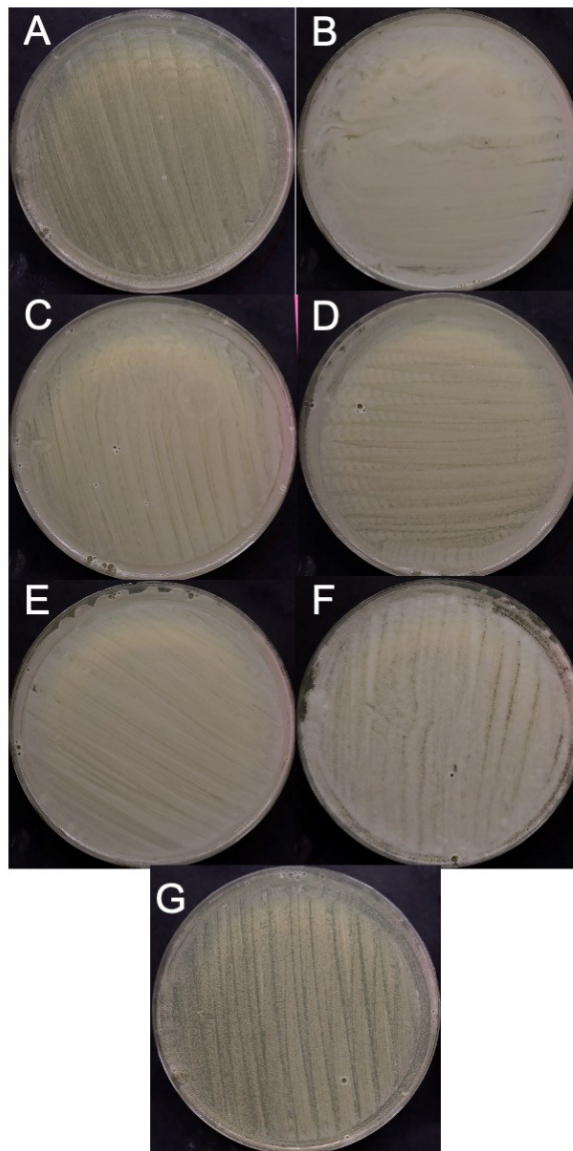
Figure S9. *Candida auris* isolates and *Candida parapsilosis* and *Issatchenkia orientalis* reference strains growing on Mueller–Hinton agar (MHA) media with chloroquine. Images of *C. auris* isolates 1-5 (A-E), *I. orientalis* (F), and *C. parapsilosis* (G) grown on MHA plus glucose methylene blue agar plates with 1031.8 µg/mL chloroquine diphosphate salt.
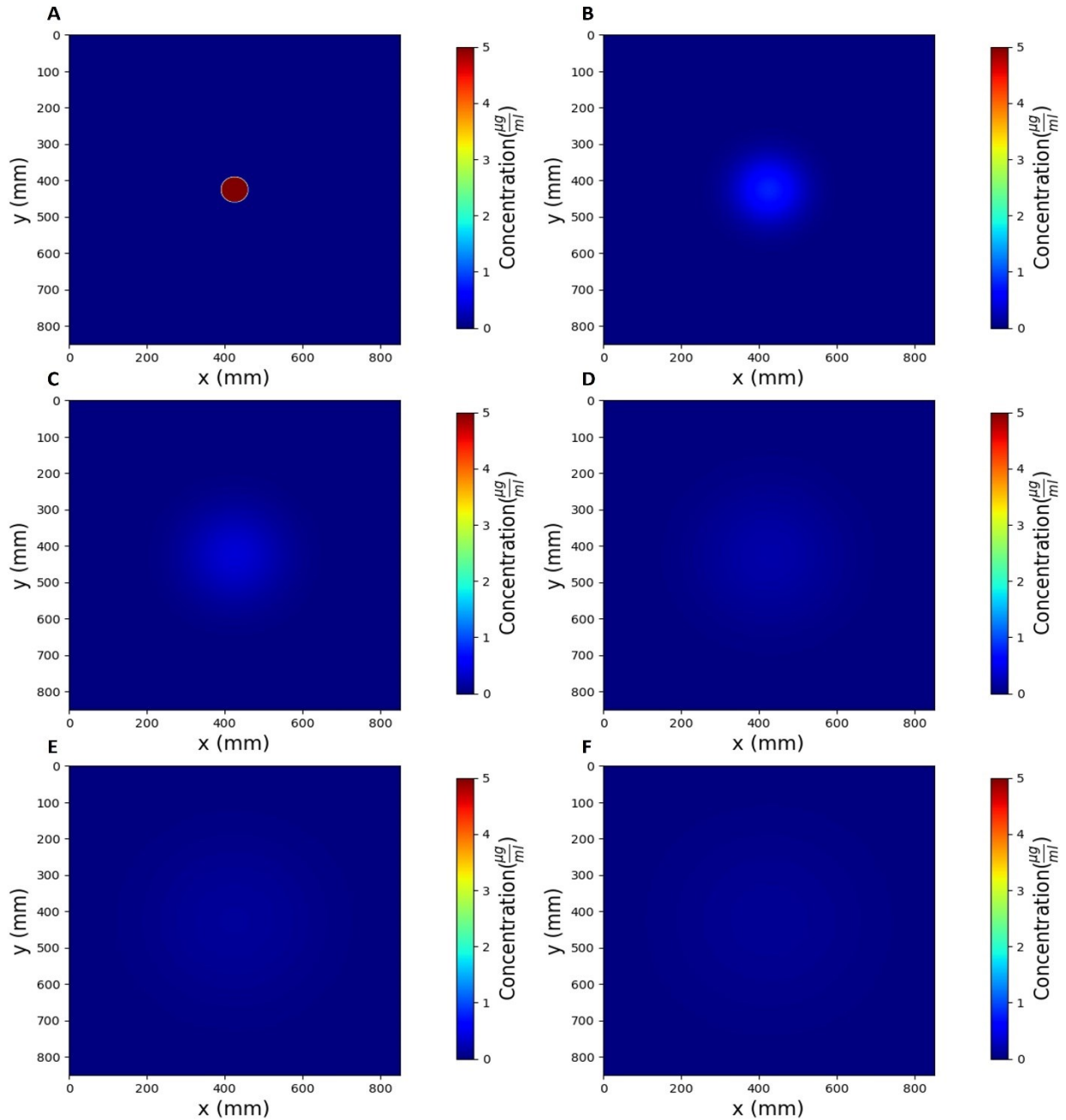
Figure S10. Temporal and spatial evolution of caspofungin diffusion in disk diffusion assay (D =9.94 × 10^{-10} m^2/s). Diffusion of 5 µg/ml caspofungin (same concentration used in experimental test) in disk diffusion assay in x and y direction (mm) at (A) 1 h, (B) 6 h, (C)12 h, (D) 24 h, (E) 36 h and (F) 48h with diffusion constant equal to 9.94 × 10^{-10} m^2/s. Red color shows the highest concentration and dark blue shows the lowest concentration. During diffusion always the concentration of caspofungin in high at the center and lower at the outer edge of the inhibition zone.
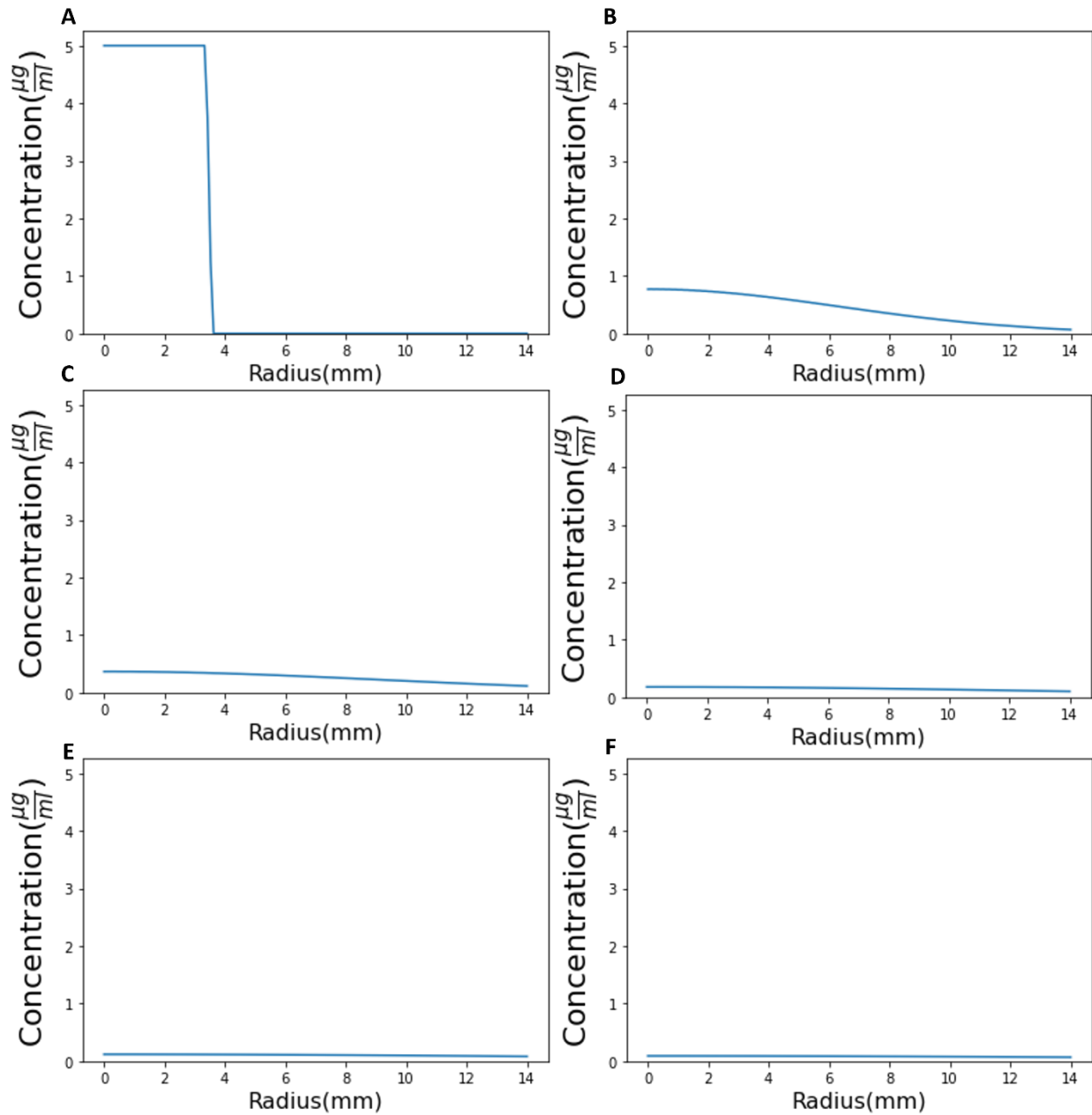
Figure S11. Temporal variation of caspofungin concentration in the zone of inhibition (D = 9.94 × 10^{-10} m^2/s). The concentration gradient (µg/ml) of caspofungin in zone of inhibition (mm) at (A) 1 h, (B) 6 h, (C) 12 h, (D) 24 h, (E) 36 h and (F) 48 h with diffusion constant equal to 9.94 × 10^{-10} m2/s. The initial concentration of caspofungin was assumed to be 5 µg/ml (same concentration used in experimental test).
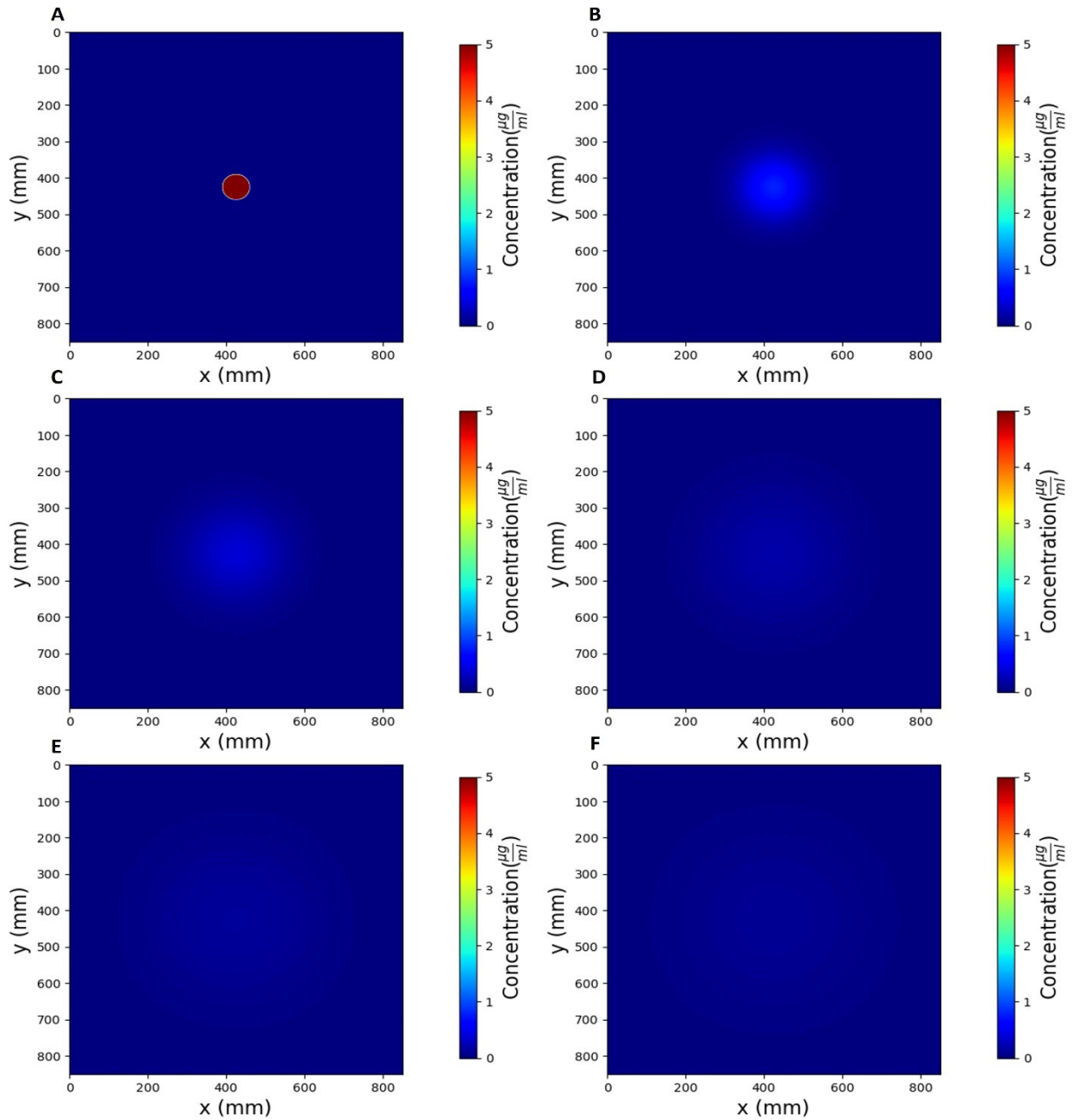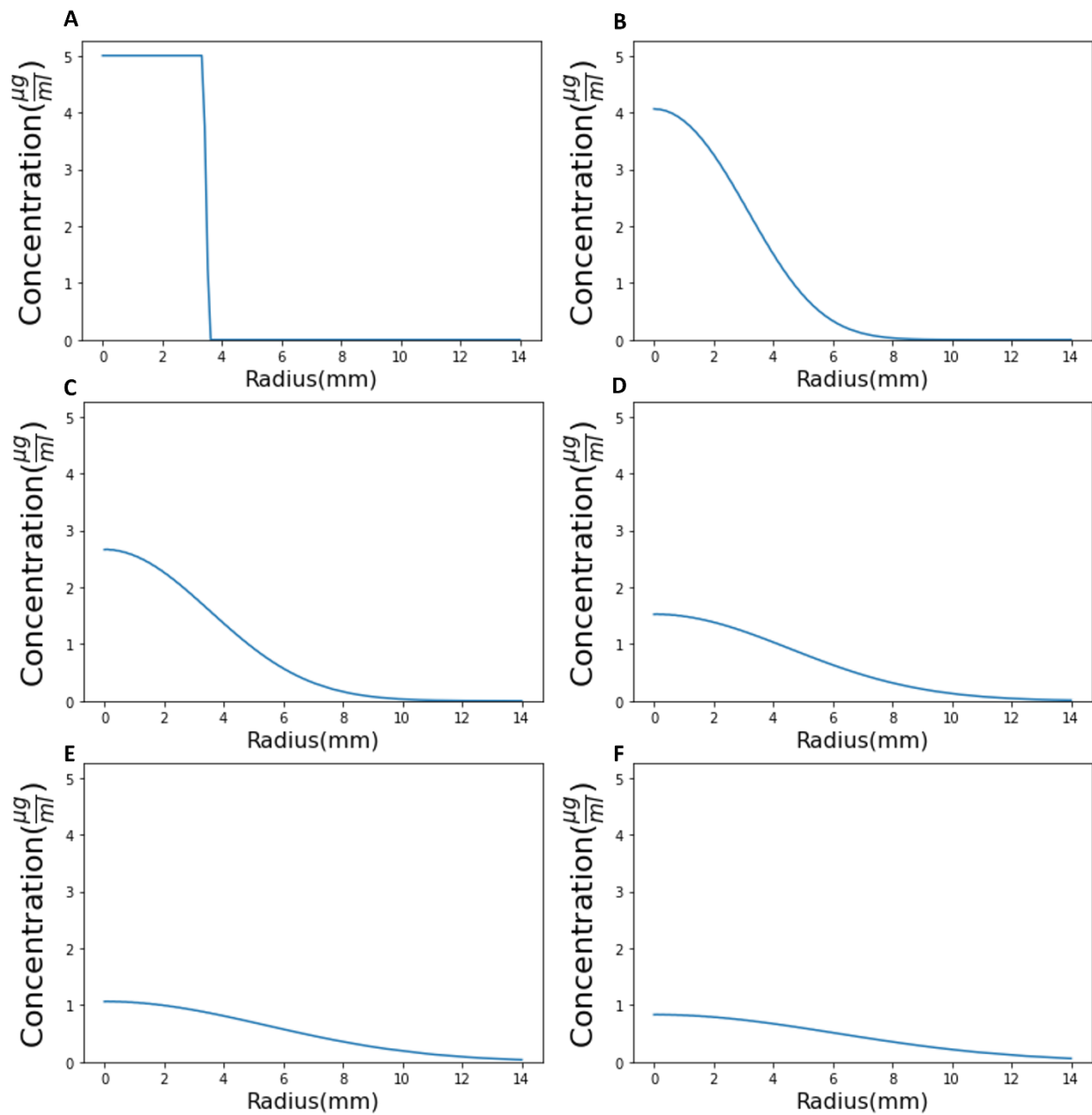
Figure S12. Temporal and Spatial Evolution of Caspofungin Diffusion in Disk Diffusion Assay (D =9.947 × 10 $^{-11}$ m^2/s). Diffusion of 5 µg/ml caspofungin (same concentration used in experimental test) in disk diffusion assay in x and y direction (mm) at (A)1 h, (B) 6 h, (C)12 h, (D) 24 h, (E) 36 h and (F) 48 h with diffusion constant equal to 9.94 × 10 $^{-11}$ m^2/s. Red color shows the highest concentration and dark blue shows the lowest concentration. During diffusion always the concentration of caspofungin in high at the center and lower at the outer edge of the inhibition zone.
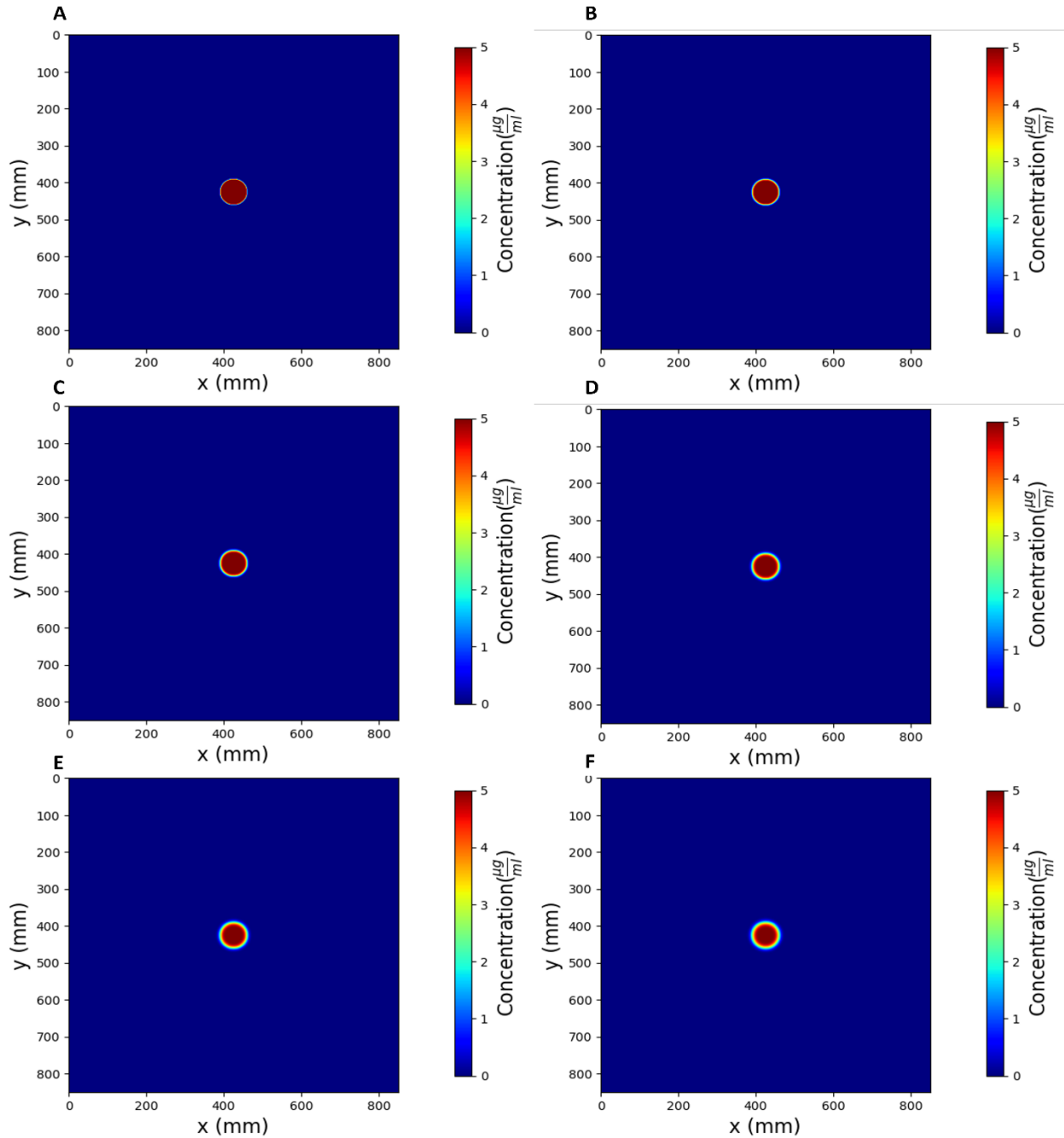
Figure S13. Temporal Variation of Caspofungin Concentration in the Zone of Inhibition (D = 9.947 ×10^{-11} m^2/s). The concentration gradient (µg/ml) of caspofungin in zone of inhibition (mm) at (A) 1h, (B) 6 h, (C) 12 h, (D) 24 h, (E) 36 h and (F) 48 h with diffusion constant equal to 9.94 × 10 $^{-11}$ m2/s. The initial concentration of caspofungin was assumed to be 5 µg/ml (same concentration used in experimental test).

Figure S14. Temporal and Spatial Evolution of Caspofungin Diffusion in Disk Diffusion Assay (D =9.94 × 10 $^{-13}$ m²/s). Diffusion of 5 µg/ml caspofungin (same concentration used in experimental test) in disk diffusion assay in x and y direction (mm) at (A)1 h, (B) 6 h, (C)12 h, (D) 24 h, (E) 36 h and (F) 48h with diffusion constant equal to 9.94 × 10 $^{-13}$ m²/s. Red color shows the highest concentration and dark blue shows the lowest concentration. During diffusion always the concentration of caspofungin in high at the center and lower at the outer edge of the inhibition zone.

Figure S15. Temporal Variation of Caspofungin Concentration in the Zone of Inhibition (D = 9.94 × 10 $^{-13}$ m^2/s). The concentration gradient (μg/ml) of caspofungin in zone of inhibition (mm) at (A) 1h, (B) 6 h, (C) 12 h, (D) 24 h, (E) 36 h and (F) 48 h with diffusion constant equal to 9.94 × 10 $^{-13}$ m2/s. The initial concentration of caspofungin was assumed to be 5 μg/ml (same concentration used in experimental test).
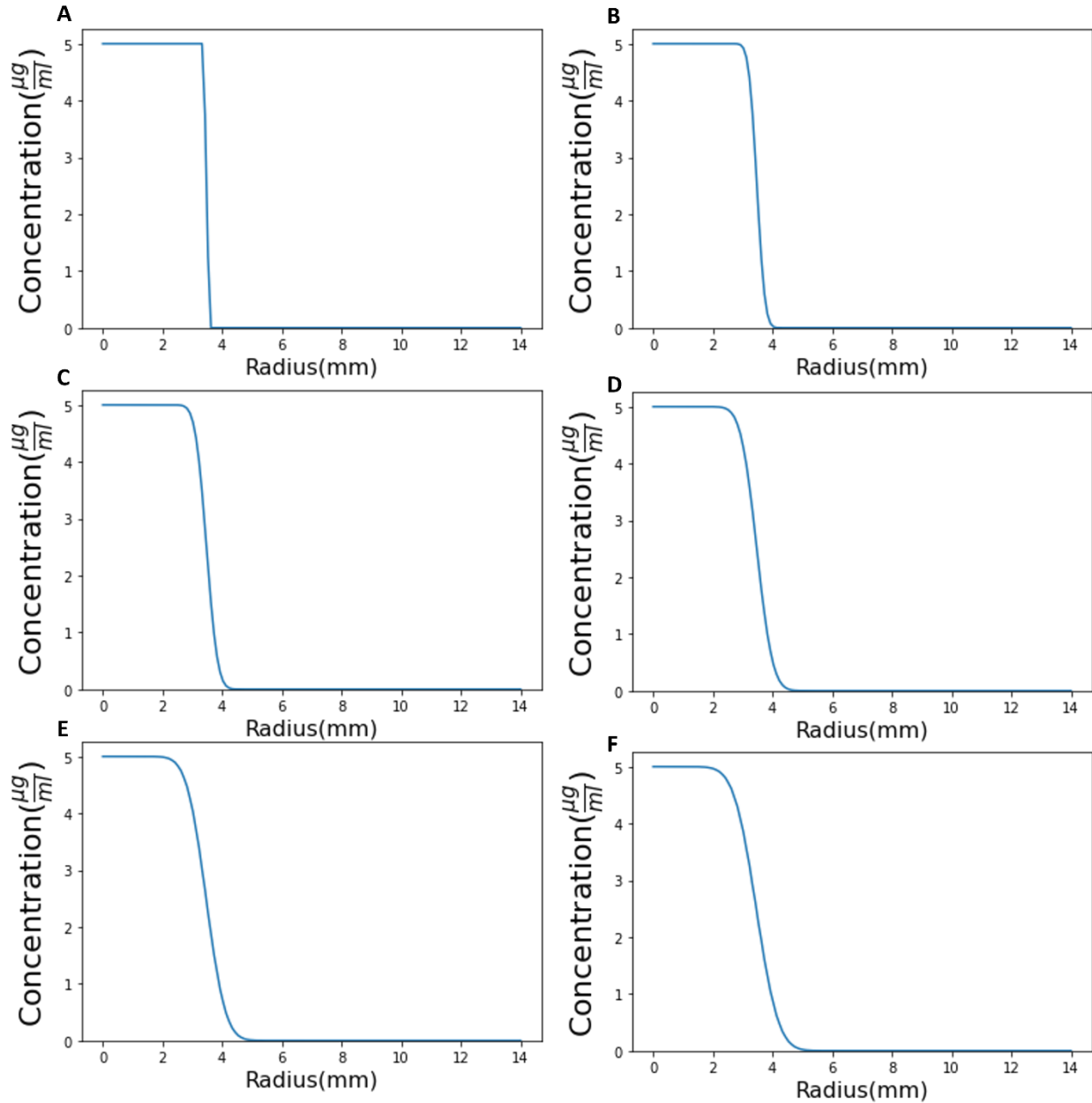
5.3   Python Codes

Code S1. Code for diffusion constant calculation:

```python
pi=3.14159
m=1.815e-24
T=308.15
rho=1000
k=1.380649e-23
eta=0.03
r=(3*m/(4*pi*rho))**(1/3)
D=(k*T)/(6*pi*eta*r)

print (D)
```

Codes S2. Temporal and Spatial Evolution of Caspofungin Diffusion in Disk Diffusion Assay

```python
import numpy as np
import matplotlib.pyplot as plt


path = "Path"

# plate size, mm
w = h = 85.
# intervals in x-, y- directions, mm
dx = dy = 0.1
# Diffusion constant, mm2.s-1
D = 9.954e-6

minall, c0 = 0, 5

nx, ny = int(w/dx), int(h/dy)

dx2, dy2 = dx*dx, dy*dy
dt = dx2 * dy2 / (2 * D * (dx2 + dy2))

u0 = minall * np.ones((nx, ny))
u = u0.copy()

# Initial conditions - circle of radius r centred at (cx,cy) (mm)
r, cx, cy = 3.5, 42.5, 42.5
r2 = r**2
for i in range(nx):
    for j in range(ny):
        p2 = (i*dx-cx)**2 + (j*dy-cy)**2
        if p2 < r2:
            u0[i,j] = c0
```

```python
def do_timestep(u0, u):
    # Propagate with forward-difference in time, central-difference in space
    u[1:-1, 1:-1] = u0[1:-1, 1:-1] + D * dt * (
            (u0[2:, 1:-1] - 2*u0[1:-1, 1:-1] + u0[:-2, 1:-1])/dx2
            + (u0[1:-1, 2:] - 2*u0[1:-1, 1:-1] + u0[1:-1, :-2])/dy2 )

    u0 = u.copy()
    return u0, u

# Number of timesteps
nsteps = int((48*3600)/dt)+2

# Output
mfig = np.linspace(0, nsteps, 49)
for i in range(len(mfig)):
    mfig[i]=int(mfig[i])


fignum = 0
print(mfig)
print(nsteps)
for m in range(nsteps):

    u0, u = do_timestep(u0, u)

    if m in mfig:
        print("here")
        flag=0
        rp = 10
        r2p = rp**2
        for i in range(nx):
            for j in range(ny):
                p2 = (i*dx-cx)**2 + (j*dy-cy)**2
                if int(p2) == r2p:
                    if u0[i,j] < 2 and u0[i,j]!=0:
                        flag=1


        fig, ax = plt.subplots()
        im = ax.imshow(u.copy(), cmap="jet", vmin=minall,vmax=c0)
        ax.set_xlabel("x (mm)")
        ax.set_ylabel("y (mm)")
        ax.set_title('{} hour'.format(int(m*dt/3600)+1))
        cbar_ax = fig.add_axes([0.9, 0.15, 0.03, 0.7])
        cbar = fig.colorbar(im, cax=cbar_ax)
        cbar.set_label(r"Concentration($\frac{\mu g}{ml})$")

        plt.savefig(path + "{}.png".format(int(m*dt/3600)), dpi = 400)
```

Code S3. Temporal Variation of Caspofungin Concentration in the Zone of Inhibition

```python
import numpy as np
import matplotlib.pyplot as plt


path = "Path"
# plate size, mm
w = h = 85.
# intervals in x-, y- directions, mm
dx = dy = 0.1
# Diffusion constant, mm2.s-1
D = 9.94e-6

radius = np.linspace(0,14,140)

minall, c0 = 0, 5

nx, ny = int(w/dx), int(h/dy)

dx2, dy2 = dx*dx, dy*dy
dt = dx2 * dy2 / (2 * D * (dx2 + dy2))

u0 = minall * np.ones((nx, ny))
u = u0.copy()

# Initial conditions - circle of radius r centred at (cx,cy) (mm)
r, cx, cy = 3.5, 42.5, 42.5
r2 = r**2
for i in range(nx):
    for j in range(ny):
        p2 = (i*dx-cx)**2 + (j*dy-cy)**2
        if p2 < r2:
            u0[i,j] = c0

def do_timestep(u0, u):
    # Propagate with forward-difference in time, central-difference in space
    u[1:-1, 1:-1] = u0[1:-1, 1:-1] + D * dt * (
          (u0[2:, 1:-1] - 2*u0[1:-1, 1:-1] + u0[-2, 1:-1])/dx2
          + (u0[1:-1, 2:] - 2*u0[1:-1, 1:-1] + u0[1:-1, :-2])/dy2 )

    u0 = u.copy()
    return u0, u

# Number of timesteps
nsteps = int((48*3600)/dt)
# print(nsteps)
# Output
mfig_list = np.linspace(0, nsteps, 48)

mfig = [int(mfig_list[0]), int(mfig_list[5])+1,  int(mfig_list[11])+1,
int(mfig_list[23])+1,  int(mfig_list[35])+1, int(mfig_list[46])+1]
```

```python
fignum = 0
for m in range(nsteps):
    u0, u = do_timestep(u0, u)
    if m in mfig:
        fignum += 1
        print(m, fignum)
        fig, ax = plt.subplots()
        ax.plot(radius, u[425, 425:565])
        ax.set_xlabel("Radius (mm)", fontsize = 16)
        ax.set_ylabel(r"Concentration ($\frac{\mu g}{ml})$" , fontsize = 16)
        ax.set_ylim([0, c0+0.05*c0])
        ax.set_title('{} hour'.format(int(m*dt/3600)+1) , fontsize = 18 )

        plt.savefig(path + "{}_his.png".format(int(m*dt/3600)), dpi = 400)
```

References

[1]   S. Rasouli Koohi, S.A. Shankarnarayan, C.M. Galon, D.A. Charlebois, Identification and
        Elimination of Antifungal Tolerance in Candida auris, Biomedicines. 11 (2023).
        https://doi.org/10.3390/BIOMEDICINES11030898.

[2]   K.S. Farquhar, S. Rasouli Koohi, D.A. Charlebois, Does transcriptional heterogeneity
        facilitate the development of genetic drug resistance?, Bioessays. 43 (2021).
        https://doi.org/10.1002/BIES.202100043.

[3]   J. Berman, D.J. Krysan, Drug resistance and tolerance in fungi, Nat Rev Microbiol. 18 (2020)
        319–331. https://doi.org/10.1038/S41579-019-0322-2.

[4]   M.M. Ansari, K. Kuche, R. Ghadi, T. Date, D. Chaudhari, R. Khan, S. Jain, Socioeconomic
        Impact of Antimicrobial Resistance and Their Integrated Mitigation by One Health
        Approach, Emerging Modalities in Mitigation of Antimicrobial Resistance. (2022) 135–156.
        https://doi.org/10.1007/978-3-030-84126-3_7/FIGURES/5.

[5]   S.W. Page, P. Gautier, Use of antimicrobial agents in livestock, Rev Sci Tech. 31 (2012) 145–
        188. https://doi.org/10.20506/RST.31.1.2106.

[6]   When Antibiotics Fail The Expert Panel on the Potential Socio-Economic Impacts of
        Antimicrobial Resistance in Canada, (n.d.).

[7]   Glossary of Terms Related to Antibiotic Resistance | NARMS | CDC, (n.d.).
        https://www.cdc.gov/narms/resources/glossary.html (accessed October 14, 2023).

[8]   A.P. Magiorakos, A. Srinivasan, R.B. Carey, Y. Carmeli, M.E. Falagas, C.G. Giske, S. Harbarth,
        J.F. Hindler, G. Kahlmeter, B. Olsson-Liljequist, D.L. Paterson, L.B. Rice, J. Stelling, M.J.
        Struelens, A. Vatopoulos, J.T. Weber, D.L. Monnet, Multidrug-resistant, extensively drug-

resistant and pandrug-resistant bacteria: an international expert proposal for interim standard definitions for acquired resistance, Clinical Microbiology and Infection. 18 (2012) 268–281. https://doi.org/10.1111/J.1469-0691.2011.03570.X.

[9]   Y. Zhi-Wen, Z. Yan-Li, Y. Man, F. Wei-Jun, Clinical treatment of pandrug-resistant bacterial infection consulted by clinical pharmacist, Saudi Pharmaceutical Journal : SPJ. 23 (2015) 377. https://doi.org/10.1016/J.JSPS.2015.01.001.

[10]   A.P. Magiorakos, A. Srinivasan, R.B. Carey, Y. Carmeli, M.E. Falagas, C.G. Giske, S. Harbarth, J.F. Hindler, G. Kahlmeter, B. Olsson-Liljequist, D.L. Paterson, L.B. Rice, J. Stelling, M.J. Struelens, A. Vatopoulos, J.T. Weber, D.L. Monnet, Multidrug-resistant, extensively drug-resistant and pandrug-resistant bacteria: an international expert proposal for interim standard definitions for acquired resistance, Clin Microbiol Infect. 18 (2012) 268–281. https://doi.org/10.1111/J.1469-0691.2011.03570.X.

[11]   S. Pokharel, P. Shrestha, B. Adhikari, Antimicrobial use in food animals and human health: time to implement 'One Health' approach, Antimicrob Resist Infect Control. 9 (2020) 1–5. https://doi.org/10.1186/S13756-020-00847-X/METRICS.

[12]   Expert Panel on Antimicrobial Availability Overcoming Resistance, (n.d.).

[13]   Council of Canadian Academies | CCA | Overcoming Resistance, (n.d.). https://cca-reports.ca/reports/pull-incentives-for-high-value-antimicrobials/ (accessed October 14, 2023).

[14]   C.J. Murray, K.S. Ikuta, F. Sharara, L. Swetschinski, G. Robles Aguilar, A. Gray, C. Han, C. Bisignano, P. Rao, E. Wool, S.C. Johnson, A.J. Browne, M.G. Chipeta, F. Fell, S. Hackett, G. Haines-Woodhouse, B.H. Kashef Hamadani, E.A.P. Kumaran, B. McManigal, R. Agarwal, S.

Akech, S. Albertson, J. Amuasi, J. Andrews, A. Aravkin, E. Ashley, F. Bailey, S. Baker, B.

Basnyat, A. Bekker, R. Bender, A. Bethou, J. Bielicki, S. Boonkasidecha, J. Bukosia, C.

Carvalheiro, C. Castañeda-Orjuela, V. Chansamouth, S. Chaurasia, S. Chiurchiù, F.

Chowdhury, A.J. Cook, B. Cooper, T.R. Cressey, E. Criollo-Mora, M. Cunningham, S. Darboe,

N.P.J. Day, M. De Luca, K. Dokova, A. Dramowski, S.J. Dunachie, T. Eckmanns, D. Eibach, A.

Emami, N. Feasey, N. Fisher-Pearson, K. Forrest, D. Garrett, P. Gastmeier, A.Z. Giref, R.C.

Greer, V. Gupta, S. Haller, A. Haselbeck, S.I. Hay, M. Holm, S. Hopkins, K.C. Iregbu, J. Jacobs,

D. Jarovsky, F. Javanmardi, M. Khorana, N. Kissoon, E. Kobeissi, T. Kostyanev, F. Krapp, R.

Krumkamp, A. Kumar, H.H. Kyu, C. Lim, D. Limmathurotsakul, M.J. Loftus, M. Lunn, J. Ma,

N. Mturi, T. Munera-Huertas, P. Musicha, M.M. Mussi-Pinhata, T. Nakamura, R. Nanavati, S.

Nangia, P. Newton, C. Ngoun, A. Novotney, D. Nwakanma, C.W. Obiero, A. Olivas-Martinez,

P. Olliaro, E. Ooko, E. Ortiz-Brizuela, A.Y. Peleg, C. Perrone, N. Plakkal, A. Ponce-de-Leon, M.

Raad, T. Ramdin, A. Riddell, T. Roberts, J.V. Robotham, A. Roca, K.E. Rudd, N. Russell, J.

Schnall, J.A.G. Scott, M. Shivamallappa, J. Sifuentes-Osornio, N. Steenkeste, A.J.

Stewardson, T. Stoeva, N. Tasak, A. Thaiprakong, G. Thwaites, C. Turner, P. Turner, H.R. van

Doorn, S. Velaphi, A. Vongpradith, H. Vu, T. Walsh, S. Waner, T. Wangrangsimakul, T.

Wozniak, P. Zheng, B. Sartorius, A.D. Lopez, A. Stergachis, C. Moore, C. Dolecek, M.

Naghavi, Global burden of bacterial antimicrobial resistance in 2019: a systematic analysis,

The Lancet. 399 (2022) 629–655. https://doi.org/10.1016/S0140-6736(21)02724-0.

[15] Canadian Antimicrobial Resistance Surveillance System (CARSS) Report 2022, (2022).

https://doi.org/10.58333/E241022.

[16] Results Report 2023 - The Global Fund to Fight AIDS, Tuberculosis and Malaria, (n.d.).

https://www.theglobalfund.org/en/results/ (accessed October 14, 2023).

[17]   Drug-Resistant Infections: A Threat to Our Economic Future, (n.d.).
        https://www.worldbank.org/en/topic/health/publication/drug-resistant-infections-a-
        threat-to-our-economic-future (accessed October 14, 2023).

[18]   Council of Canadian Academies | CCA | When Antibiotics Fail, (n.d.). https://cca-
        reports.ca/reports/the-potential-socio-economic-impacts-of-antimicrobial-resistance-in-
        canada/ (accessed October 14, 2023).

[19]   J. Houšť, J. Spížek, V. Havlíček, Antifungal Drugs, Metabolites 2020, Vol. 10, Page 106. 10
        (2020) 106. https://doi.org/10.3390/METABO10030106.

[20]   K.M. Pianalto, J.A. Alspaugh, New Horizons in Antifungal Therapy, J Fungi (Basel). 2 (2016).
        https://doi.org/10.3390/JOF2040026.

[21]   D. Denning, HIDDEN CRISIS: HOW 150 PEOPLE DIE EVERY HOUR FROM FUNGAL INFECTION
        WHILE THE WORLD TURNS A BLIND EYE www.gaffi.org info@gaffi.org @gaffi_org Jag
        Jugessur jjugessur@gaffi.org, (n.d.). www.gaffi.org (accessed July 25, 2023).

[22]   Y. Lee, N. Robbins, L.E. Cowen, Molecular mechanisms governing antifungal drug
        resistance, Npj Antimicrobials and Resistance 2023 1:1. 1 (2023) 1–9.
        https://doi.org/10.1038/s44259-023-00007-2.

[23]   M. Hutchings, A. Truman, B. Wilkinson, Antibiotics: past, present and future, Curr Opin
        Microbiol. 51 (2019) 72–80. https://doi.org/10.1016/J.MIB.2019.10.008.

[24]   M.A. Ghannoum, L.B. Rice, Antifungal Agents: Mode of Action, Mechanisms of Resistance,
        and Correlation of These Mechanisms with Bacterial Resistance, Clin Microbiol Rev. 12
        (1999) 501. https://doi.org/10.1128/CMR.12.4.501.

[25] A.W. de Jong, F. Hagen, Attack, Defend and Persist: How the Fungal Pathogen Candida auris was Able to Emerge Globally in Healthcare Environments, Mycopathologia. 184 (2019) 353–365. https://doi.org/10.1007/S11046-019-00351-W/FIGURES/1.

[26] J. Osei Sekyere, Candida auris: A systematic review and meta-analysis of current updates on an emerging multidrug-resistant pathogen, Microbiologyopen. 7 (2018) e00578. https://doi.org/10.1002/MBO3.578.

[27] T. Hirayama, T. Miyazaki, Y. Ito, M. Wakayama, K. Shibuya, K. Yamashita, T. Takazono, T. Saijo, S. Shimamura, K. Yamamoto, Y. Imamura, K. Izumikawa, K. Yanagihara, S. Kohno, H. Mukae, Virulence assessment of six major pathogenic Candida species in the mouse model of invasive candidiasis caused by fungal translocation, Sci Rep. 10 (2020). https://doi.org/10.1038/S41598-020-60792-Y.

[28] C.N. Ciurea, I.B. Kosovski, A.D. Mare, F. Toma, I.A. Pintea-Simon, A. Man, Candida and Candidiasis—Opportunism Versus Pathogenicity: A Review of the Virulence Traits, Microorganisms. 8 (2020) 1–17. https://doi.org/10.3390/MICROORGANISMS8060857.

[29] A. Casadevall, D.P. Kontoyiannis, V. Robert, Environmental Candida auris and the Global Warming Emergence Hypothesis, MBio. 12 (2021) 1–3. https://doi.org/10.1128/MBIO.00360-21.

[30] N.E. Nnadi, D.A. Carter, Climate change and the emergence of fungal pathogens, PLoS Pathog. 17 (2021). https://doi.org/10.1371/JOURNAL.PPAT.1009503.

[31] A. Casadevall, D.P. Kontoyiannis, V. Robert, On the emergence of candida auris: climate change, azoles, swamps, and birds, MBio. 10 (2019). https://doi.org/10.1128/MBIO.01397-19.

[32]   J.H. Ellwanger, J.A.B. Chies, Candida auris emergence as a consequence of climate change:

         Impacts on Americas and the need to contain greenhouse gas emissions, The Lancet

         Regional Health - Americas. 11 (2022) 100250.

         https://doi.org/10.1016/j.lana.2022.100250.

[33]   A. Sanyaolu, C. Okorie, A. Marinkovic, A.F. Abbasi, S. Prakash, J. Mangat, Z. Hosein, N.

         Haider, J. Chan, Candida auris: An Overview of the Emerging Drug-Resistant Fungal

         Infection, Infect Chemother. 54 (2022) 236. https://doi.org/10.3947/IC.2022.0008.

[34]   E.J. Eckbo, T. Wong, A. Bharat, M. Cameron-Lane, L. Hoang, M. Dawar, M. Charles, First

         reported outbreak of the emerging pathogen Candida auris in Canada, Am J Infect Control.

         49 (2021) 804–807. https://doi.org/10.1016/J.AJIC.2021.01.013.

[35]   S. Fan, C. Li, J. Bing, G. Huang, H. Du, Discovery of the Diploid Form of the Emerging Fungal

         Pathogen Candida auris, ACS Infect Dis. 6 (2020) 2641–2646.

         https://doi.org/10.1021/ACSINFECDIS.0C00282/ASSET/IMAGES/LARGE/ID0C00282_0005.J

         PEG.

[36]   M. Ademe, F. Girma, Candida auris: From multidrug resistance to pan-resistant strains,

         Infect Drug Resist. 13 (2020) 1287–1294. https://doi.org/10.2147/IDR.S249864.

[37]   H. Du, J. Bing, T. Hu, C.L. Ennis, C.J. Nobile, G. Huang, Candida auris: Epidemiology, biology,

         antifungal resistance, and virulence, PLoS Pathog. 16 (2020) e1008921.

         https://doi.org/10.1371/JOURNAL.PPAT.1008921.

[38]   K. Satoh, K. Makimura, Y. Hasumi, Y. Nishiyama, K. Uchida, H. Yamaguchi, Candida auris sp.

         nov., a novel ascomycetous yeast isolated from the external ear canal of an inpatient in a

Japanese hospital, Microbiol Immunol. 53 (2009) 41–44. https://doi.org/10.1111/J.1348-0421.2008.00083.X.

[39]   G. Desoubeaux, A.T. Coste, C. Imbert, C. Hennequin, Overview about Candida auris: What's up 12 years after its first description?, Journal of Medical Mycology. 32 (2022) 101248. https://doi.org/10.1016/J.MYCMED.2022.101248.

[40]   H. Il Choi, J. An, J.J. Hwang, S.Y. Moon, J.S. Son, Otomastoiditis caused by Candida auris: Case report and literature review, Mycoses. 60 (2017) 488–492. https://doi.org/10.1111/MYC.12617.

[41]   F. Safari, M. Madani, H. Badali, A.A. Kargoshaie, H. Fakhim, M. Kheirollahi, J.F. Meis, H. Mirhendi, A Chronic Autochthonous Fifth Clade Case of Candida auris Otomycosis in Iran, Mycopathologia. 187 (2022) 121–127. https://doi.org/10.1007/S11046-021-00605-6/METRICS.

[42]   N.A. Chow, T. De Groot, H. Badali, M. Abastabar, T.M. Chiller, J.F. Meis, Potential Fifth Clade of Candida auris, Iran, 2018, Emerg Infect Dis. 25 (2019) 1780. https://doi.org/10.3201/EID2509.190686.

[43]   B. Spruijtenburg, H. Badali, M. Abastabar, H. Mirhendi, S. Khodavaisy, J. Sharifisooraki, M. Taghizadeh Armaki, T. de Groot, J.F. Meis, Confirmation of fifth Candida auris clade by whole genome sequencing, Emerg Microbes Infect. 11 (2022) 2405–2411. https://doi.org/10.1080/22221751.2022.2125349/SUPPL_FILE/TEMI_A_2125349_SM7355 .ZIP.

[44]   C. Suphavilai, K.K.K. Ko, K.M. Lim, M.G. Tan, P. Boonsimma, J.J.K. Chu, S.S. Goh, P. Rajandran, L.C. Lee, K.Y. Tan, B.B.S. Ismail, M.K. Aung, Y. Yang, J.X.Y. Sim, I. Venkatachalam,

B.P.Z. Cherng, B. Spruijtenburg, K.S. Chan, L.L.E. Oon, A.L. Tan, Y.E. Tan, L. Wijaya, B.H. Tan, M.L. Ling, T.H. Koh, J.F. Meis, C.K.M. Tsui, N. Nagarajan, Discovery of the sixth Candida auris clade in Singapore, MedRxiv. (2023) 2023.08.01.23293435. https://doi.org/10.1101/2023.08.01.23293435.

[45]   S.A. Lone, A. Ahmad, Candida auris—the growing menace to global health, Mycoses. 62 (2019) 620–637. https://doi.org/10.1111/MYC.12904.

[46]   S. Ahmad, W. Alfouzan, Candida auris: Epidemiology, Diagnosis, Pathogenesis, Antifungal Susceptibility, and Infection Control Measures to Combat the Spread of Infections in Healthcare Facilities, Microorganisms 2021, Vol. 9, Page 807. 9 (2021) 807. https://doi.org/10.3390/MICROORGANISMS9040807.

[47]   F. Chaabane, A. Graf, L. Jequier, A.T. Coste, Review on Antifungal Resistance Mechanisms in the Emerging Pathogen Candida auris, Front Microbiol. 10 (2019) 499266. https://doi.org/10.3389/FMICB.2019.02788/BIBTEX.

[48]   L. Forgács, A.M. Borman, E. Prépost, Z. Tóth, G. Kardos, R. Kovács, A. Szekely, F. Nagy, I. Kovacs, L. Majoros, Comparison of in vivo pathogenicity of four Candida auris clades in a neutropenic bloodstream infection murine model, Emerg Microbes Infect. 9 (2020) 1160–1169. https://doi.org/10.1080/22221751.2020.1771218.

[49]   A. Al-Rashdi, A. Al-Maani, A. Al-Wahaibi, A. Alqayoudhi, A. Al-Jardani, S. Al-Abri, Characteristics, Risk Factors, and Survival Analysis of Candida auris Cases: Results of One-Year National Surveillance Data from Oman, Journal of Fungi. 7 (2021) 1–12. https://doi.org/10.3390/JOF7010031.

[50]   S. Silva, M. Negri, M. Henriques, R. Oliveira, D.W. Williams, J. Azeredo, Candida glabrata, Candida parapsilosis and Candida tropicalis: biology, epidemiology, pathogenicity and antifungal resistance, FEMS Microbiol Rev. 36 (2012) 288–305. https://doi.org/10.1111/J.1574-6976.2011.00278.X.

[51]   E.S. Spivak, K.E. Hanson, Candida auris: an Emerging Fungal Pathogen, J Clin Microbiol. 56 (2018). https://doi.org/10.1128/JCM.01588-17.

[52]   G. Bravo Ruiz, A. Lorenz, What do we know about the biology of the emerging fungal pathogen of humans Candida auris?, Microbiol Res. 242 (2021). https://doi.org/10.1016/J.MICRES.2020.126621.

[53]   A. Jeffery-Smith, S.K. Taori, S. Schelenz, K. Jeffery, E.M. Johnson, A. Borman, R. Manuel, C.S. Browna, Candida auris: a Review of the Literature, Clin Microbiol Rev. 31 (2018). https://doi.org/10.1128/CMR.00029-17.

[54]   A. Jeffery-Smith, S.K. Taori, S. Schelenz, K. Jeffery, E.M. Johnson, A. Borman, R. Manuel, C.S. Browna, Candida auris: A review of the literature, Clin Microbiol Rev. 31 (2018). https://doi.org/10.1128/CMR.00029-17.

[55]   P.G. Pappas, M.S. Lionakis, M.C. Arendrup, L. Ostrosky-Zeichner, B.J. Kullberg, Invasive candidiasis, Nat Rev Dis Primers. 4 (2018). https://doi.org/10.1038/NRDP.2018.26.

[56]   S. Dahiya, A.K. Chhillar, N. Sharma, P. Choudhary, A. Punia, M. Balhara, K. Kaushik, V.S. Parmar, Candida auris and Nosocomial Infection, Curr Drug Targets. 21 (2020) 365–373. https://doi.org/10.2174/1389450120666190924155631.

[57]   Y. Lee, E. Puumala, N. Robbins, L.E. Cowen, Antifungal Drug Resistance: Molecular

        Mechanisms in Candida albicans and Beyond, Chem Rev. 121 (2021) 3390–3411.

        https://doi.org/10.1021/ACS.CHEMREV.0C00199.

[58]   E.S. Spivak, K.E. Hanson, Candida auris: An emerging fungal pathogen, J Clin Microbiol. 56

        (2018). https://doi.org/10.1128/JCM.01588-17/FORMAT/EPUB.

[59]   Y. Lee, E. Puumala, N. Robbins, L.E. Cowen, Antifungal Drug Resistance: Molecular

        Mechanisms in Candida albicans and Beyond, Chem Rev. 121 (2021) 3390–3411.

        https://doi.org/10.1021/ACS.CHEMREV.0C00199.

[60]   M. V. Horton, C.J. Johnson, R. Zarnowski, B.D. Andes, T.J. Schoen, J.F. Kernien, D. Lowman,

        M.D. Kruppa, Z. Ma, D.L. Williams, A. Huttenlocher, J.E. Nett, Candida auris Cell Wall

        Mannosylation Contributes to Neutrophil Evasion through Pathways Divergent from

        Candida albicans and Candida glabrata, MSphere. 6 (2021).

        https://doi.org/10.1128/MSPHERE.00406-21.

[61]   N.A. Chow, J.F. Muñoz, L. Gade, E.L. Berkow, X. Li, R.M. Welsh, K. Forsberg, S.R. Lockhart, R.

        Adam, A. Alanio, A. Alastruey-Izquierdo, S. Althawadi, A.B. Araúz, R. Ben-Ami, A. Bharat, B.

        Calvo, M. Desnos-Ollivier, P. Escandón, D. Gardam, R. Gunturu, C.H. Heath, O. Kurzai, R.

        Martin, A.P. Litvintseva, C.A. Cuomo, Tracing the Evolutionary History and Global

        Expansion of Candida auris Using Population Genomic Analyses, MBio. 11 (2020).

        https://doi.org/10.1128/MBIO.03364-19.

[62]   J.F. Muñoz, L. Gade, N.A. Chow, V.N. Loparev, P. Juieng, E.L. Berkow, R.A. Farrer, A.P.

        Litvintseva, C.A. Cuomo, Genomic insights into multidrug-resistance, mating and virulence

        in Candida auris and related emerging species, Nature Communications 2018 9:1. 9 (2018)

        1–13. https://doi.org/10.1038/s41467-018-07779-6.

[63]   A. Rosenberg, I. V. Ene, M. Bibi, S. Zakin, E.S. Segal, N. Ziv, A.M. Dahan, A.L. Colombo, R.J. Bennett, J. Berman, Antifungal tolerance is a subpopulation effect distinct from resistance and is associated with persistent candidemia, Nature Communications 2018 9:1. 9 (2018) 1–14. https://doi.org/10.1038/s41467-018-04926-x.

[64]   J. Violet, J. Smid, A. Pielaat, J.-W. Sanders, S. V. Avery, The Influence of Heteroresistance on Minimum Inhibitory Concentration, Investigated Using Weak-Acid Stress in Food Spoilage Yeasts, Appl Environ Microbiol. 89 (2023). https://doi.org/10.1128/AEM.00125-23/SUPPL_FILE/AEM.00125-23-S0001.DOCX.

[65]   L. Dewachter, M. Fauvart, J. Michiels, Bacterial Heterogeneity and Antibiotic Survival: Understanding and Combatting Persistence and Heteroresistance, Mol Cell. 76 (2019) 255–267. https://doi.org/10.1016/J.MOLCEL.2019.09.028.

[66]   A. Rodloff, T. Bauer, S. Ewig, P. Kujath, E. Müller, Susceptible, Intermediate, and Resistant – The Intensity of Antibiotic Action, Dtsch Arztebl Int. 105 (2008) 657. https://doi.org/10.3238/ARZTEBL.2008.0657.

[67]   I. Keren, N. Kaldalu, A. Spoering, Y. Wang, K. Lewis, Persister cells and tolerance to antimicrobials, FEMS Microbiol Lett. 230 (2004) 13–18. https://doi.org/10.1016/S0378-1097(03)00856-5.

[68]   T.K. Wood, S.J. Knabel, B.W. Kwan, Bacterial Persister Cell Formation and Dormancy, Appl Environ Microbiol. 79 (2013) 7116. https://doi.org/10.1128/AEM.02636-13.

[69]   S.G. Mohiuddin, S. Ghosh, H.G. Ngo, S. Sensenbach, P. Karki, N.K. Dewangan, V. Angardi, M.A. Orman, Cellular Self-Digestion and Persistence in Bacteria, Microorganisms 2021, Vol. 9, Page 2269. 9 (2021) 2269. https://doi.org/10.3390/MICROORGANISMS9112269.

[70]   M. Ayrapetyan, T. Williams, J.D. Oliver, Relationship between the Viable but Nonculturable

State and Antibiotic Persister Cells, J Bacteriol. 200 (2018).

https://doi.org/10.1128/JB.00249-18.

[71]   J.S. Kim, N. Chowdhury, R. Yamasaki, T.K. Wood, Viable but non-culturable and persistence

describe the same bacterial stress state, Environ Microbiol. 20 (2018) 2038–2048.

https://doi.org/10.1111/1462-2920.14075.

[72]   R. Bellmann, P. Smuszkiewicz, Pharmacokinetics of antifungal drugs: practical implications

for optimized treatment of patients, Infection. 45 (2017) 737.

https://doi.org/10.1007/S15010-017-1042-Z.

[73]   M.C. Fisher, A. Alastruey-Izquierdo, J. Berman, T. Bicanic, E.M. Bignell, P. Bowyer, M.

Bromley, R. Brüggemann, G. Garber, O.A. Cornely, S.J. Gurr, T.S. Harrison, E. Kuijper, J.

Rhodes, D.C. Sheppard, A. Warris, P.L. White, J. Xu, B. Zwaan, P.E. Verweij, Tackling the

emerging threat of antifungal resistance to human health, Nature Reviews Microbiology

2022 20:9. 20 (2022) 557–571. https://doi.org/10.1038/s41579-022-00720-1.

[74]   P. Wal, N. Saraswat, H. Vig, A Detailed Insight onto the Molecular and Cellular Mechanism

of Action of the Antifungal Drugs Used in the Treatment of Superficial Fungal Infections,

Curr Drug Ther. 17 (2022) 148–159.

https://doi.org/10.2174/1574885517666220328141054.

[75]   I. Abe, Bacterial Squalene Cyclase, in: Comprehensive Natural Products II, Elsevier, 2010:

pp. 709–732. https://doi.org/10.1016/B978-008045382-8.00737-1.

[76]   U. Sankawa, Overview, Comprehensive Natural Products Chemistry. (1999) 1–22.

https://doi.org/10.1016/B978-0-08-091283-7.00163-6.

[77] N. Grover, Echinocandins: A ray of hope in antifungal drug therapy, Indian J Pharmacol. 42
(2010) 9. https://doi.org/10.4103/0253-7613.62396.

[78] E. Darmon, D.R.F. Leach, Bacterial Genome Instability, Microbiol Mol Biol Rev. 78 (2014) 1.
https://doi.org/10.1128/MMBR.00035-13.

[79] M. Pigliucci, Phenotypic plasticity: beyond nature and nurture, 2001.
https://books.google.com/books?hl=en&lr=&id=JoCFupYhdNQC&oi=fnd&pg=PR9&ots=K6
7aQFghrM&sig=djXYfBCPVKiTnBObEp864GwAQn8 (accessed September 26, 2023).

[80] M.A. Fortuna, The phenotypic plasticity of an evolving digital organism, R Soc Open Sci. 9
(2022). https://doi.org/10.1098/RSOS.220852.

[81] H.F. Nijhout, Development and evolution of adaptive polyphenisms, Evol Dev. 5 (2003) 9–
18. https://doi.org/10.1046/J.1525-142X.2003.03003.X.

[82] E. Jablonka, M. Lachmann, M.J. Lamb, Evidence, mechanisms and models for the
inheritance of acquired characters, J Theor Biol. 158 (1992) 245–268.
https://doi.org/10.1016/S0022-5193(05)80722-2.

[83] A.D. Bradshaw, Evolutionary Significance of Phenotypic Plasticity in Plants, Adv Genet. 13
(1965) 115–155. https://doi.org/10.1016/S0065-2660(08)60048-6.

[84] X. Li, T. Guo, Q. Mu, X. Li, J. Yu, Genomic and environmental determinants and their
interplay underlying phenotypic plasticity, Proc Natl Acad Sci U S A. 115 (2018) 6679–6684.
https://doi.org/10.1073/PNAS.1718326115.

[85] A. Selmecki, A. Forche, J. Berman, Aneuploidy and isochromosome formation in drug-
resistant Candida albicans, Science. 313 (2006) 367–370.
https://doi.org/10.1126/SCIENCE.1128242.

[86] C. Gilchrist, R. Stelkens, Aneuploidy in yeast: Segregation error or adaptation mechanism?, Yeast. 36 (2019) 525. https://doi.org/10.1002/YEA.3427.

[87] W. Mulla, J. Zhu, R. Li, Yeast: A simple model system to study complex phenomena of aneuploidy, FEMS Microbiol Rev. 38 (2014) 201. https://doi.org/10.1111/1574-6976.12048.

[88] J. Bing, T. Hu, Q. Zheng, J.F. Muñoz, C.A. Cuomo, G. Huang, Experimental Evolution Identifies Adaptive Aneuploidy as a Mechanism of Fluconazole Resistance in Candida auris, Antimicrob Agents Chemother. 65 (2021). https://doi.org/10.1128/AAC.01466-20.

[89] A. Selmecki, M. Gerami-Nejad, C. Paulson, A. Forche, J. Berman, An isochromosome confers drug resistance in vivo by amplification of two genes, ERG11 and TAC1, Mol Microbiol. 68 (2008) 624–641. https://doi.org/10.1111/J.1365-2958.2008.06176.X.

[90] K.L. Gorringe, Loss of Heterozygosity, ELS. (2016) 1–8. https://doi.org/10.1002/9780470015902.A0026643.

[91] LOH (Loss of Heterozygosity), (n.d.). https://www.genome.gov/genetics-glossary/Loss-of-Heterozygosity (accessed August 14, 2023).

[92] O. Pös, J. Radvanszky, G. Buglyó, Z. Pös, D. Rusnakova, B. Nagy, T. Szemes, DNA copy number variation: Main characteristics, evolutionary significance, and pathological aspects, Biomed J. 44 (2021) 548. https://doi.org/10.1016/J.BJ.2021.02.003.

[93] J. Dawan, J. Ahn, Bacterial Stress Responses as Potential Targets in Overcoming Antibiotic Resistance, Microorganisms. 10 (2022). https://doi.org/10.3390/MICROORGANISMS10071385.

[94]   L.E. Cowen, Hsp90 Orchestrates Stress Response Signaling Governing Fungal Drug

Resistance, PLoS Pathog. 5 (2009) e1000471.

https://doi.org/10.1371/JOURNAL.PPAT.1000471.

[95]   T.R. O'Meara, N. Robbins, L.E. Cowen, The Hsp90 Chaperone Network Modulates Candida

Virulence Traits, Trends Microbiol. 25 (2017) 809.

https://doi.org/10.1016/J.TIM.2017.05.003.

[96]   H. Carolus, S. Pierson, J.F. Muñoz, A. Subotić, R.B. Cruz, C.A. Cuomo, P. Van Dijck, Genome-

Wide Analysis of Experimentally Evolved Candida auris Reveals Multiple Novel

Mechanisms of Multidrug Resistance, MBio. 12 (2021).

https://doi.org/10.1128/MBIO.03333-20.

[97]   C. Papp, F. Bohner, K. Kocsis, M. Varga, A. Szekeres, L. Bodai, J.R. Willis, T. Gabaldón, R.

Tóth, J.D. Nosanchuk, C. Vágvölgyi, A. Gácser, Triazole Evolution of Candida parapsilosis

Results in Cross-Resistance to Other Antifungal Drugs, Influences Stress Responses, and

Alters Virulence in an Antifungal Drug-Dependent Manner, MSphere. 5 (2020).

https://doi.org/10.1128/MSPHERE.00821-20.

[98]   M.C. Fisher, A. Alastruey-Izquierdo, J. Berman, T. Bicanic, E.M. Bignell, P. Bowyer, M.

Bromley, R. Brüggemann, G. Garber, O.A. Cornely, S.J. Gurr, T.S. Harrison, E. Kuijper, J.

Rhodes, D.C. Sheppard, A. Warris, P.L. White, J. Xu, B. Zwaan, P.E. Verweij, Tackling the

emerging threat of antifungal resistance to human health, Nat Rev Microbiol. 20 (2022)

557. https://doi.org/10.1038/S41579-022-00720-1.

[99]   F. Yang, V. Gritsenko, Y.S. Futterman, L. Gao, C. Zhen, H. Lu, Y.Y. Jiang, J. Berman,

Tunicamycin Potentiates Antifungal Drug Tolerance via Aneuploidy in Candida albicans,

MBio. 12 (2021). https://doi.org/10.1128/MBIO.02272-21.

[100] F. Yang, F. Teoh, A.S.M. Tan, Y. Cao, N. Pavelka, J. Berman, H. Malik, Aneuploidy Enables Cross-Adaptation to Unrelated Drugs, Mol Biol Evol. 36 (2019) 1768–1782. https://doi.org/10.1093/MOLBEV/MSZ104.

[101] F. Yang, H. Lu, H. Wu, T. Fang, J. Berman, Y. Jiang, Aneuploidy Underlies Tolerance and Cross-Tolerance to Drugs in Candida parapsilosis, Microbiol Spectr. 9 (2021). https://doi.org/10.1128/SPECTRUM.00508-21.

[102] J. Coates, B.R. Park, D. Le, E. Şimşek, W. Chaudhry, M. Kim, Antibiotic-induced population fluctuations and stochastic clearance of bacteria, Elife. 7 (2018). https://doi.org/10.7554/ELIFE.32976.

[103] C.C. Bell, O. Gilan, Principles and mechanisms of non-genetic resistance in cancer, British Journal of Cancer 2019 122:4. 122 (2019) 465–472. https://doi.org/10.1038/s41416-019-0648-6.

[104] D.A. Charlebois, Effect and evolution of gene expression noise on the fitness landscape, Phys Rev E Stat Nonlin Soft Matter Phys. 92 (2015) 022713. https://doi.org/10.1103/PHYSREVE.92.022713/FIGURES/5/MEDIUM.

[105] G. Bergers, S. Song, N. Meyer-Morse, E. Bergsland, D. Hanahan, Benefits of targeting both pericytes and endothelial cells in the tumor vasculature with kinase inhibitors, J Clin Invest. 111 (2003) 1287–1295. https://doi.org/10.1172/JCI17929.

[106] D.A. Charlebois, Quantitative systems-based prediction of antimicrobial resistance evolution, NPJ Syst Biol Appl. 9 (2023). https://doi.org/10.1038/S41540-023-00304-6.

[107] J. Cairns, Mutation selection and the natural history of cancer, Nature 1975 255:5505. 255 (1975) 197–200. https://doi.org/10.1038/255197a0.

[108] A. Brock, H. Chang, S. Huang, Non-genetic heterogeneity — a mutation-independent driving force for the somatic evolution of tumours, Nature Reviews Genetics 2009 10:5. 10 (2009) 336–342. https://doi.org/10.1038/nrg2556.

[109] D. Fraser, M. Kærn, A chance at survival: gene expression noise and phenotypic diversification strategies, Mol Microbiol. 71 (2009) 1333–1340. https://doi.org/10.1111/J.1365-2958.2009.06605.X.

[110] W.J. Blake, G. Bor Balá Zsi, M.A. Kohanski, F.J. Isaacs, K.F. Murphy, Y. Kuang, C.R. Cantor, D.R. Walt, J.J. Collins, Phenotypic consequences of promoter-mediated transcriptional noise, Cell.ComWJ Blake, G Balázsi, MA Kohanski, FJ Isaacs, KF Murphy, Y Kuang, CR Cantor, DR WaltMolecular Cell, 2006•cell.Com. 24 (n.d.) 853–865. https://doi.org/10.1016/j.molcel.2006.11.003.

[111] D. Zhuravel, D. Fraser, S. St-Pierre, L. Tepliakova, W.L. Pang, J. Hasty, M. Kærn, Phenotypic impact of regulatory noise in cellular stress-response pathways, Syst Synth Biol. 4 (2010) 105. https://doi.org/10.1007/S11693-010-9055-2.

[112] D. Charlebois, Computational Investigations of Noise-mediated Cell Population Dynamics, (2014). https://doi.org/10.20381/RUOR-3454.

[113] D.A. Charlebois, M. Kærn, What all the noise is about: The physical basis of cellular individuality, Can J Phys. 90 (2012) 919–923. https://doi.org/10.1139/P2012-091.

[114] V. Shahrezaei, P.S. Swain, Analytical distributions for stochastic gene expression, Proc Natl Acad Sci U S A. 105 (2008) 17256–17261. https://doi.org/10.1073/PNAS.0803850105/SUPPL_FILE/APPENDIX_PDF.PDF.

[115]   D. Fraser, M. Kærn, A chance at survival: gene expression noise and phenotypic

diversification strategies, Mol Microbiol. 71 (2009) 1333–1340.

https://doi.org/10.1111/J.1365-2958.2009.06605.X.

[116]   Kirby-Bauer Disk Diffusion Susceptibility Test Protocol | ASM.org, (n.d.).

https://asm.org/Protocols/Kirby-Bauer-Disk-Diffusion-Susceptibility-Test-Pro (accessed

September 25, 2023).

[117]   GitHub - acgerstein/diskImageR: diskImageR package, (n.d.).

https://github.com/acgerstein/diskImageR (accessed August 15, 2023).

[118]   A.C. Gerstein, A. Rosenberg, I. Hecht, J. Berman, diskImageR: quantification of resistance

and tolerance to antimicrobial drugs using disk diffusion assays, Microbiology (Reading).

162 (2016) 1059–1068. https://doi.org/10.1099/MIC.0.000295.

[119]   R.T.-(No Title), undefined 2010, R: A language and environment for statistical computing,

Cir.Nii.Ac.Jp. (n.d.). https://cir.nii.ac.jp/crid/1370294721063650048 (accessed October 28,

2023).

[120]   ImageJ.JS, (n.d.). https://ij.imjoy.io/ (accessed October 28, 2023).

[121]   T. Levinson, A. Dahan, A. Novikov, Y. Paran, J. Berman, R. Ben-Ami, Impact of tolerance to

fluconazole on treatment response in Candida albicans bloodstream infection, Mycoses.

64 (2021) 78–85. https://doi.org/10.1111/MYC.13191.

[122]   A. Rosenberg, I. V. Ene, M. Bibi, S. Zakin, E.S. Segal, N. Ziv, A.M. Dahan, A.L. Colombo, R.J.

Bennett, J. Berman, Antifungal tolerance is a subpopulation effect distinct from resistance

and is associated with persistent candidemia, Nature Communications 2018 9:1. 9 (2018)

1–14. https://doi.org/10.1038/s41467-018-04926-x.

[123] A.C. Gerstein, A. Rosenberg, I. Hecht, J. Berman, diskImageR: quantification of resistance and tolerance to antimicrobial drugs using disk diffusion assays, Microbiology (N Y). 162 (2016) 1059. https://doi.org/10.1099/MIC.0.000295.

[124] P.W. Van der Pas, The discovery of the Brownian motion, Scientiarum Historia: Tijdschrift Voor de Geschiedenis van de Wetenschappen En de Geneeskunde. 13 (1971) 27–35. https://dspace.library.uu.nl/handle/1874/293495 (accessed August 16, 2023).

[125] biological physics energy information life phyliips... - Google Scholar, (n.d.). https://scholar.google.com/scholar?hl=en&as_sdt=0%2C5&q=biological+physics+energy+i nformation+life+phyliips+nelson+- +Google+Scholar%2C+%28n.d.%29.+https%3A%2F%2Fscholar.google.com%2Fscholar%3Fh l%3Den%26as_sdt%3D0%252C5%26q%3Dbiological%2Bphysics%2Benergy%2Binformatio n%2Blife%2Bphyliips%2Bnelson%26btnG%3D+%28accessed+July+2%2C+2023%29.&btnG = (accessed August 16, 2023).

[126] Diffusion in Solids: Fundamentals, Methods, Materials, Diffusion-Controlled ... - Helmut Mehrer - Google Books, (n.d.). https://books.google.ca/books?hl=en&lr=&id=IUZVffQLFKQC&oi=fnd&pg=PA27&dq=Diffus ion+in+solids:+fundamentals,+methods,+materials,+diffusion- controlled+processes&ots=66qaxNN73q&redir_esc=y#v=onepage&q=Diffusion%20in%20s olids%3A%20fundamentals%2C%20methods%2C%20materials%2C%20diffusion- controlled%20processes&f=false (accessed August 16, 2023).

[127] H. Mehrer, Diffusion in Solids, 155 (2007). https://doi.org/10.1007/978-3-540-71488-0.

[128] H. Mehrer, Diffusion in solids: fundamentals, methods, materials, diffusion-controlled processes, 2007.

https://books.google.com/books?hl=en&lr=&id=IUZVffQLFKQC&oi=fnd&pg=PA27&dq=Diff

usion+in+solids:+fundamentals,+methods,+materials,+diffusion-

controlled+processes&ots=66qaxNN73q&sig=Gbm2CVGqw3TMhFysCZAyBU7vpnk

(accessed July 2, 2023).

[129] R.M.B.S.G.D. Nelson PC, Biological physics: energy, information, life, 2008.

[130] biological physics energy information life phyliips nelson - Google Scholar, (n.d.).

https://scholar.google.com/scholar?hl=en&as_sdt=0%2C5&q=biological+physics+energy+i

nformation+life+phyliips+nelson&btnG= (accessed July 2, 2023).

[131] Numerical Methods in Engineering and Science (C,... - Google Scholar, (n.d.).

https://scholar.google.com/scholar?hl=en&as_sdt=0%2C5&q=Numerical+Methods+in+En

gineering+and+Science+%28C%2C+C%2B%2B%2C+and+MATLAB%29+B.S.+Grewel&btnG=

(accessed July 2, 2023).

[132] Finite difference methods for diffusion processes, (n.d.). http://hplgit.github.io/num-

methods-for-PDEs/doc/pub/diffu/sphinx/index.html (accessed July 2, 2023).

[133] B.S. Grewal, Numerical Methods in Engineering and Science:(C, and C++, and MATLAB),

(2018).

https://books.google.com/books/about/Numerical_Methods_in_Engineering_and_Sci.ht

ml?id=BCdtDwAAQBAJ (accessed August 16, 2023).

[134] Finite difference methods for diffusion processes, (n.d.). http://hplgit.github.io/num-

methods-for-PDEs/doc/pub/diffu/sphinx/index.html (accessed August 16, 2023).

[135] Analytical Solution of Fick's 2nd law — MATLAB Number ONE, (n.d.).

https://matlab1.com/analytical-solution-ficks-2nd-law/ (accessed October 18, 2023).

[136] J. Leveque ; C, R.J. Leveque, Finite Difference Methods for Differential Equations, (1998).

[137] Grewal.J. Grewal BS, Numerical methods in Engineering and Science, 1996.

[138] J. Leveque ; C, R.J. Leveque, Finite Difference Methods for Differential Equations, (1998).

[139] H. Mehrer, Diffusion in Solids, 155 (2007). https://doi.org/10.1007/978-3-540-71488-0.

[140] K. Samprovalaki, P.T. Robbins, P.J. Fryer, Investigation of the diffusion of dyes in agar gels, J Food Eng. 111 (2012) 537–545. https://doi.org/10.1016/J.JFOODENG.2012.03.024.

[141] S. Miyamoto, K. Atsuyama, K. Ekino, T. Shin, Estimating the Diffusion Coefficients of Sugars Using Diffusion Experiments in Agar-Gel and Computer Simulations, Chem Pharm Bull (Tokyo). 66 (2018) 632–636. https://doi.org/10.1248/CPB.C18-00071.

[142] S. Miyamoto, K. Shimono, Molecular Modeling to Estimate the Diffusion Coefficients of Drugs and Other Small Molecules, Molecules 2020, Vol. 25, Page 5340. 25 (2020) 5340. https://doi.org/10.3390/MOLECULES25225340.

[143] V. Chandrasekar, S.J. Knabel, R.C. Anantheswaran, Modeling development of inhibition zones in an agar diffusion bioassay, Food Sci Nutr. 3 (2015) 394–403. https://doi.org/10.1002/FSN3.232.

[144] I. Sebti, D. Blanc, A. Carnet-Ripoche, R.E. Saurel, V.E. Coma, Experimental study and modeling of nisin diffusion in agarose gels, J Food Eng. 63 (2004) 185–190. https://doi.org/10.1016/S0260-8774(03)00299-1.

[145] Caspofungin | C52H88N10O15 | CID 2826718 - PubChem, (n.d.). https://pubchem.ncbi.nlm.nih.gov/compound/2826718 (accessed July 3, 2023).

[146] M44: Antifungal Disk Diffusion Susceptibility, Yeasts, (n.d.).

https://clsi.org/standards/products/microbiology/documents/m44/ (accessed October 28,

2023).

[147] A. Rosenberg, I. V. Ene, M. Bibi, S. Zakin, E.S. Segal, N. Ziv, A.M. Dahan, A.L. Colombo, R.J.

Bennett, J. Berman, Antifungal tolerance is a subpopulation effect distinct from resistance

and is associated with persistent candidemia, Nature Communications 2018 9:1. 9 (2018)

1–14. https://doi.org/10.1038/s41467-018-04926-x.

[148] S.A. Shankarnarayan, D.A. Charlebois, Machine learning to identify clinically relevant

Candida yeast species, BioRxiv. (2023) 2023.09.08.556885.

https://doi.org/10.1101/2023.09.08.556885.